Curriculum Vitae

Peter Ammon Hecker

pheck001@umaryland.edu

Education

University of Maryland, Baltimore
Ph.D. Candidate – Molecular Medicine 2008-2012

- *Mentor*: William C. Stanley
- *Thesis*: Glucose-6-phosphate dehydrogenase, macronutrient intake, and heart failure
- Additional studies of the effects of adiponectin, fish oils, microRNA-29b, obscurin D, and perilipin 5, in heart failure and metabolism
- Received an NIH T32 Cardiovascular Training Grant (10/2009-9/2011)

Brigham Young University
B. S. – Molecular Biology 2003-2008

- Admitted 1 year early from high school, received multiple performance-based scholarships
- Phi Eta Sigma Honor Society

Relevant Experience

Lab Rotations
University of Maryland, Baltimore 11/2008-3/2009

- Tested anti-cancer properties of an attenuated HSV-2 virus
- Protein purification for use in *Clostridium difficile* vaccine

Mentored Research
Brigham Young University 9/2006-4/2008

- Made a ribosome library in E. coli and screened it for translational stalling mutations
- Sequenced rainbow trout DNA from lakes and streams in the mountain west

Molecular Biology Teaching Assistant
Brigham Young University 1/2007-6/2008

- Held regular review sessions and tutored students
- Graded assignments, quizzes, and tests

Publications

1. **Hecker PA**, Mapanga RF, Kimar CP, Ribeiro Jr RF, Brown BH, O'Connell KA, Cox JW, Shekar KC, Asemu G, Essop MF, Stanley WC. Effects of glucose 6-phosphate dehydrogenase deficiency on the metabolic and cardiac responses to obesogenic or high fructose diets. [Submitted].

2. **Hecker PA**, Lionetti V, Ribeiro RF Jr, Rastogi S, Brown BH, O’Connell KA, Cox JW, Shekar KC, Gamble D, Sabbah HN, Leopold JA, Gupte SA, Recchia FA, Stanley WC. Glucose-6-phosphate dehydrogenase deficiency increases redox stress and moderately accelerates the development of heart failure. [Submitted].

3. Rawat DK, **Hecker P**, Watanabe M, Levy RJ, Okada T, Edwards JG, Gupte SA. G6PD insufficiency suppresses cardiac myocyte L-type calcium channel activity and myocardial contractility, and increases end-diastolic diameter. [Submitted].

4. **Hecker PA**, Galavao TF, O’Shea KM, Brown BH, Henderson R, Riggle H, Gupte SA, Stanley WC. High sugar intake does not adversely affect metabolic and cardiac dysfunction in genetic cardiomyopathy. *Nutrition*. Epub 2012 Feb 2.

5. Galvao TF, Brown BH, **Hecker PA**, O’Connell K, O’Shea KM, Sabbah HN, Rastogi S, Daneault C, Des Rosiers C, Stanley WC. High saturated fat intake improves survival in heart failure compared to a high polyunsaturated fat or low fat diet despite persistent mitochondrial defects. *Cardiovascular Research*. 2012 Jan 1;93(1):24-32. Epub 2011 Sep 29.

6. **Hecker PA**, O’Shea KM, Galvao TF, Brown BH, Stanley WC. Role of adiponectin in the development of high-fat diet-induced metabolic abnormalities in mice. *Hormone and Metabolic Research*. 2011 Feb;43(2):100-5. Epub 2010 Dec 16.

7. O'Shea KM, Chess DJ, Khairallah RJ, **Hecker PA**, Lei B, Walsh K, Des Rosiers C, Stanley WC. Omega-3 polyunsaturated fatty acids prevent pressure overload-induced ventricular dilation and decrease in mitochondrial enzymes despite no change in adiponectin. *Lipids in Health and Disease*. 2010 Sep 6;9:95.

8. Khairallah RJ, Sparagna GC, Khanna N, O'Shea KM, **Hecker PA**, Kristian T, Fiskum G, Des Rosiers C, Polster BM, Stanley WC. Dietary supplementation with docosahexaenoic acid, but not eicosapentaenoic acid, dramatically alters cardiac mitochondrial phospholipid fatty acid composition and prevents permeability transition. *Biochim Biophys Acta*. 2010 Aug;1797(8):1555-62. Epub 2010 May 21.

9. O'Shea KM, Chess DJ, Khairallah RJ, Rastogi S, **Hecker PA**, Sabbah HN, Walsh K, Stanley WC. Effects of adiponectin deficiency on structural and metabolic remodeling in mice subjected to pressure overload. *Am J Physiol Heart Circ Physiol*. 2010 Jun;298(6):H1639-45. Epub 2010 Mar 26.

10. O'Shea KM, Khairallah RJ, Sparagna GC, Xu W, **Hecker PA**, Robillard-Frayne I, Des Rosiers C, Kristian T, Murphy RC, Fiskum G, Stanley WC. Dietary omega-3 fatty acids alter cardiac mitochondrial phospholipid composition and delay Ca^{2+}-induced permeability transition. *J Mol Cell Cardiol*. 2009 Dec;47(6):819-27. Epub 2009 Aug 22.

Abstracts

1. **Hecker PA**, Lionetti V, Stanley WC. Glucose-6-phosphate dehydrogenase deficiency exacerbates LV dilation but does not affect function after myocardial infarction. *European Society of Cardiology* [poster presentation]. 2012.

2. **Hecker PA**, Ribeiro RF, Brown BH, O'Connell K, Stanley WC. Glucose-6-phosphate dehydrogenase deficiency promotes susceptibility to pressure overload induced left ventricular dysfunction and hypertrophy. *American Heart Association* [oral presentation]. 2011.

3. **Hecker PA**, Galavao TF, O’Shea KM, Brown BH, Henderson R, Riggle H, Gupte SA, Stanley WC. High sugar intake may improve survival and does not adversely affect cardiac and metabolic dysfunction in genetic cardiomyopathy. *American Heart Association* [poster presentation]. 2011.

4. **Hecker PA**, Galavao TF, O’Shea KM, Brown BH, Henderson R, Riggle H, Gupte SA, Stanley WC. Metabolic and cardiac dysfunction are unaffected by high sugar intake in a hamster model of heart failure. *Experimental Biology* [poster presentation]. 2011.

5. **Hecker PA**, Galavao TF, O’Shea KM, Brown BH, Henderson R, Riggle H, Stanley WC. Metabolic and cardiac dysfunction in cardiomyopathic hamsters is unaffected by high sugar intake. *Annual Retreat - Vascular Biology Training Program & Training Program in Cardiovascular Cell Biology* [oral presentation]. 2010.

6. **Hecker PA**, O’Shea KM, Galvao TFG, Brown BH, Stanley WC. Role of adiponectin in the development of diet-induced cardiometabolic syndrome. *Society for Heart and Vascular Metabolism* [poster presentation]. 2010.

Abstract

Glucose 6-Phosphate Dehydrogenase, Macronutrient Intake, and Heart Failure

Peter Ammon Hecker, Doctor of Philosophy, 2012

Dissertation Directed by Dr. William C. Stanley, Professor, Department of Cardiology

Glucose 6-phosphate dehydrogenase (G6PD) catalyzes the conversion of G6P to 6-phosphogluconolactone and formation of NADPH. Human G6PD deficiency is very common, and may affect the development of metabolic abnormalities and heart failure through its affects on reactive oxygen species (ROS). NADPH fuels antioxidant pathways, but also fuels oxidant production by NADPH oxidase, uncoupled nitric oxide synthase, and other enzymes. Evidence suggests that high sugar intake, obesity, and heart failure increase [NADPH] and ROS formation, possibly by increasing the flux of glucose through G6PD. Therefore the goal of this project was to determine whether G6PD deficiency protects against or exacerbates oxidative stress and cardiac dysfunction in the context of obesity, high sugar intake, and heart failure. First, we found that G6PD deficiency decreased obesity but not metabolic abnormalities after long term dietary treatment. Second, G6PD deficiency moderately exacerbated redox stress and heart failure mediated by myocardial infarction, severe pressure overload, or mild pressure overload with high fructose intake. Third, although high sugar intake increased superoxide production, this did not correspond with increases in [NADPH] or mortality in a genetic model of cardiomyopathy. The results indicate that G6PD deficiency moderately exacerbates oxidative stress, diet-induced metabolic dysfunction, and heart failure.

Glucose 6-Phosphate Dehydrogenase, Macronutrient Intake, and Heart Failure

by
Peter Ammon Hecker

Dissertation submitted to the faculty of the Graduate School of the
University of Maryland, Baltimore in partial fulfillment
of the requirements for the degree of
Doctor of Philosophy
2012

Table of Contents

List of Tables

List of Figures

Abbreviations

4-HA – 4-Hydroxyalkenals

6PG – 6-Phosphogluconate

6PGD – 6-Phosphogluconate dehydrogenase

AAB – Abdominal aortic banding

ACC – American College of Cardiology

ACE inhibitors – Angiotensin converting enzyme inhibitors

AHA – American Heart Association

ANP – Atrial natriuretic peptide

$APN^{-/-}$ – Adiponectin deficient

ARB – Angiotensin II receptor blocker

AT1 – Angiotensin II receptor type 1

AWT – Absolute wall thickness

BH4 – tetrahydrobiopterin

CHF – Congestive heart failure

CS – Citrate synthase

DIO – Diet induced obesity

dV – End diastolic volume

EDA – End diastolic area

EDD – End diastolic diameter

EF – Ejection fraction

ESA – End systolic area

ESD – End systolic diameter

ET – Ejection time

FFA – Free fatty acids

FS – Fractional shortening

G6P – Glucose 6-phosphate

G6PD – Glucose 6-phosphate dehydrogenase

G6PDX mice – G6PD deficient mice

GSH – Glutathione, reduced form

GSSG – Glutathione, oxidized form

HDL – High density lipoprotein

ICDH – Isocitrate dehydrogenase

IVCT – Isovolumetric contraction time

IVRT – Isovolumetric relaxation time

LAD – left anterior descending coronary artery

LDL – Low density lipoprotein

LV – Left Ventricle

LVAW;d – LV anterior wall at diastole

LVAW;s – LV anterior wall at systole

LVPW;d – LV posterior wall at diastole

LVPW;s – LV posterior wall at systole

MCAD – Medium chain acyl-coenzyme A dehydrogenase

MDA – Malondialdehyde

MHC – Myosin heavy chain

MPI – Myocardial performance index

MPTP – Mitochondrial permeability transition pore

NAD+ – Nicotinamide adenine dinucleotide, oxidized form

NADH – Nicotinamide adenine dinucleotide, reduced form

NADP+ – Nicotinamide adenine dinucleotide phosphate, oxidized form

NADPH – Nicotinamide adenine dinucleotide phosphate, reduced form

NYHA – New York Heart Association

ob/ob mice – Obese leptin deficient mice

PCR – Polymerase chain reaction

qRT-PCR – Quantitative real time PCR

RAAS – Renin angiotensin aldosterone system

ROS – Reactive oxygen species

RV – Right Ventricle

RWT – Relative wall thickness

SOD – Superoxide dismutase

sV – End systolic volume

TAC – Transverse aortic constriction

TG – Triglycerides

Chapter 1 – Introduction

G6PD Deficiency

G6PD Overview

Glucose 6-phosphate dehydrogenase (G6PD) deficiency affects over 400 million people, and is the most common enzyme deficiency in the world[1, 2]. G6PD is the first and rate determining enzyme of the pentose phosphate pathway. The activity of this pathway determines cytoplasmic [NADPH], and thereby affects the redox status of the cell[3]. Although the effects of G6PD deficiency on blood cells have been well studied, its effects in other tissues are relatively undefined. Because G6PD affects redox status, G6PD deficiency may play a role in human disease[3, 4, 4-13].

Epidemiology of G6PD Deficiency

Hundreds of G6PD mutations have been found throughout the world, and many of these result in a decrease in the activity of the enzyme[2]. The severity of G6PD deficiency is classified by the World Health Organization on the basis of enzyme activity (Figure 1.1)[2, 14]. The *g6pdx* gene is X-linked, and so G6PD deficiency most commonly affects males rather than females. G6PD deficiency is highly distributed throughout sub-Saharan Africa, regions in the Mediterranean, and parts of Southeast Asia. The deficiency may be well preserved in these populations because G6PD deficient patients have few or no complications, and because it confers a selective advantage against malaria[15]. The most common allele that results in G6PD deficiency, G6PD A-, is largely found in African populations and results in a residual G6PD activity of ~20%[16]. Most Americans that have

G6PD deficiency are of African descent. Approximately 10% of black Americans are G6PD deficient, and, overall between 0.5 and 2.9% of Americans are G6PD deficient[2]. Thus, G6PD deficiency is a common enzymopathy which affects a great number of Africans and African Americans.

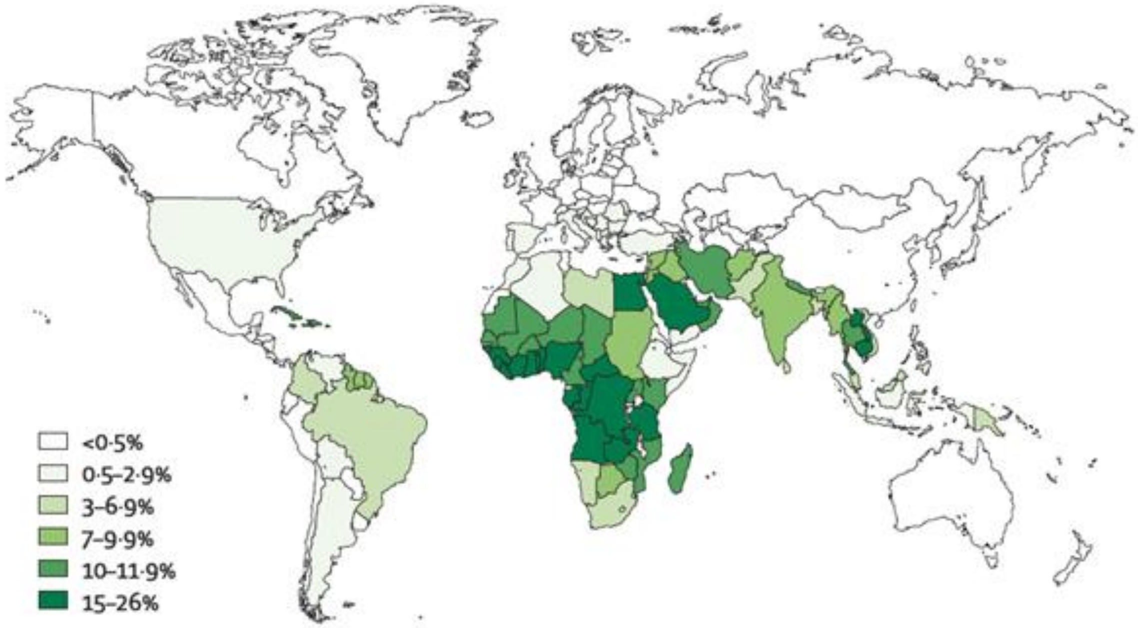

Classes of G6PD deficiency

Class I
Severely deficient, associated with chronic non-spherocytic haemolytic anaemia

Class II
Severely deficient (1–10% residual activity), associated with acute haemolytic anaemia

Class III
Moderately deficient (10–60% residual activity)

Class IV
Normal activity (60–150%)

Class V
Increased activity (>150%)

Figure 1.1.

Top Panel. Worldwide distribution of G6PD deficiency.

Bottom Panel. World Health Organization classes of G6PD deficiency

Modified from Cappellini 2008, Lancet.

G6PD Biochemistry

Warburg and Christian discovered G6PD in 1931[17]. The *g6pdx* gene was sequenced in 1986 by two separate groups, and resides on the long arm of the X chromosome (band Xq28)[18, 19]. The gene contains 13 exons, is ~20 kilobases long, and encodes a 545 amino acid product. The second exon contains the start codon. The crystal structure of G6PD was first solved in *Leuconostoc mesenteroides*, a gram positive species of bacteria, in 1994, and then adapted to a human homology model in 1996[20, 21] (Figure 1.2). The structure of the human enzyme was finally solved in 2000[22, 23]. The active G6PD enzyme consists of identical ~56 kDa subunits which interact as dimers or tetramers[18, 24]. Activity of the enzyme requires allosteric interactions with multiple NADP+ molecules[25, 26]. The binding of structural NADP+ molecules on each subunit are required for formation of the enzyme, and further interaction is required for catalytic activity[23]. The enzyme resides in the cytoplasm, and catalyzes the oxidation of glucose 6-phosphate (G6P) to 6-phosphogluconolactone and the reduction of NADP+ to NADPH(Figure 1.3)[27]. The most common G6PD mutations affect the catalytic domain, and lead to a defective enzyme which is rapidly degraded[2, 20, 28].

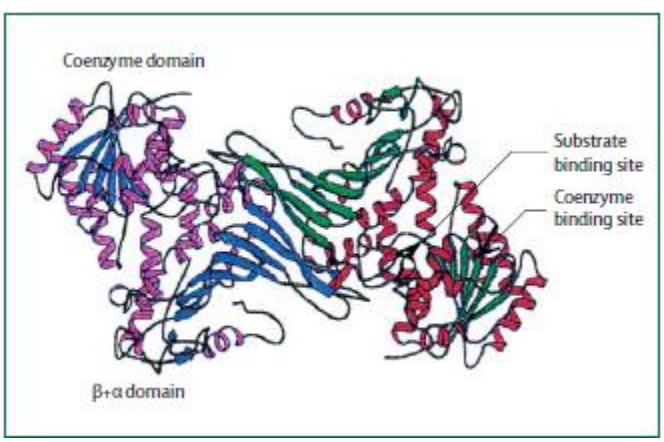

Figure 1.2. *Three-dimensional structure of a G6PD dimer*. *Naylor 1996, Blood*.

G6PD activity varies widely according to cell type and disease state, and its role is of major functional importance. G6PD controls the entry of G6P into the pentose phosphate pathway (Figure 1.3). The pentose phosphate pathway is characterized by the following reactions: 1) G6PD oxidizes G6P to 6-phosphogluconolactone, 2) lactontase hydrolyzes circular 6-phosphogluconolactone to form a linear product, 6-phosphogluconate, 3) 6-phosphogluconate dehydrogenase (6PGD) converts 6-phosphogluconate to ribulose-5-phosphate. The reaction catalyzed by 6PGD cleaves the 1˚ carbon from 6-phosphogluconate, and releases CO_2. The above 3 reactions are known as the oxidative phase of the pathway. In the non-oxidative phase, ribulose-5-phosphate may be used for nucleotide synthesis or aromatic amino acid synthesis, or may be converted to fructose-6-phosphate and glyceraldehydes-3-phosphate through a series of aldolases and transketolases which re-enter the pathway or are oxidized as fuel.

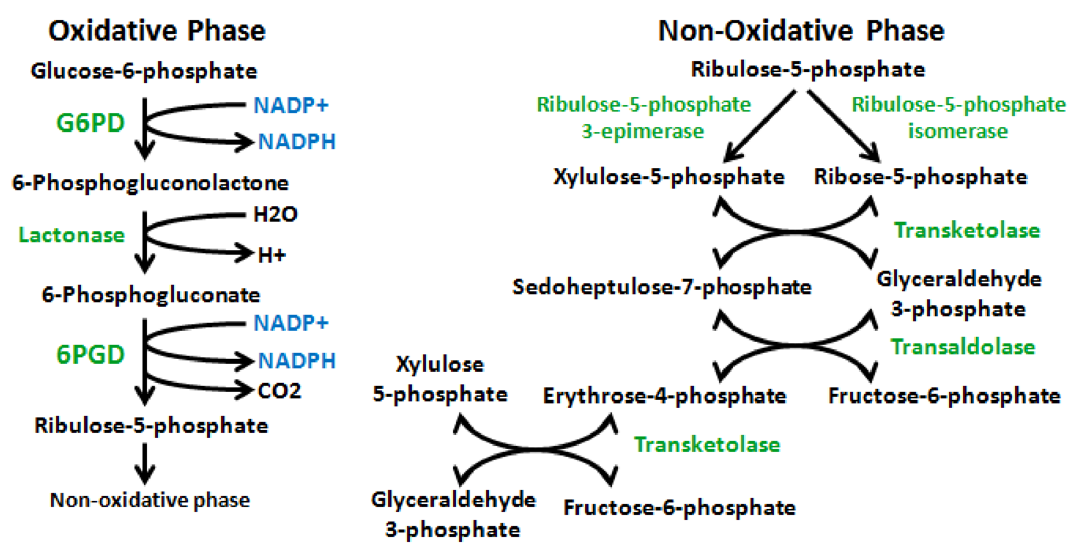

Figure 1.3. *The pentose phosphate pathway*. The oxidative phase of the pentose phosphate pathway produces NADPH from NADP+, and ribulose-5 phosphate. If ribulose-5-phosphate is not used for nucleotide synthesis, then it converted to glyceraldehydes-3-phosphate and fructose-6-phosphate through a series of non-oxidative

reactions. 6PGD, 6-phosphogluconate dehydrogenase; G6PD, glucose 6-phosphate dehydrogenase. *Redrawn from King 1996, themedicalbiochemistrypage.org*.

G6PD and 6PGD both produce NADPH from NADP+, but the reaction catalyzed by G6PD is the rate-determining step of the pentose phosphate pathway, and decreasing the activity of G6PD lowers NADPH levels[3, 4, 6, 27, 29]. The mitochondrial enzymes isocitrate dehydrogenase and malic enzyme also produce NADPH from NADP+ in the mitochondria, but G6PD is the sole producer of cytoplasmic NADPH. Of interest, red blood cells do not contain mitochondria, and so the entire red blood cell production of NADPH is dependent on G6PD. However, non-blood cells still depend on G6PD for cytoplasmic NADPH[9, 10].

Clinical Consequences of G6PD Deficiency

NADPH is used required by the antioxidant glutathione system to reduce reactive oxygen species (ROS)[30]. Excessive ROS can damage the cell, resulting in oxidized proteins, ribonucleotides, and lipids[31]. By producing NADPH, G6PD and 6PGD fuel cytoplasmic antioxidant capacity[10]. Red blood cells depend on the pentose phosphate pathway for antioxidant defense, and therefore G6PD deficiency can manifest in adverse hemolytic responses. Severe G6PD deficiency results in chronic hemolytic anemia, and complete deficiency is embryonic lethal[1, 16, 32]. However, most G6PD deficient individuals are moderately deficient (Class II-III), and have few problems. The most common complication is acute hemolytic anemia in response to oxidizing stimuli such as fava bean consumption, microbrial infection, or certain antimalarial medications such as primaquine, pamaquine, or chloroquine. Hemolytic anemia usually presents with weakness, fatigue, and jaundice. A blood transfusion is generally sufficient to alleviate these conditions because the transfused blood cells are not usually deficient for G6PD and are more resistant to stress. Thus, in most patients, G6PD deficiency only manifests as a treatable acute hemolytic anemia in response to oxidizing stimulants.

Before the discovery of G6PD in 1931[17], the effects of G6PD deficiency were known as favism, because of a hemolytic response in certain individuals after the consumption of fava beans. Broad beans contain high levels of vicine, divicine, convicine, and isouramil, which are all oxidants, and G6PD deficient cell show are exquisitely sensitive to oxidant stress[10, 33]. People have known about favism for thousands of years. Herodotus, the first known historian wrote that Egyptian priests prohibited the consumption of fava beans, and Pythagoras, a Greek philosopher-mathematician who lived during the 5th century BC, also refused them[1, 16]. However, despite the known effects of fava beans to some individuals, the cause of favism was not known until the mid 1900s.

The discovery of G6PD deficiency was made in the 1950s in prisoner volunteers that were being treated with antimalarial medications[1]. These prisoners were given the antimalarial drug, primaquine in order to assess the toxicity of the drug. Most of these prisoners did not manifest any adverse reactions to the drug, but some had a hemolytic response. In the subjects with a hemolytic response, blood which was transfused from primaquine-insensitive subjects did not undergo hemolysis, and thus it was found that the sensitivity was due to some intrinsic factor of the blood cells themselves[34]. At this time the addition of NADPH was known to reduce oxidized glutathione (GSSG) via G6PD[30], and upon further investigation, it was discovered that the serum of primaquine-sensitive subjects had a decreased ability to reduce GSSG which was corrected by adding NADPH to the hemolysate, but not by adding NADP+[35-38]. This indicated that G6PD was the defect in these subjects, because G6PD is the only enzyme that reduces NADP+ to NADPH in red blood cells. Thus, investigators became aware that G6PD deficiency was the cause of drug-induced hemolysis and that it resulted in decreased red blood cell antioxidant capacity.

The most adverse complication in G6PD deficient subjects is acute bilirubin encephalopathy leading to kernicterus, or brain damage in newly born infants. Kernicterus occurs in response to jaundice after acute hemolytic anemia[39, 40]. G6PD deficient newborns have an increased risk of severe jaundice and are thus at risk for kernicterus[2, 40].

Assessment and Management of G6PD Deficiency

Screening for G6PD deficiency is performed on a routine basis in many states, and in countries where the prevalence of G6PD deficiency is high. Testing for G6PD deficiency may also be performed in cases of neonatal jaundice or acute hemolysis, especially when it occurs in response to antimalarial drugs or the consumption of broad beans. Assessment of G6PD deficiency can be achieved quickly via the Beutler spot test, and is more readily confirmed by a more sensitive laboratory method to assess the specific activity of the enzyme[41, 42]. The Beutler spot test involves combining a small sample of blood with G6P and NADP+, then drying a spot of this reaction mixture on filter paper. NADPH, but not NADP+, fluoresces under long wave ultraviolet light because it absorbs light at 340nm. If the spot does not fluoresce under ultraviolet light, then the test is positive for G6PD deficiency. The Beutler spot test may then be confirmed by a more sensitive laboratory method to assess the specific activity of the enzyme. The DNA mutation can also be confirmed by direct sequencing or by PCR genotyping of the *g6pdx* gene.

For most people with G6PD deficiency, treatment entails simply avoiding any agent that triggers hemolysis. This includes the avoidance of fava beans and a specific list of drugs. If a severe hemolytic crisis does occur, then a blood transfusion is normally sufficient. Vaccination against common pathogens also helps prevent hemolysis, because hemolysis may be triggered by an infection[43]. Overall, G6PD deficiency is generally only a problem in the most severely deficient individuals, and the majority of G6PD deficient patients live normal lives without any resultant complications.

Animal Model of G6PD Deficiency

The generation of G6PD deficient (G6PDX) mice was first reported in 1988[44]. This was done by treating male mice with a DNA ethylating agent, 1-ethyl-1-nitrosourea, to induce random DNA mutations. G6PD deficiency was then identified in subsequent offspring. G6PDX mice have an A:T mutation in the 5˚ untranslated region at the splice site of the 3˚ end of exon 1[45]. This mutation results in decreased translation of G6PD, and leads to ~20-40% residual G6PD activity in G6PDX mice compared to WT littermate control mice (Figure 1.4). A residual activity of ~20% is similar to the degree by which activity is decreased in humans with the A- G6PD allele, and is classified as a type III, or moderate, deficiency[2, 16]. G6PDX mice are born in normal Mendelian ratios, and mature normally. Thus, they provide an acceptable model for the study of G6PD deficiency.

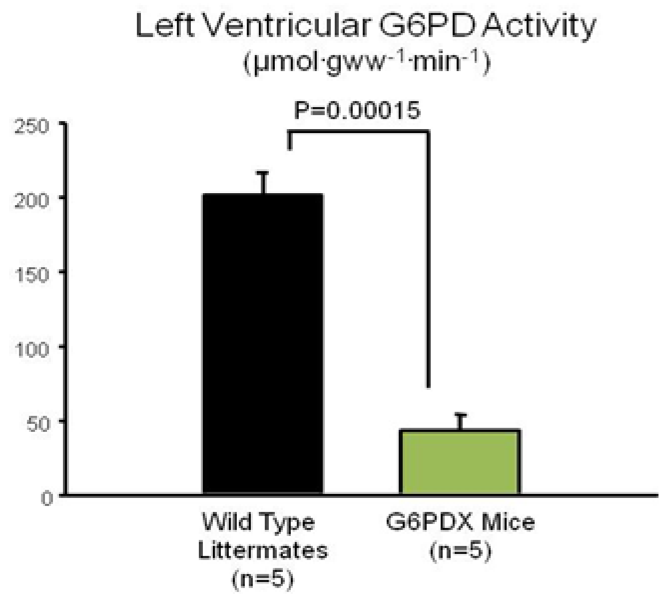

Figure 1.4. *G6PD activity of G6PDX vs WT mice*. G6PD activity was assessed in myocardium of mice at 8 weeks of age. *Hecker, unpublished data*.

Heart Failure

Definition of Heart Failure

Heart failure is a syndrome defined by an impaired ability of the ventricle to fill with or eject blood[46]. This results in an inability to adequately supply blood to other organs in response to increased demand such as exercise. The severity of heart failure is characterized clinically according to the New York Heart Association (NYHA) classification system based on its effects on physical activity and quality of life[47]. In mild to moderate heart failure, patients experience undue dyspnea and fatigue in response to physical activity and exercise (NYHA classes II-III). In severe heart failure, patients experience symptoms even at rest (NYHA class IV). Another classification system defined by the American Heart Association (AHA) and the American College of Cardiology (ACC) is based on the progression of heart failure. In this system patients progress from being at risk of developing heart failure (stage A), to developing cardiac structural abnormalities (stage B), to developing symptoms of heart failure (stage C), to requiring ambulatory care or constant hospitalization for heart failure (stage D)[46]. Of the 5 million patients with heart failure, most are in stage C[48]. Thus, heart failure is a progressive clinical syndrome defined by an impaired ability of the ventricle to meet the body's demands for blood perfusion, leading to a decreased quality of life and eventual death.

Assessment of Heart Failure

Although impaired filling and impaired blood ejection are both used in the definition of heart failure, either one can occur distinctly from the other[46]. An impairment in ventricular filling may be due to a reduced ability of the ventricle to relax, known as diastolic dysfunction. Diastolic dysfunction may result from increased ventricular stiffness and fibrosis[49]. Impaired ejection of blood may be due to a reduced ability of the ventricle to contract, known as systolic dysfunction. Thus, there is a distinction between impaired ejection and filling. Experimental means have been devised to assess each of these, as described below.

Echocardiography is a useful tool for the diagnosis of heart failure, because it can be used to assess structural abnormalities and contractile dysfunction (Figure 1.5)[46]. This method uses ultrasound technology to create an image of a working heart by which cardiac dimensions may be obtained. With these measurements, one can then calculate the systolic and diastolic volumes and determine the ejection fraction, which is the percentage of blood that is pumped out of the ventricle with each beat of the heart. Healthy patients usually have an ejection fraction between 50 and 70%. A decreased ejection fraction is indicative of systolic dysfunction and heart failure[46].

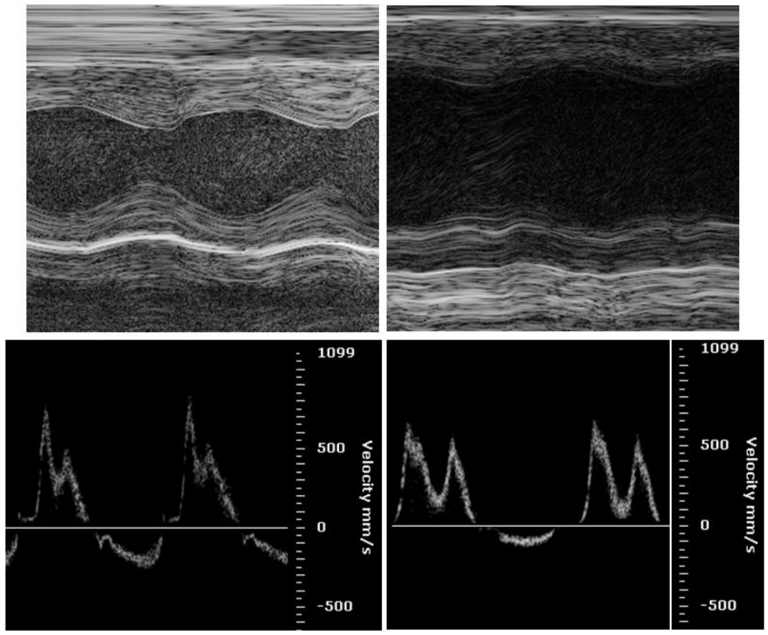

Figure 1.5. *Healthy and failing murine myocardium as assessed by echocardiography*. *Top left*. M-mode linescan of healthy myocardium taken from the short axis of the left ventricle. *Bottom left*. Doppler images of healhy myocardium taken from the apical view of the left ventricle *Top right*. Failing myocardium is evidenced by an increase in end diastolic diameter, and a decrease in shortening. *Bottom right*. A decrease in the E/A peak ratio is indicative of diastolic dysfunction. *Hecker, unpublished data.*

Diastolic dysfunction is detected via Doppler echocardiography. By this method, one determines the velocity of blood entering the ventricle. Blood enters the ventricle in 2 waves, known as the early (E) and late (atrial; A) wave. In a normal healthy heart, blood enters the ventricle most rapidly during the E wave. However, when diastolic dysfunction occurs, the E wave is decreased resulting in a subsequent decrease in the E/A ratio. Thus, a decrease in E/A is indicative of diastolic function[46]. Heart failure may also result in a decreased ejection time (ET), and an increased isovolumetric relaxation contraction time (IVRT) and isovolumetric contraction time (IVCT)[46]. Myocardial performance index

(MPI) is defined as the ratio of these factors ((IVCT+IVRT)/ET), and an increase in MPI may denote dysfunction.

Ventricular catheterization is another method which is employed to assess cardiac dysfunction. By this method one determines the ventricular end systolic and end diastolic pressures, as well as the change in pressure over time (dp/dt max & dp/dt min). Either an increase in end diastolic pressure or a decrease in dp/dt min is indicative of diastolic dysfunction, and suggest an impaired ability of the ventricle to relax. A decrease in end systolic pressure or dp/dt max is indicative of systolic dysfunction. Thus, in addition to echocardiography, cardiac function may also be determined by ventricular catheterization.

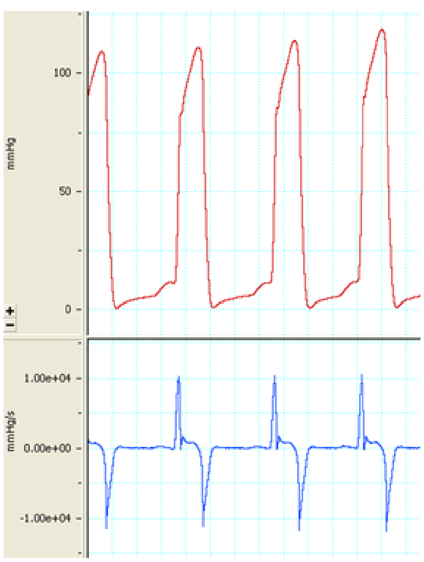

Figure 1.6. *Changes in murine ventricular pressure as determined by catheterization.*

Top panel. Top peaks represent the LV end systolic pressure. The humps at the base of the peak represent the LV end diastolic pressure.

Bottom panel. The top and bottom peaks represent the maximal changes in pressure over time (dp/dt max, and dp/dt min).

Hecker, unpublished data.

Heart failure patients commonly experience edema, or swelling due to a buildup of interstitial fluid[46, 50]. Edema may be found in the periphere, such as the ankles, the jugular vein, the abdomen (ascites), or in the lungs (congestion). Fluid buildup in the lungs is a hallmark of congestive heart failure (CHF)[51]. Edema occurs in heart failure as a result of increased venous pressure and fluid retention[52]. Edema is a common indicator of heart failure, however the presence of edema does not necessarily denote heart failure because a number of other factors such as liver cirrhosis or renal insufficiency may also contribute to edema[52]. Pulmonary edema may lead to difficulty breathing, and indicates a worsened prognosis and increased risk of mortality[50]. Thus, edema is indicated in the pathophysiology of heart failure, and its presence may help guide diagnosis.

Heart failure generally occurs in combination with an enlargement of the heart, or cardiac hypertrophy[53]. Left ventricular mass varies widely but the average mass of a healthy middle aged man or woman is estimated to be ~190g or ~140g respectively, and this may increase by 60-80% in heart failure[54-56]. Cardiac hypertrophy is divided into two types, concentric hypertrophy and eccentric hypertrophy (Figure 1.7)[57]. Concentric hypertrophy is characterized by thickening of the myocardial walls. This occurs as individual cardiomyocytes lay down an increased amount of sarcomeres in parallel. Concentric hypertrophy occurs in response to high blood pressure perhaps to decrease myocardial wall stress[58, 59]. Continued wall stress and volume overload may lead to eccentric hypertrophy, the second type of hypertrophy. Eccentric hypertrophy is characterized by expansion and dilation of the ventricle, without necessarily an increase in wall thickness, and occurs in response to cardiomyocyte stretch[58, 59]. Concentric and eccentric hypertrophy both denote a worsened prognosis, and lead to an increased risk of arrhythmia and sudden cardiac death[60-64].

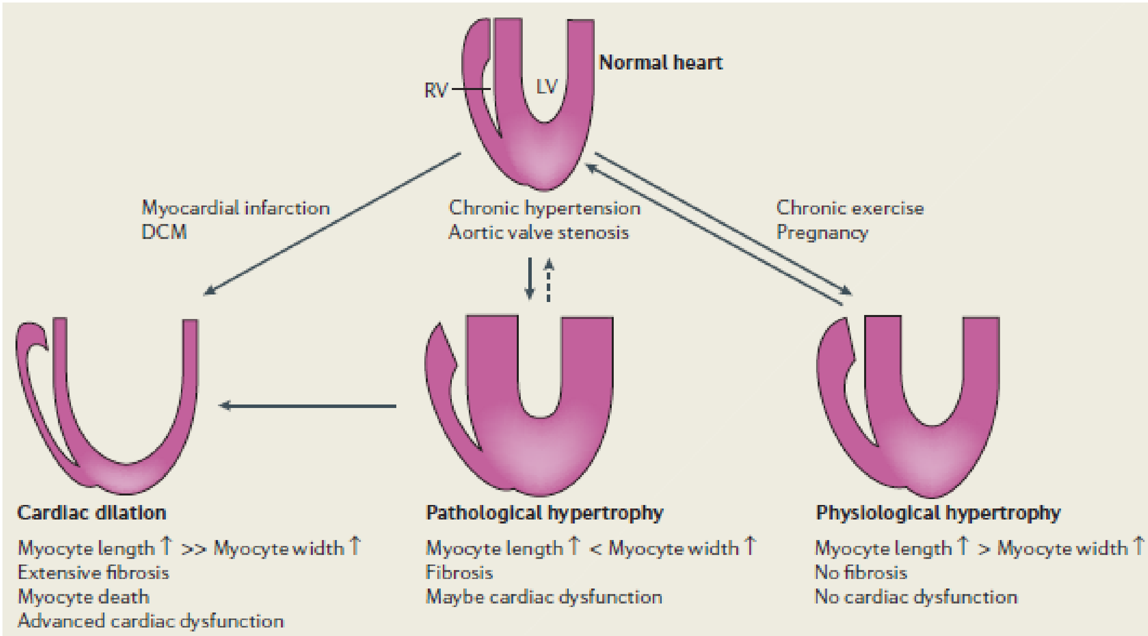

Figure 1.7. *Types of cardiac hypertrophy*. *Heineke 2006, Nat Rev Mol Cell Biol*.

The failing heart often reverts to a fetal program of gene expression. This includes changes in metabolic and contractile proteins[65-67]. In particular, expression of the contractile protein myosin heavy chain β (MHCβ) may be increased, and MHCα may be decreased. An increase in the ratio of MHCβ/MHCα is a commonly used indicator of hypertrophy and heart failure. Other genes that are upregulated in the failing heart include more compliant titin isoforms (N3BA1 and N2BA2)[65, 68], alpha skeletal actin[69, 70], atrial natriuretic peptide (ANP), and brain natriuretic peptide (BNP)[71, 72]. ANP and BNP are synthesized and secreted into the blood in increased amounts in response to stress or hypertrophy. Increased natriuretic peptide gene expression and circulating protein levels are commonly used as indicators of heart failure[72, 73]. Thus, these changes in gene expression can be used to assess heart failure.

Another common characteristic of heart failure is a decreased capacity for energy production and contractile reserve (Figure 1.8)[74, 75]. The human heart produces approximately 6 kg of ATP in order to pump 10 tons of blood per day[75]. To provide the required ATP, roughly one third of the heart volume is made up of mitochondria, the major energy-producing cellular organelles. Decreased mitochondrial function is evident in heart failure, and may result from a decrease in oxidative enzymes and respiratory-chain complexes[76]. The decrease in overall oxidative capacity corresponds with a decrease in mitochondrial enzyme activities, including aconitase, isocitrate dehydrogenase (ICDH), citrate synthase (CS), and medium chain acyl-coenzyme A dehydrogenase (MCAD)[77-79]. Thus, a decrease in oxidative enzyme capacity and mitochondrial function may be used in the assessment of heart failure[80-82].

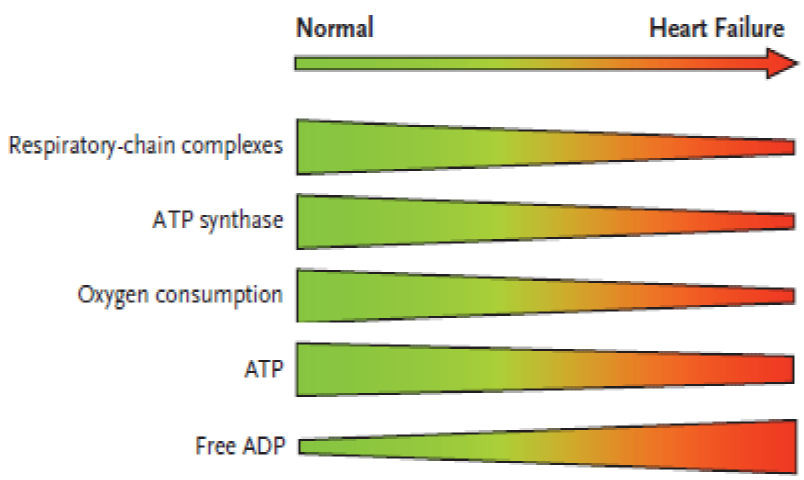

Figure 1.8. *Changes in myocardial energetics during the transition heart failure*. Respiratory enzymes and complexes are decreased, resulting in a decreased maximal capacity for fuel generation in the failing myocardium.

Modified from Neubauer 2007, NEJM.

We have discussed common indicators used to denote heart failure. These include but are not limited to cardiac hypertrophy, decreased functional parameters as assessed by echocardiography and ventricular catheterization, increased fetal gene expression, and decreased overall oxidative capacity. All of these parameters were used in the assessment of heart failure and function described in the experiments in chapters 2-4.

Management of Heart Failure

Standard pharmacological treatment for heart failure generally includes neurohormonal inhibitors that target components of adrenergic signaling and the renin-angiotensin-aldosterone system (RAAS)[46]. There is an additive benefit to the combined use of RAAS and adrenergic inhibitors[83]. Additional support is provided through the use of diuretics to alleviate fluid retention. The combination of a beta blocker, a RAAS inhibitor, and a diuretic is routine care for a heart failure patient. Depending on the circumstances, further care may include a variety of other treatments such as digoxin, vasodilators, antiarrhythmogenic drugs, exercise training, heart transplantation, or implantation of ventricular assist devices[46]. Here, we briefly discuss routine treatment, which includes the use of inhibitors of the RAAS, beta blockers, and diuretics.

Sympathetic stimulation and adrenergic signaling may be overactivated in patients with heart failure[84]. Increased sympathetic activity acutely increases cardiac contractility which may be beneficial in the short term, but any beneficial short term contractile effects are far outweighed by a number of adverse effects in the long term[46]. Adverse effects of chronically increased sympathetic activity include increased heart rate, blood pressure, myocyte apoptosis, cardiac hypertrophy, and risk of arrhythmia [84-87]. Beta blockers reduce these adverse effects by inhibiting beta adrenergic receptor signaling. These drugs have been shown to improve cardiac function and survival in heart failure patients, and are recommended as a mainstay for all patients with heart failure unless contraindicated[46, 88-91].

The RAAS is activated via the kidneys in response to a decrease in renal blood perfusion[92, 93]. In this cascade, the kidneys secrete renin into the bloodstream, which cleaves angiotensinogen to angiotensin I. Angiotensin I is then converted to angiotensin II by angiotensin converting enzyme (ACE). Angiotensin II activates vascular smooth muscle contraction via Gq-protein signaling and increases blood pressure[94]. Angiotensin II also increases salt and water retention, and stimulates the release of aldosterone from the adrenal cortex. Aldosterone further acts to increase water and sodium retention[95]. Thus, the RAAS stimulates increased blood pressure and fluid retention. This mechanism is adaptive in response to acute effects such as orthostatic hypotension or extensive bleeding. However, in the case of heart failure the RAAS may be constantly activated in response to chronically decreased renal perfusion[92, 93]. Specific drugs that target the RAAS include ACE inhibitors, angiotensin II receptor blockers (ARBs), and aldosterone antagonists. ACE inhibitors are recommended for standard treatment, but ARBs may be prescribed if the patient develops side-effects such as a dry cough in response to ACE inhibition[96]. Aldosterone antagonists are recommended in addition to ACE inhibitors for patients with moderate to severe heart failure where continued monitoring of blood electrolytes and renal function is available[46, 97]. Inhibitors of the RAAS decrease blood pressure and edema, and thus reduce the load against which the heart must pump in order to eject blood. These drugs also reduce cardiac hypertrophy and fibrosis by inhibiting the direct stimulatory effects of angiotensin II and aldosterone on the heart[94]. Inhibition of the RAAS through the use of ACE inhibitors or ARBs improves cardiac outcomes and survival, and is recommended in all patients with heart failure unless contraindicated[46, 98, 99].

In addition to neurohormonal inhibitors, diuretics are also included in heart failure therapy because of their effects on edema[46]. Edema occurs in patients with heart failure as a result of increased neurohormonal activation, fluid retention, and hydrostatic blood pressure[51, 52]. Loop diuretics act on the kidney to inhibit the sodium-potassium-chloride transporter, increase sodium and fluid excretion, and reduce swelling and edema[100]. Diuretics reduce symptoms of fluid retention rapidly, acting within hours to days after the initiation of treatment, whereas beta blockers and ACE inhibitors may require several months to manifest any observable benefit[46]. By decreasing fluid retention, diuretic treatment reduces blood volume, and decrease the load on the heart. Thus, treatment with diuretics may beneficially effect symptoms of heart failure including edema and reduced cardiac function[46].

Despite Available Treatments, Heart Failure is still a Major Concern

Despite the treatments mentioned above, heart failure is still a major clinical concern. Heart failure accounts for nearly 30 billion annual US dollars per year in the United States, and is the greatest contributor toward Medicare expenditure[46]. Heart failure is primarily responsible for over 57,000 deaths and 1 million hospitalizations in the United States each year[48]. After diagnosis, 1 in 5 heart failure patients die within a year, and 5 year mortality is ~50%. Thus, heart failure is a great burden, and more effective treatments are needed.

Models of Heart Failure

To gain more insight into the development and progression of heart failure, several animal models of chronic heart failure have been developed[101]. Two commonly used models are pressure overload induced by transverse aortic constriction (TAC), and myocardial infarction via ligation of the left anterior descending coronary artery (LAD). These two models are described below.

TAC entails a constriction of the aorta, which is the outflow tract of the left ventricle. This greatly increases the load placed on the heart. This model mimics the effects of exaggerated hypertension or aortic stenosis[61, 102, 103], and results in cardiac hypertrophy and systolic dysfunction over a course of weeks (Figure 1.9).

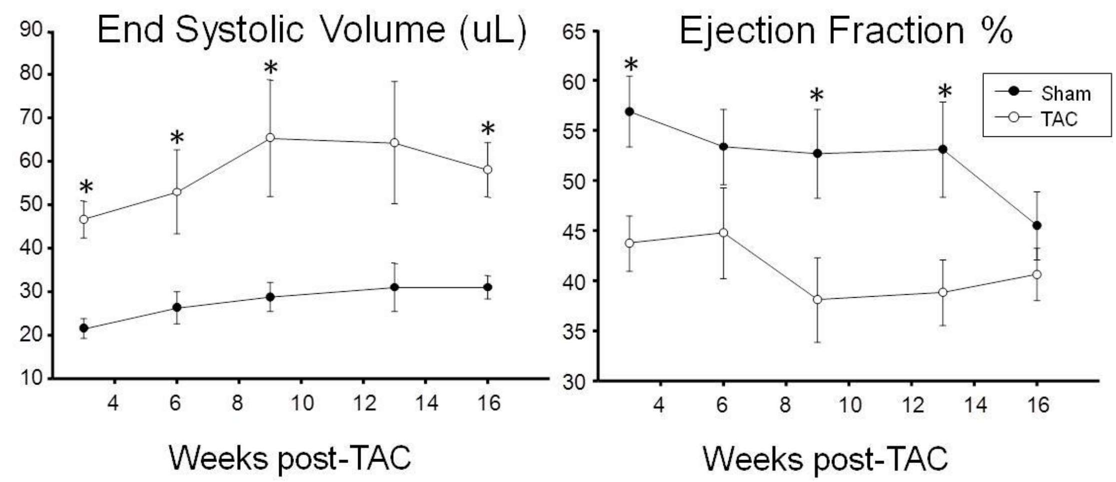

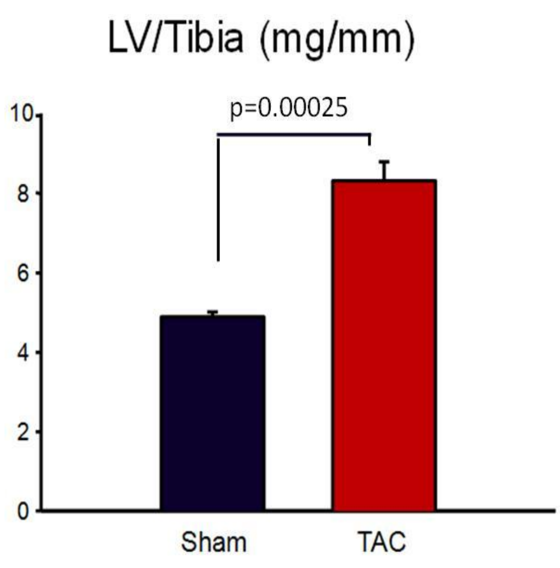

Figure 1.9. *Top Panel*. A typical response to TAC includes an increase in systolic volume and a decrease in ejection fraction, indicating LV chamber expansion and systolic failure. *Bottom Panel*. Measurement of LV mass reveals 70% hypertrophy 17 weeks after TAC; sham n=7; TAC n=9. Data are mean±SEM. Statistical comparison was made via 2 tailed t-test. P<0.05 was considered significant. Hecker, unpublished data.

The second animal heart failure model, myocardial infarction, is induced by complete occlusion of the LAD. The LAD is a major supplier of blood to the tissue of the heart, and occlusion of this vessel leads to ischemia and necrosis in the apical portion of the left ventricular wall. As a result of LAD ligation, an infarct is formed which consists mainly of collagen scar tissue, while the rest of the heart must compensate for the lack of healthy tissue. Over a course of weeks, this model results in ventricular dilation, and systolic and diastolic dysfunction.

Myocardial infarction and TAC result in increased oxidative stress, increased fetal gene expression, decreased oxidative capacity, and decreased contractile function. Both of these models have great utility for translational research, and have been used successfully in preclinical studies[101, 104-106]. We have employed both models in our studies to examine the effects of G6PD deficiency on heart failure in the experiments described in chapter 3.

Reactive Oxygen Species and Heart Failure

Increased ROS is indicated in heart failure. Particularly, patients with heart failure have increased myocardial superoxide and hydrogen peroxide production and a decreased antioxidant reserve[6, 107]. One source of ROS in the failing heart is NADPH oxidase, a phagocytic enzyme which produces superoxide using NADPH as a reducing agent[107, 108]. NADPH oxidase inhibition decreased superoxide and hydrogen peroxide production in myocardial lystates from patients with heart failure and from dogs with experimental heart failure[3, 6]. Further, the genetic deletion of NADPH oxidase subunits, p47phox or Nox4[109-111], attenuated the development of heart failure. Another enzyme which produces superoxide in heart failure is nitric oxide synthase (NOS) when it is uncoupled from its essential cofactor, BH4[112, 113]. Inhibition of this NOS in myocardial tissue from heart failure patients decreased NADPH dependant superoxide production[6], and treatment with BH4 in mice with pressure overload induced heart failure reversed cardiac superoxide production, hypertrophy, fibrosis, and dysfunction[114]. A third enzyme, xanthine oxidase is also known to produce NADPH dependant superoxide[115]. Pharmacological inhibition of xanthine oxidase by allopurinol increased cardiac efficiency in heart failure patients, and decreased oxidative stress and heart failure in a genetic model of cardiomyopathy[116, 117]. Finally, mitochondria produce superoxide during respiration, and antioxidants targeted to the mitochondria decreased ROS and cardiac dysfunction in a number of heart failure models[118, 119]. Thus, there is an increase in ROS in failing myocardium which may be a target for treatment.

Macronutrient Intake and Heart Failure

Introduction to Macronutrient Intake

Dietary intervention may be an independent way of preventing and controlling heart failure which is independent of pharmacological therapy[120]. Dietary intervention in heart failure patients is of great potential value because it is relatively inexpensive to undertake, and is unlikely to interfere with concurrent pharmacological therapy. Therefore, any benefit of dietary intervention would come as an added benefit to most medicinal treatments. Here we focus on the effects of macronutrient intake on metabolic and cardiac health. Macronutrients are the energy producing components of food and include carbohydrate, protein, and fat, as opposed to micronutrients which include vitamins and minerals. In particular, we examine the effects of high sugar intake and diet induced obesity (DIO).

Obesity

Obesity is a result of an imbalance between the intake of macronutrients and expenditure of energy. If more energy from macronutrients are consumed than expended for an extended period of time, then energy storage as fat, weight gain and eventual obesity will occur. Overweight and obesity are defined in terms of body mass index (BMI), which indicates relative weight based on height (BMI = [body mass (kg)] / [height $(m)^2$]). A BMI of 25 to < 30 is defined as overweight, and BMI 30 or above is defined as obese. According to these standards, approximately one third of Americans are overweight, and another third are obese[121]. Obesity often leads to a host of metabolic abnormalities such as hyperglycemia, insulin resistance, impaired glucose tolerance, dyslipidemia, and high blood pressure[122]. All of these factors precipitate in an increased risk of cardiovascular disease and heart failure (Figure 1.10)[123-127].

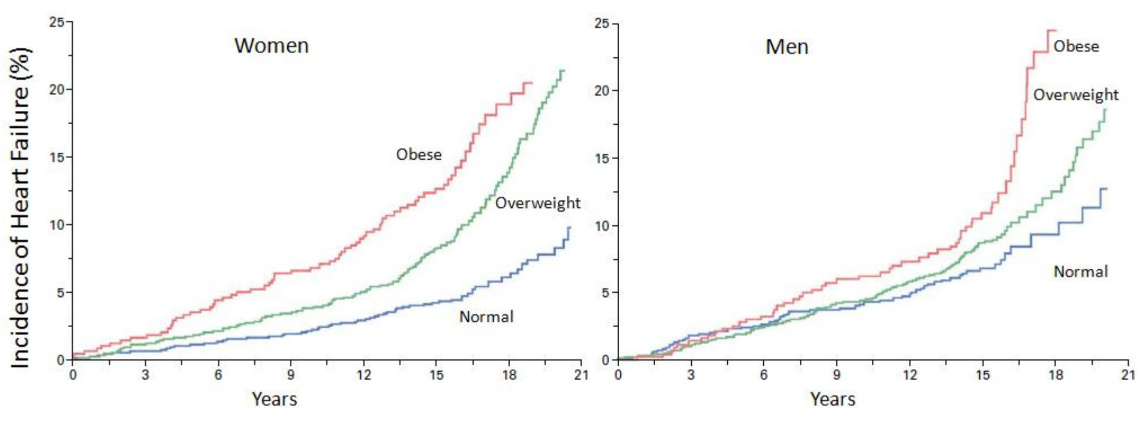

Figure 1.10. **Heart Failure Risk among the Obese and Overweight**. The incidence of heart failure was increased in obese and overweight groups among 5881 men and women. *Modified from Kenchaiah 2002, NEJM.*

Models of Obesity

Diet induced obesity (DIO) and leptin deficiency or leptin signaling deficiencies are the most commonly used animal models of obesity. Other genetically altered rodent models may also be used and include agouti overexpressing mice, New Zealand Obese mice, Tsumura Suzuki Obese Diabetes mice, Wistar fatty rats, and Otsuka Long Evans Tokushima Fatty rats[128]. We briefly describe DIO and leptin deficient models below because they have been used to study the effects of ROS and G6PD, and pertain to the work described in this dissertation.

DIO is employed using a high fat/high sugar diet in order to induce obesity. Mice in DIO groups typically eat the same mass of food as control-fed mice, but DIO mice become obese because the high fat/high sugar diet is more energy dense than most control diets. DIO results in decreased glucose tolerance, hyperinsulinemia, dyslipidemia, and insulin resistance, and other metabolic abnormalities similar to humans (Figure 1.11 A-B)[129]. However, these effects may depend on the duration of DIO, and on the species and strain used[128]. DIO has been used extensively by researchers to uncover the effects of obesity on cardiac and metabolic health.

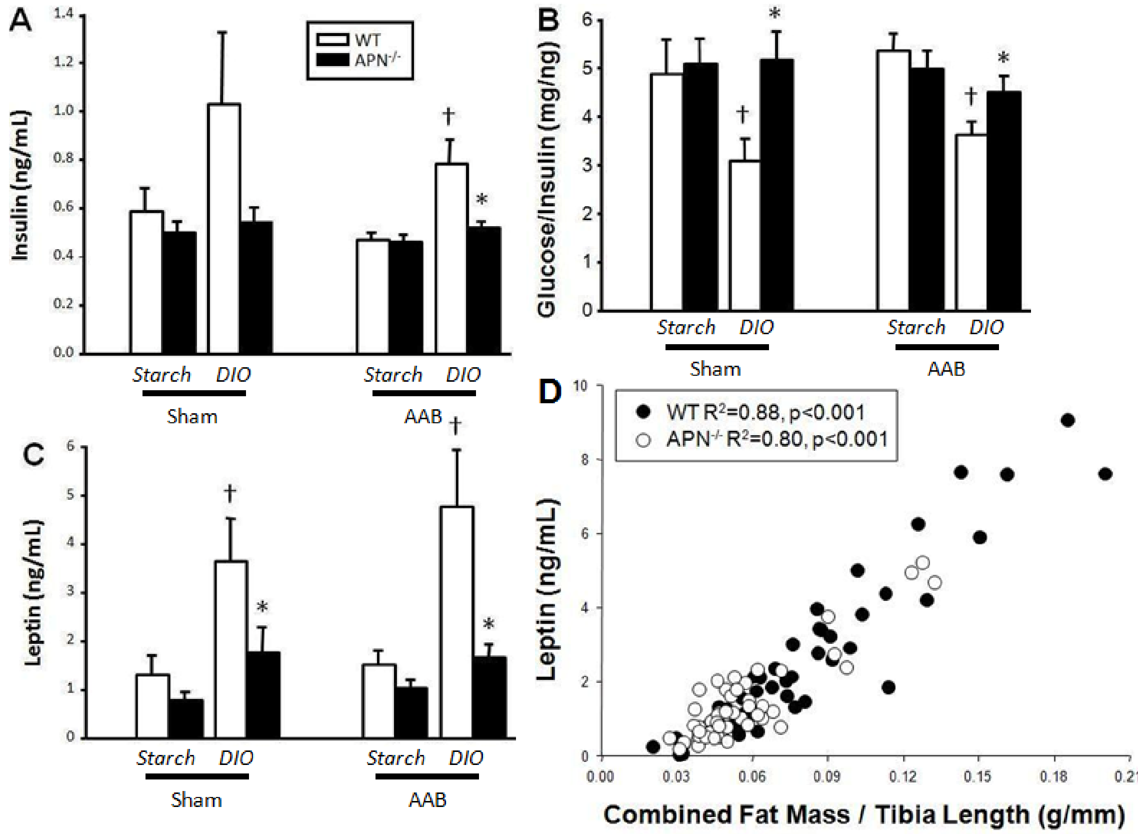

Figure 1.11. *Metabolic abnormalities in mice with Diet induced obesity (DIO). A.* Serum insulin was increased in WT mice, but not in adiponectin deficient (APN$^{-/-}$) mice, in response to DIO. *B.* DIO decreased the serum glucose/insulin ratio in WT mice, but not in APN$^{-/-}$ mice. *C.* DIO increased serum leptin in WT mice, but not in APN$^{-/-}$ mice. A similar pattern was observed with an increase in fat mass in WT mice, but not in APN$^{-/-}$ mice, in response to DIO (Data not shown). *D.* Serum leptin concentration increased linearly with combined fat mass in WT and APN$^{-/-}$ mice. WT (C57BL/6J) and APN$^{-/-}$ mice received abdominal aortic banding (AAB) or sham surgery, and were then placed on a control high starch diet or a high fat/high sugar diet to induce obesity (DIO) for 8 weeks. Data are mean ± SEM; Sham n=8-11/group, AAB n=13-19/group; *P <0.05 vs. WT; †P <0.05 vs. STD. *Hecker 2011, Horm. Metab. Res.*

Rodents with deficiencies in leptin signaling are also commonly used by researchers to study obesity. Leptin is a hormone which is secreted by adipocytes (fat cells) in proportion to adipose tissue mass (Figure 1.11 C-D). This hormone regulates hunger to decrease food intake by signaling in the hypothalamus. The leptin gene is mutated, and leptin is not present in ob/ob mice. Because of this, ob/ob mice consume more energy than they expend and obesity occurs. Metabolic syndrome, cardiac dysfunction, and mortality ensue as obesity progresses[130, 131]. Leptin deficient mice become grossly obese (~60 grams by 6 months of age for ob/ob mice vs. ~30 grams at 6 months for WT mice)[132]. Leptin receptor mutations also result in obesity, and rats and mice with these mutations (db/db mice and Zucker obese rats) are commonly used to study obesity.

Although animals with deficiencies in leptin signaling become grossly obese, results from these animals are difficult to interpret due to the confounding effects of leptin deficiency on metabolism. Leptin is a signaling molecule with other functions other than hunger regulation. Other actions of leptin include effects on adrenergic signaling and blood pressure, and these actions may have confounding effects on the cardiovascular system[133, 134]. Also, congenital leptin deficiency is extremely rare[135]. Therefore, animals with deficiencies in leptin signaling have limited relevance as a model of human obesity. Because of these issues, we have chosen to employ DIO for our studies in chapter 2.

Obesity and Heart Failure

Studies have shown that obesity adversely affects cardiac function and leads to the development of heart failure[127]. DIO in mice for 5 or 6 months increased heart mass, indicating cardiac hypertrophy in response to obesity[136, 137]. Leptin deficient ob/ob mice also develop cardiac hypertrophy and systolic impairment[130]. Not only does obesity lead to the development of cardiac dysfunction, but it accelerates the progression of heart failure. Obesity exacerbated cardiac hypertrophy and left ventricular chamber dilation in mice after myocardial infarction by LAD occlusion, and then 1 week of reperfusion[138]. Other experiments with ischemia-reperfusion injury or permanent LAD occlusion also showed that DIO increased lung congestion, LV hypertrophy, and heart failure, indicating that obesity accelerated heart failure in this heart failure model[136, 139]. Heart failure induced by pressure overload in response to TAC was also accelerated by obesity[140]. After TAC, LV dilation and fetal gene expression (increased MHCβ/MHCα) were increased by DIO in mice. In summary, obesity increases cardiac hypertrophy, adversely affects heart function, and exacerbates the development and progression of heart failure.

High Sugar Intake

The average American consumes roughly 90 grams of added sugars per day, representing 16% of energy intake[141]. However, the world health organization advises that sugar consumption be no more than 10% of total energy intake, and the American Heart Association recommends no more than 5%[142, 143]. High sugar intake may have adverse effects on the heart and metabolism[120]. In particular, a high sugar diet is associated with increased obesity and insulin resistance in humans[144, 145]. A high sugar diet may also result in the development dyslipidemia, including increased circulating triglycerides and LDL cholesterol, and decreased circulating HDL cholesterol[141]. These metabolic abnormalities are risk factors for cardiovascular disease[146, 147].

One aspect of sugar that can have profound effects on metabolism is its ability to be digested rapidly and quickly absorbed into the bloodstream. The rapid absorption of sugar results in transient increases in blood sugar and insulin which may negatively affect cardiometabolic health[146]. Glycemic index is a measure of how quickly a food is digested and enters the blood stream. A scale of 1 to 100 is used for glycemic index, with 100g of pure glucose being 100. Glycemic load is defined as total carbohydrate content of a food in grams multiplied by its glycemic index, and thus is an indicator of the quantity and the quality of carbohydrates consumed[148]. Clinical studies indicate that high dietary glycemic index or glycemic load result in increased risk of developing coronary heart disease (Figure 1.12)[120, 146, 148-150]. Thus, eating a diet high in sugar or other rapidly absorbed constituents results in greater cardiovascular disease risk.

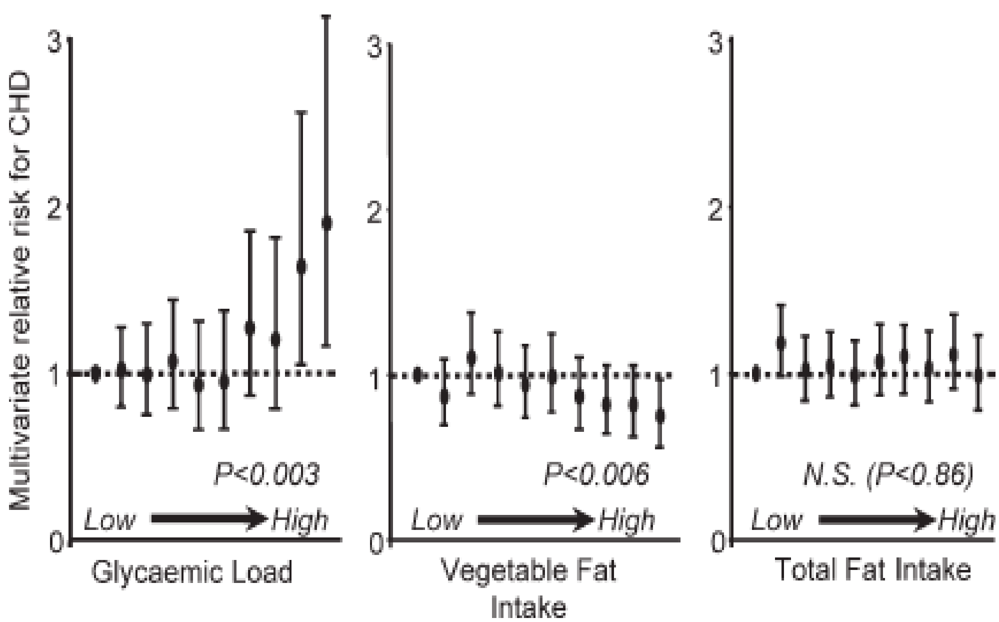

Figure 1.12. Multivariate risk analysis indicates an increased risk with high sugar intake, and no effect of total fat intake on the risk of developing coronary heart disease. *Chess 2007, Cardiovascular Research; Data from Halton 2006, N Engl J Med.*

Sugar and Heart Failure

Studies in our lab and others found that high sugar intake hastened the progression of heart failure in rats and mice compared to control complex carbohydrate (starch) diets. High sugar intake increased fetal gene expression, apoptosis, contractile dysfunction, and mortality in salt-sensitive hypertensive rats (Figure 1.13)[151, 152]. Mortality, cardiac hypertrophy, and fetal gene expression were similarly increased by high sugar intake in mice with pressure overload induced by TAC[153, 154]. And finally, in a volume overload model generated by an arterial-venous shunt, a high fructose diet exacerbated chamber dilation and systolic dysfunction in rats[155]. Thus, high sugar intake negatively affected heart failure in rodent models. Although a direct connection between high sugar intake and the development and progression of heart failure has yet to be demonstrated in humans, experiments in animals clearly indicate that high sugar intake can accelerate progression of heart failure[156].

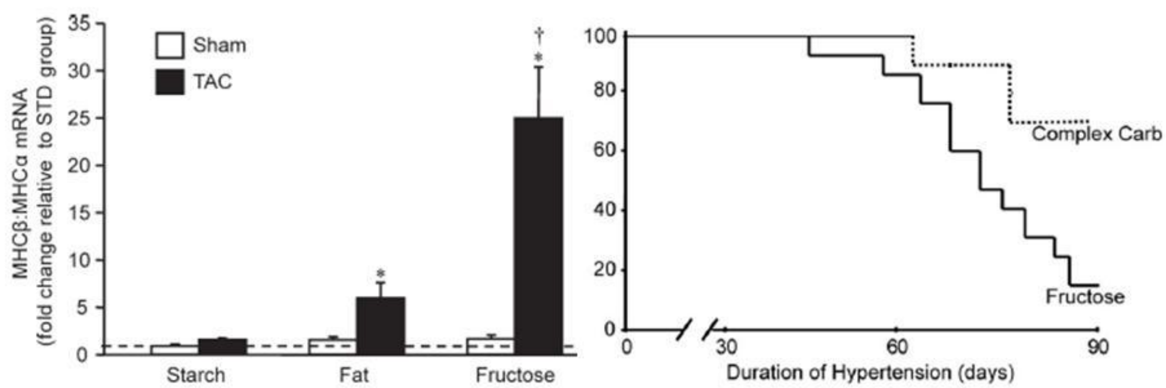

Figure 1.13. **High fructose intake exacerbates heart failure and accelerates mortality**. *Left Panel*. In mice with transverse aortic constriction (TAC), fetal gene expression was increased by a high fat which resulted in obesity (60% of total energy from fat) or by a high fructose diet (61% of total energy from fructose). *Right Panel*. Mortality was accelerated by a high fructose diet (52% of total energy from fructose) in hypertensive Dahl salt-sensitive rats. *Modified from Chess 2007, Cardiovascular Research.*

Macronutrient Intake and Reactive Oxygen Species

Increased ROS may be responsible for the adverse effects of high sugar on the heart. A high fructose diet increases superoxide formation in the heart and may result in cardiac dysfunction after long-term treatment[146, 157]. A study in our lab provided evidence for ROS as a mechanism of sugar toxicity to the heart when it showed that antioxidant treatment with a superoxide dismutase mimetic, tempol, prevents the acceleration of heart failure by high fructose intake[154]. In this study, tempol decreased cardiac lipid peroxidation products, hypertrophy, and dysfunction after TAC and with high fructose intake, thus indicating that decreasing ROS may prevent the accelerated development of heart failure by high sugar intake.

Obesity also increases the production of ROS in the heart. Increased superoxide production was seen in cardiac tissue from rats with DIO and obese Zucker rats[8, 158]. The increase in superoxide production corresponded with decreased antioxidant enzymes and GSH/GSSG, indicating an overall decrease in antioxidant capacity in the hearts of obese rats. Studies have also demonstrated increased ROS and decreased GSH/GSSG in cardiac tissue and cardiomyocytes isolated from ob/ob mice[131, 159, 160]. These results indicate increased cardiac oxidative stress in the heart in response to obesity.

Increased ROS generation via NADPH oxidase and uncoupled NOS may be a mechanism by which obesity adversely affects the development and progression of heart failure. Increased NADPH oxidase activity corresponded with increases in ROS production in the hearts of obese Zucker rats[8]. Pharmacological inhibition of NADPH oxidase by apocynin prevented obesity from exacerbating heart failure after myocardial infarction induced by permanent LAD occlusion[138]. Uncoupled NOS is also implicated in obesity, and genetic deletion of endothelial NOS decreased ROS, cardiac remodeling, cardiac dysfunction, and death after TAC in obese mice[161]. Thus, inhibition of NADPH oxidase and NOS resulted in decreased ROS production and prevented the exacerbation of heart failure by obesity. Therefore, oxidant production through these enzymes in the heart may be a pathological mechanism of obesity.

Effects of G6PD Deficiency

Overview of G6PD and Oxidative Stress

Increased flux of glucose through nonoxidative pathways may be responsible for increased ROS in the context of diabetes and obesity[162]. Heart failure increases the rate of glucose uptake and glycolysis[74, 75]. However, high sugar intake and obesity increase circulating lipids and thereby suppress glucose oxidation[74, 141]. This results in increased glucose flux through nonoxidative pathways. One such pathway is the pentose phosphate pathway (Figure 1.14)[3, 4, 6, 8], which is the main cytoplasmic source of NADPH[27]. The production of NADPH provides reducing equivalents for the production of superoxide as well as for the antioxidant glutathione system. NADPH is used by glutathione reductase to reduce GSSG to GSH which is used by glutathione peroxidase to reduce hydrogen peroxide to water. ROS such as hydrogen peroxide and superoxide react with and damage cellular lipids, nucleic acids, and proteins. Sources of ROS in the cardiovascular system include complex I and III within mitochondria[163] and NADPH dependent ROS-producing enzymes such as NADPH oxidase[107], xanthine oxidase[117], and uncoupled nitric oxide synthase[112]. The latter 3 enzymes produce superoxide by reducing oxygen with NADPH. Thus, while NADPH produced by the pentose phosphate pathway may be used by the antioxidant system to remove ROS via the glutathione antioxidant system, it is also be used by pro-oxidant pathways to produce ROS.

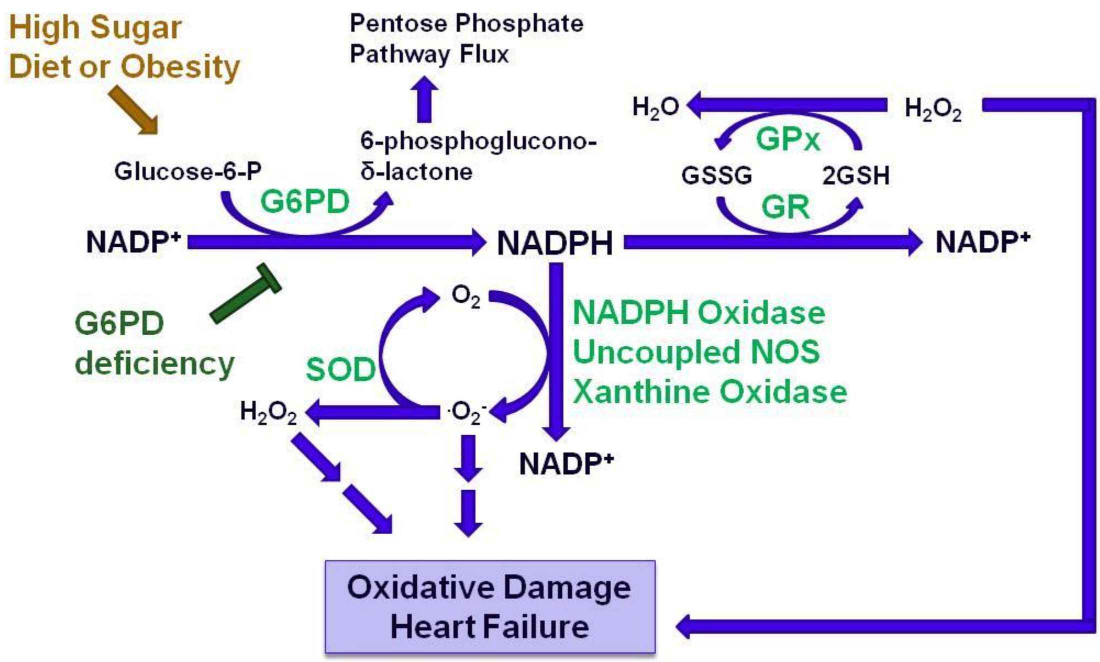

Figure 1.14. *NADPH and the formation and negation of reactive oxygen species*. High sugar intake or obesity may increase intracellular glucose 6-phosphate which can be used by G6PD to produce NADPH. NADPH may then be used either to remove ROS through the antioxidant glutathione pathway or to produce ROS through NADPH oxidase, uncoupled NOS, and xanthine oxidase. G6PD, glucose 6-phosphate dehydrogenase; GPx, glutathione peroxidase; GR, glutathione reductase; NOS, nitric oxide synthase; ROS, reactive oxygen species; SOD, superoxide dismutase.

G6PD and the Production of Reactive Oxygen Species

The NADPH produced by G6PD may be used to produce ROS. The oxidant enzymes, NADPH oxidase[107, 108], xanthine oxidase[115, 117], and uncoupled nitric oxide synthase[112, 113] are implicated in heart failure. It was reported that G6PD deficiency led to a decreased risk of heart disease risk and cardiovascular death in patients[164, 165], perhaps because G6PD deficiency reduced the substrate for NADPH-dependent oxidant enzymes[3]. G6PD expression and [NADPH] were increased in failing myocardium from dogs and humans, and in the myocardium of obese Zucker rats, and in these experiments the pharmacological inhibition of G6PD decreased [NADPH] and ROS production[3, 6]

(Figure 1.15). A similar decrease in [NADPH] and ROS was observed after G6PD inhibition in genetically obese rats[4, 8]. Thus, G6PD fuels ROS production by providing NADPH for oxidant enzymes in heart failure and obesity.

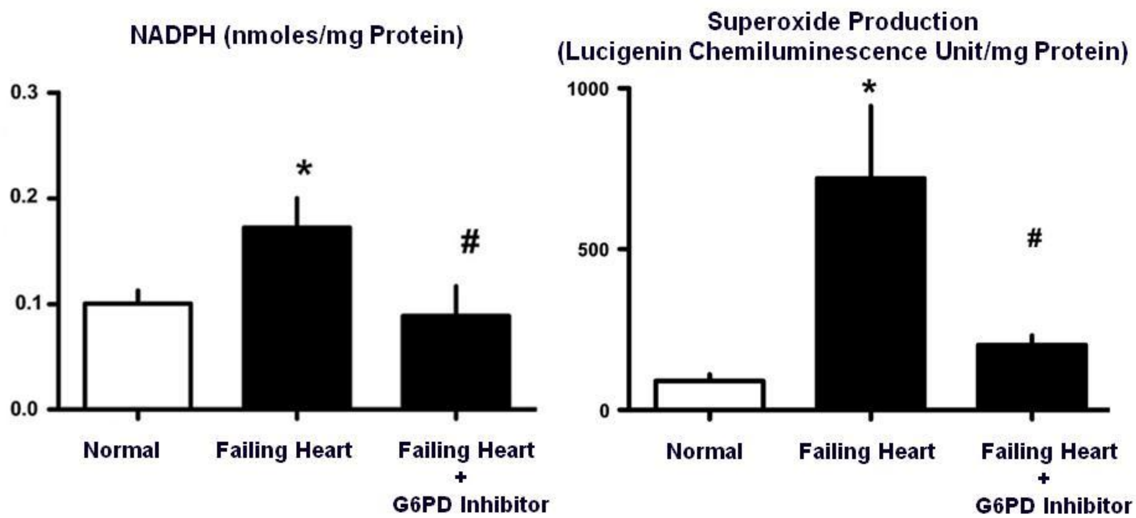

Figure 1.15. G6PD inhibition decreases [NADPH] and superoxide formation in failing myocardium from humans. *Modified from Gupte 2007, J. Card. Fail.*

Although pharmacological G6PD inhibition prevented ROS formation in samples of failing and obese myocardium in the experiments described above, it is important to determine whether decreased G6PD activity is beneficial in the living animal. Rajasekaran et al, demonstrated that G6PD deficiency may limit disease progression in desmin-related cardiomyopathy, a genetic disease resulting in heart failure[7]. Desmin-related cardiomyopathy in these experiments was induced by overexpressing mutant αB-crystallin (hR120GCryAB) in mice (CryAB mice). Cross-breeding CryAB mice with G6PDX mice rescued progeny from hR120GCryAB-associated protein aggregation and prevented cardiac hypertrophy, thus indicating that G6PD inhibition *per se* may be beneficial *in vivo* (Figure 1.16). However, cardiomyopathy in response to genetic alteration may be of limited clinical significance, and further studies in more relevant heart failure models are needed.

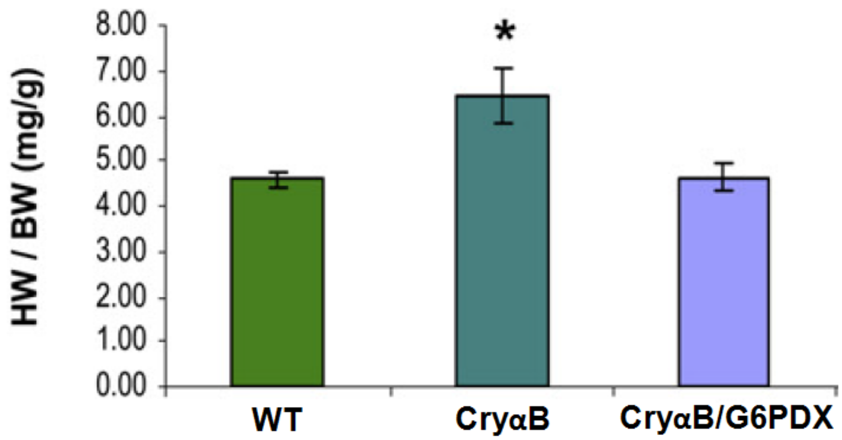

Figure 1.16. G6PD deficiency prevents cardiac hypertrophy in a genetic model of cardiomyopathy. *Modified from Rajasekaran 2007, Cell.*

G6PD may play a role in ROS production in other tissues besides the heart. G6PD expression is increased in various cell types in both heart failure and obesity, and this may allow increased flux through the pentose phosphate pathway and result in increased NADPH and ROS generation in these cell types[3, 4, 6, 8, 166]. Specifically, in cultured adipocytes and β-cells, G6PD overexpression increased ROS generation, exocrine dysfunction, and cell death, and this could lead to insulin resistance if it took place *in vivo*[166-168].

G6PD may play a role in the vascular response to dyslipidemia and hypertension. G6PD deficiency prevented vascular oxidative stress in response to angiotensin II infusion, and this led to a decreased rise in blood pressure[169]. It is important to see if G6PD deficiency decreases blood pressure in response to more physiologically relevant stimuli such as obesity. Similar experiments showed that G6PD deficiency decreased superoxide production and atherosclerotic lesions in apolipoprotein E null mice[170]. Thus, there is evidence for a deleterious role of G6PD in the cardiovascular system. However, the data are inconclusive and additional studies need to be performed in order to demonstrate the relevance of these experiments to human disease.

G6PD Deficiency and Antioxidant Capacity

In terms of the antioxidant utility, the NADPH supplied by G6PD can aid in defense against oxidative stress. Inhibiting G6PD makes cells more susceptible to ROS-induced cell death[9, 10]. G6PDX mice display β-cell apoptosis and glucose intolerance, presumably by a decreased resistance to ROS[13]. Studies in patients have suggested an increased risk of diabetes in G6PD deficient subjects[171-176]. Decreased levels of G6PD have been observed in diet induced obesity, and are thought to contribute to increased ROS in the liver[177, 178]. G6PD deficient mice also have increased oxidative stress in the kidneys which results in kidney failure and albuminuria[11, 179]. These mice also develop mild hypertrophic cardiomyopathy as they age, and cardiac cells deficient for G6PD have decreased contractility[27]. Finally, after acute ischemia-reperfusion injury, isolated perfused hearts from G6PDX mice display a greater impairment in relaxation and contraction compared to WT mice[180]. These impairments in relaxation and pressure development were rescued by antioxidants, but were not rescued by ribose supplementation, demonstrating that the deficit was due to a deficiency in antioxidant defenses rather than a ribose deficiency. Thus, G6PD deficiency makes cells more sensitive to ROS, and may adversely impact cardiometabolic health.

G6PD Deficiency, Macronutrient Intake, and Heart Failure

Cell culture studies have shown an increase in ROS generation via NADPH oxidase in response to increased glucose, and this increase in ROS was prevented by inhibition of G6PD[181]. However, it remains to be determined whether G6PD deficiency will decrease oxidative stress *in vivo*, and whether G6PD deficiency is beneficial or deleterious in the heart in the presence of high sugar intake and obesity. Because NADPH production via G6PD activity is required for maximal antioxidant capacity, G6PD deficiency could be derogatory in response to cardiometabolic stress. On the other hand, if ROS are produced in a limited measure due to a decrease in NADPH production, then antioxidant systems may still function without maximal G6PD activity. Thus on one hand G6PD deficiency may result in a decreased production of ROS with beneficial cardiometabolic effects, while on the other hand G6PD deficiency may allow the antioxidant systems to become overwhelmed and worsen cardiometabolic defects in response to high sugar intake and obesity.

Based on the evidence that G6PD fuels superoxide production by supplying NADPH for superoxide-producing enzymes in heart failure and obesity[3, 4, 6, 8, 182], we hypothesized that in the face of cardiometabolic stress induced by high sugar intake, obesity, G6PD deficiency would be protective against cardiac and metabolic dysfunction. To address this hypothesis, we performed studies in G6PDX mice with high sugar intake, DIO, and heart failure. Overall, we found that contrary to our hypothesis G6PD deficiency mildly worsened metabolic abnormalities and heart failure in the context of obesity and a high sugar diet.

Project Aims

Rationale Leading to Aims

Heart failure results in a switch from predominantly fatty acid utilization toward increased glucose utilization[75]. However, high fructose intake and obesity increase circulating lipids which further increase intracellular glucose but inhibit glycolysis and glucose oxidation[74, 141]. This increased glucose may then proceed through nonoxidative pathways which have adverse effects on the heart[146, 157, 162, 183]. One such nonoxidative pathway is through the pentose phosphate pathway which is controlled by the activity of G6PD. G6PD deficiency affects over 400 million people worldwide[15], and there is limited evidence suggesting that these patients have a decreased risk of heart disease[165] and cardiovascular death[164] despite having an increased risk for diabetes[171-176]. G6PD is the rate-determining enzyme of the pentose phosphate pathway, and its activity determines cytoplasmic [NADPH][27]. Although NADPH may be used by glutathione reductase to reduce glutathione (GSSG to GSH) and thereby facilitate the removal of H_2O_2, NADPH is also used by NADPH oxidase[107, 108], xanthine oxidase[115, 117], and uncoupled nitric oxide synthase[112, 113] to produce superoxide which can stress the heart. G6PD, [NADPH], and ROS production were increased in liver and cardiac tissue from genetically obese Zucker rats and in failing myocardium from dogs and human patients[3, 4, 6, 8]. In these studies, pharmacological G6PD inhibition in tissue samples decreased ROS production, indicating that increased flux through G6PD may increase intracellular NADPH and promote the formation of ROS[3, 4, 6, 8]. Recent studies in our lab and others have indicated an increased severity of heart failure in mice and rats that were obese or received a high sugar diet, and that these effects were alleviated by antioxidant treatment[120, 138, 151, 152, 154].

Statement of Hypothesis

Given that both obesity and fructose intake may mediate damage of the heart through ROS formation, we hypothesized that increased flux through G6PD mediates this increase in ROS formation and thus mediates the adverse effects of high fructose and obesity on the heart.

Aim 1. Determine the role of G6PD in mediating the adverse metabolic and cardiac effects of diet induced obesity and high fructose intake.

G6PDX and WT mice were subjected to both short and long-term dietary treatment of a control high starch diet, a high fructose diet, or to a diet high in both fat and sugar to induce obesity. Based on our hypothesis, we anticipated that G6PD deficiency would protect the heart against the adverse effects of diet induced obesity and high fructose intake. These experiments are reported in chapter 2.

Aim 2. Determine the role of G6PD in mediating the adverse effects of high fructose on the outcome of high pressure-induced heart failure.

G6PDX and WT mice received high fructose or high starch diets, and heart failure was induced by transverse aortic constriction (TAC). Based on our hypothesis, we anticipated that G6PD deficiency would protect the heart against pressure overload-induced heart failure, particularly in animals fed a high fructose diet. These experiments are reported in chapter 3.

Aim 3. Determine whether G6PD, [NADPH], and ROS production are increased by high sugar intake in a genetic model of cardiomyopathy.

Cardiomyopathic TO-2 hamsters received either a long-term high sugar diet or a control high starch diet, and were compared to healthy F1B hamsters that received a high starch diet. Based on our hypothesis, we anticipated that high sugar intake would increase G6PD, [NADPH], and ROS generation, and that this would lead to decreased cardiac function and survival in this genetic model of cardiomyopathy. These experiments are reported in chapter 4.

Chapter 2 – Glucose 6-Phosphate Dehydrogenase Deficiency Decreases Weight Gain, But Does Not Prevent Metabolic Dysfunction in Diet Induced Obesity

Chapter Abstract

Glucose 6-phosphate dehydrogenase (G6PD) deficiency, the most common enzyme deficiency, may influence the development of cardiometabolic syndrome by affecting cellular redox status. G6PD generates cytoplasmic NADPH, which replenishes the antioxidant system, but also may increase NADPH-dependant oxidant production. We hypothesized that G6PD deficiency worsens diet induced metabolic dysfunction by increasing oxidative stress throughout the body, but prevents diet induced oxidative stress and dysfunction in the heart. G6PD deficient (G6PDX) and WT mice received a standard high starch diet, a high fructose diet, or a high fat/high sucrose diet to induce obesity (DIO), and tissue was analyzed after 12 and 31 weeks of treatment. DIO increased fat and total body mass, but to a lesser extent in G6PDX than WT mice. G6PD deficiency increased sensitivity diet induced metabolic abnormalities such as increased free fatty acids and triglycerides, and DIO decreased glucose tolerance to a similar extent in WT and G6PDX mice. Modest cardiac hypertrophy and dilation were evident in young G6PDX mice, but not in older mice. Likewise, DIO increased cardiac hypertrophy in WT mice, but did not exacerbate left ventricular dilation or hypertrophy in G6PDX mice. These results reveal a complex interplay between diet induced cardiometabolic effects and G6PD deficiency, in which G6PD deficiency decreased obesity without decreasing metabolic dysfunction.

Introduction

Diabetes and obesity are highly prevalent. Roughly one third of Americans are obese, and another third are overweight[126]. Obesity may result in metabolic dysfunction and other abnormalities such as increased serum glucose, triglycerides, and free fatty acids, and abnormal insulin secretion. These metabolic abnormalities increase the risk of cardiovascular problems, including coronary heart disease and heart failure.

Altered flux of glucose through non-oxidative pathways may mediate the adverse effects of diabetes and obesity[162]. Non-oxidative glucose pathways include the formation of advanced glycation end-products (AGEs), the polyol pathway, the hexosamine biosynthetic pathway (HBP), and the pentose phosphate pathway (PPP). It has been suggested that in obesity, flux through these pathways is increased by oxidative stress[184-186]. G6PD is the rate-determining enzyme of the PPP, and the main cytoplasmic source of NADPH[27, 29]. It is unclear how these pathways interact, and what impact G6PD deficiency has on the activation of these other pathways.

Cardiovascular problems associated with metabolic dysfunction are highly prevalent in African Americans[48]. Glucose 6-phosphate dehydrogenase (G6PD) deficiency, the most common enzyme deficiency in the world, is particularly common among individuals of African descent[2]. Severely deficient patients commonly have <10% residual G6PD activity, with less severe forms (20-60% residual activity) being more common and clinically undetected[2, 187].

The effects of G6PD deficiency on the interaction between metabolic dysfunction and the heart are unclear. Clinical studies suggest that G6PD deficiency may reduce the risk of heart disease[164, 165]. The risk of developing heart disease is highly linked with the development of metabolic dysfunction and diabetes. However, despite playing a possible cardioprotective role, G6PD deficiency has been suggested to increase the risk of diabetes, and studies in G6PD deficient (G6PDX) mice with ~20% residual activity found that G6PD deficiency may increase β-cell apoptosis and result in insulin resistance[13, 176]. Thus, there may be an unexplored interaction in which G6PD deficiency negatively affects metabolic derangements while protecting against heart disease.

By producing NADPH, G6PD helps provide reducing equivalents for the antioxidant system[31]. In cultured cells, G6PD deficiency decreases antioxidant capacity and increases cell death in response to oxidant challenge[9, 10, 27]. G6PD deficiency increased pancreatic β-cell death and associated metabolic dysfunction in aging mice[13]. G6PD deficiency also increased susceptibility for ischemia/reperfusion injury, and led to moderate cardiac dysfunction in older mice[27, 180]. Thus, G6PD deficiency may decrease resistance to oxidant stress and adverse cardiometabolic effects.

On the other hand, G6PD provides reducing equivalents required for the generation of reactive oxygen species (ROS)[3, 4, 6, 8]. Specifically, G6PD supplies NADPH for superoxide production through generation of by NADPH oxidase[108, 169, 170, 188], uncoupled nitric oxide synthase[114, 189], and xanthine oxidase[117]. Thus, G6PD deficiency can result in decreased ROS generation. Recent investigations reported that G6PD activity and [NADPH] were increased in the liver and myocardium of genetically obese rats, and that increased superoxide generation in obesity was decreased by inhibiting G6PD in vitro[4, 8, 190]. Similar findings were seen in myocardium from humans and dogs with heart failure[3, 6]. Thus, in contrast to the antioxidant effects of G6PD activity, excessive flux through G6PD may promote the formation of NADPH dependent ROS.

Evidence suggests that high sugar intake and obesity increase oxidative stress in the myocardium, and that blocking these oxidant effects may have beneficial cardiovascular effects[13, 146, 157, 179, 191]. Specifically, decreasing ROS prevented the exacerbation of heart failure by obesity or high sugar intake[138, 154, 192]. In cultured adipocytes, high glucose increased ROS that was decreased by G6PD knockdown[193]. G6PDX mice may have a decreased antioxidant defense capacity[194]. However, because a decrease in G6PD activity may decrease diet-induced ROS formation, G6PD deficiency may decrease overall ROS and beneficially affect the cell in certain circumstances.

The purpose of the present investigation was to determine the effects of G6PD deficiency on diet induced cardiometabolic defects, oxidant stress, and other non-oxidative glucose pathways. We hypothesized that G6PD deficiency would exacerbate diet induced metabolic dysfunction, while on the other hand preventing the adverse effects of high fructose intake and obesity in the myocardium. To test this hypothesis, we subjected wild type (WT) and G6PDX mice to dietary stress via high fructose intake and diet-induced obesity (DIO) until they were 31 weeks of age. We predicted that DIO and high fructose intake would decrease cardiac and metabolic function in WT mice. We predicted further that G6PD deficiency would exacerbate diet induced metabolic dysfunction, but that G6PD deficiency would prevent diet induced cardiac dysfunction despite increased metabolic dysfunction. Finally, we predicted that by altering the flux of glucose through G6PD, G6PD deficiency would affect the activation of other non-oxidative glucose pathways.

Experimental Design

Sixty female G6PDX and 60 female WT littermate control mice were weaned at 3 weeks of age and subsequently placed on a high starch diet (Starch), a high fructose diet (Fructose), or a high fat/high sucrose diet intended to induce obesity (DIO) (n=20/group) (Table 2.1). Dietary energy intake was determined by measuring the amount of food which was fed to the mice throughout the study, subtracting the weight of the uneaten food at the end of the study, and dividing the amount of eaten food by the (number of mice * days). Blood pressure was assessed by tail cuff plethysmography at 11 and 23 weeks of age, heart function was assessed by echocardiography at 12 and 24 weeks, and metabolic function was assessed by intraperitoneal glucose tolerance test at 28 weeks. A subset of mice (n=10/group) were euthanized at 12 weeks of age, and the remaining mice were euthanized at 31±0.2 weeks (28-33 weeks) of age for biochemical analysis.

Table 2.1.

	Fat		Carbohydrate				Protein
Diet	Soy Oil	Lard	Cornstarch	Maltodextrin	Fructose	Sucrose	Casein
Starch	6	4	57	12	0	1	20
Fructose	6	4	9	0	60	1	20
DIO	6	39	7	10	0	17	20

Values are energy contribution to the diet (% of total). Diets were matched for vitamin and mineral content. DIO, diet induced obesity.

Values are shown as mean ± standard error (SE). Survival was assessed by Log-Rank Kaplan Meier analysis. Comparisons between strain and diet grouping were made using a two-way ANOVA with the Holm-Sidak correction. $P<0.05$ was considered significant.

Results

G6PD Deficiency Decreases Obesity

Compared to WT mice, G6PD activity was decreased in G6PDX mice in all tissues in which we assayed its activity (Figure 2.1). Of interest, high fructose intake increased G6PD activity in the heart and liver (Figure 2.1A-2.1C), while DIO decreased G6PD activity in the liver and skeletal muscle (Figure 2.1A, 2.1B, and 2.1F). Such dietary effects on G6PD activity have been well characterized[195-200]. Energy intake was greater with the high fructose diet than the starch diet, and was the greatest in animals fed the high fat/high sugar diet (Table 2.2). G6PD deficiency had no effect on energy intake. Over the course of the study, there were no differences in survival among groups (Figure 2.2).

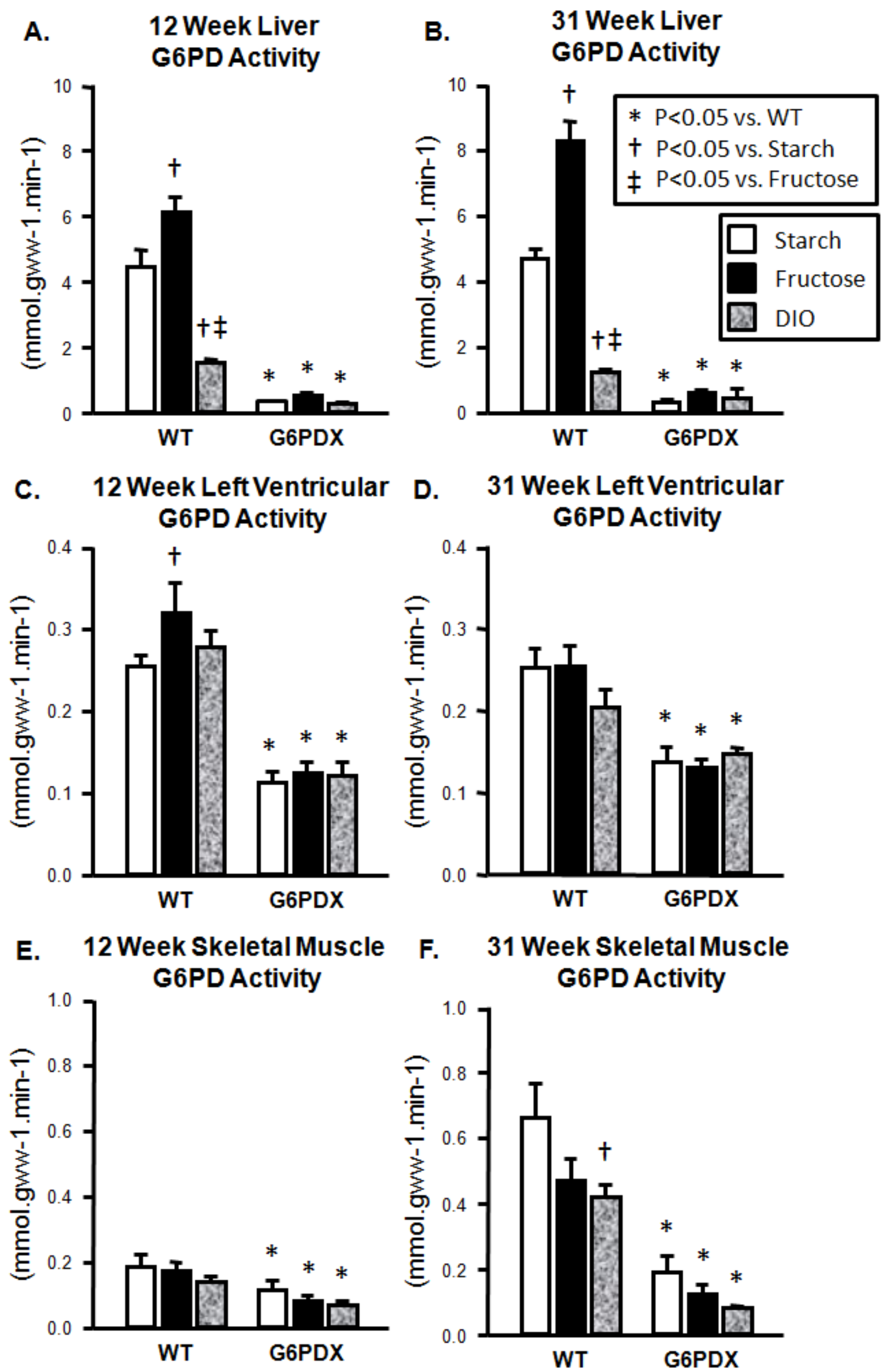

Figure 2.1. *G6PD Activity*. **A-B**. Liver G6PD activity. **C-D**. Left ventricular G6PD activity **E-F**. Hind-limb skeletal muscle G6PD Activity. Data were obtained using tissue from mice at 12 and 31 weeks. DIO, Diet Induced Obesity; G6PDX, glucose 6-phosphate dehydrogenase deficient mice; WT, wild type; n=7-10/group.

Table 2.2.

Parameter	Wild Type Starch	Wild Type Fructose	Wild Type DIO	G6PD Deficient Starch	G6PD Deficient Fructose	G6PD Deficient DIO
Duration of the Study						
Energy Intake (Calories mouse^{-1} day^{-1})	*8.33±0.43*	*9.71±0.40†*	*10.89±0.29†‡*	*8.22±0.29*	*9.31±0.28†*	*10.44±0.26†‡*
12 weeks						
Tibia Length (mm)	*19.1±0.2*	*19.5±0.3*	*19.6±0.2*	*19.6±0.2*	*19.6±0.2*	*19.8±0.2*
Kidney Mass (mg)	*135±5*	*147±3*	*162±4†‡*	*134±3*	*154±3†*	*160±7†*
Liver Mass (g)	*1.05±0.03*	*1.28±0.11†*	*1.15±0.03*	*1.07±0.04*	*1.38±0.05†*	*1.08±0.04‡*
Liver Glycogen (mg/gww)	*47.8±4.2*	*47.3±8.8*	*36.8±3.8*	*49.6±4.3*	*49.0±6.3*	*27.7±2.8†‡*
Liver Triglycerides (mg/gww)	*9.17±0.76*	*7.53±0.68*	*10.1±0.76*	*7.76±0.65*	*6.88±0.48*	*12.14±1.06†‡*
31 weeks						
Tibia Length (mm)	*19.8±0.1*	*20.1±0.1*	*19.6±0.1*	*19.4±0.3*	*19.5±0.2**	*18.8±0.4**
Kidney Mass (mg)	*162±4*	*177±4*	*169±4*	*155±7*	*163±5*	*153±8*
Liver Mass (g)	*1.42±0.06*	*1.81±0.04†*	*1.51±0.05‡*	*1.24±0.06**	*1.80±0.08†*	*1.18±0.03†‡*
Liver Glycogen (mg/gww)	*56.4±2.2*	*51.7±4.9*	*38.2±2.9†‡*	*53.5±4.7*	*53.4±5.0*	*38.0±3.5†‡*
Liver Triglycerides (mg/gww)	*12.0±1.3*	*11.0±1.8*	*19.9±1.3†‡*	*8.10±1.05*	*10.8±1.1*	*15.0±2.1*†*

Values are means ± SE; *P <0.05 vs. WT; †P <0.05 vs. Starch; ‡P<0.05 vs Fructose; n=4 cages/group for energy intake; for all other parameters n=10/group at 12 weeks, n=7-10/group at 31 weeks of age. DIO, Diet Induced Obesity; gww, grams of wet tissue weight.

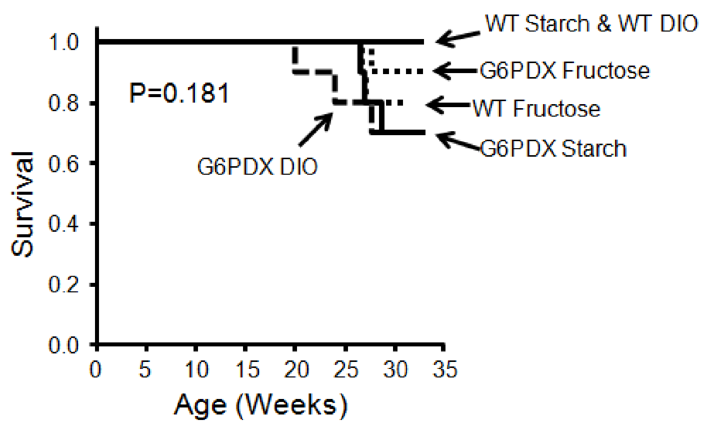

Figure 2.2. *Survival*. There was no statistically significant difference in overall survival throughout the study (p=0.181). Survival was assessed by Log-Rank Kaplan Meier analysis; n=20/group until 12 weeks and n=10/group thereafter. DIO, Diet Induced Obesity; G6PDX, glucose 6-phosphate dehydrogenase deficient mice; WT, wild type.

There were no differences in initial body mass at 3 weeks when mice were weaned and placed into dietary groups (body mass=11.1±0.3g for all groups). Until 16 weeks, both WT and G6PDX mice experienced greater weight gain in response to DIO compared to the high starch or high fructose diets (Figure 2.3A). However, after 16 weeks, G6PDX mice ceased increasing their body mass in response to DIO (Figure 2.3B and 2.3C). DIO increased fat pad mass in WT and G6PDX mice, but to a lesser extent in G6PDX mice at 31 weeks (Figure 2.3D and 2.3E). These results indicate that despite similar energy intake between G6PDX and WT mice, G6PD deficiency decreased obesity in response to a high fat/high sugar diet.

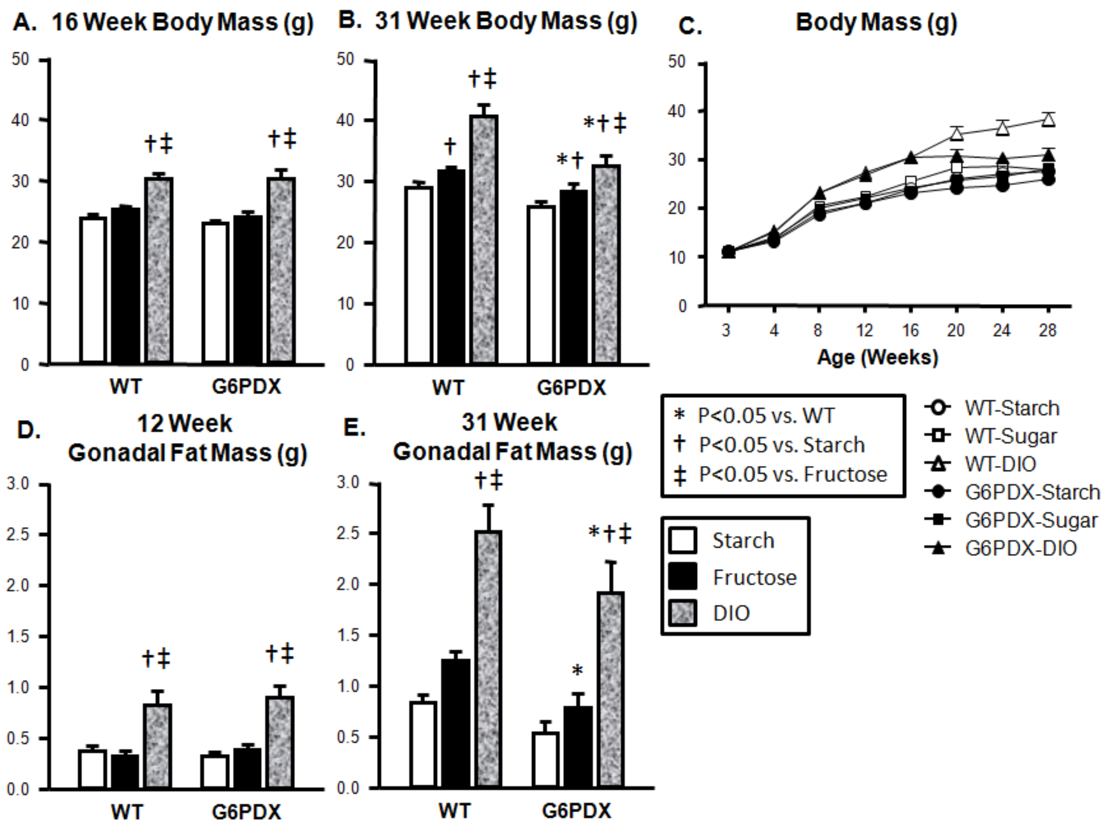

Figure 2.3. *G6PD deficiency results in decreased obesity*. **A**. DIO increased 16 week body mass to the same extent in G6PDX and WT mice. **B**. DIO increased terminal 31 week body mass to a lesser extent in G6PDX mice compared to WT mice. **C**. Body mass data indicate that there was an increase in body mass over the course of the study, with a greater increase in body mass in response to the high fat/high sugar diet (DIO). Further, the data indicate that in G6PDX mice there was a cessation in the increase in body mass around 16 weeks. **D**. DIO increased gonadal fat mass the same extent in G6PDX and WT mice at 12 weeks. **E**. DIO increased gonadal fat mass to a lesser extent in G6PDX mice compared to WT mice at 31 weeks. DIO, Diet Induced Obesity; G6PDX, glucose 6-phosphate dehydrogenase deficient mice; WT, wild type; n=7-10/group.

Effect of G6PD Deficiency on Diet Induced Metabolic Dysfunction

Normally, decreasing obesity results in fewer metabolic abnormalities, and greater metabolic function[201]. Thus, we determined whether metabolic parameters were affected by the decrease in obesity in response to G6PD deficiency. Increase serum triglycerides and free fatty acids may indicate of state of metabolic syndrome and increased fat mobilization. DIO increased serum free fatty acids, and high fructose intake increased serum triglycerides in G6PDX mice (Figure 2.4A and 2.4B). Leptin secretion is increased in obesity, and corresponds to increased fat mass[201]. We observed an increase in leptin in WT and G6PDX mice, but to a lesser extent in G6PDX mice, corresponding to the extent of fat pad mass increase in response to DIO (Figure 2.4C; Table 2.3). Increased insulin secretion is indicative of a pre-diabetic state[202]. DIO increased serum insulin in WT mice; however G6PDX mice failed to increase serum insulin in response to DIO (Figure 2.4D). Decreased insulin, and may be due to β-cell apoptosis and dysfunction in G6PDX mice, as reported by Zhang, et al[13]. Metabolic dysfunction can lead to renal failure, and G6PD deficiency is associated with increased serum creatinine and albuminuria[11, 179, 203]. In our study, DIO resulted in increased serum creatinine in G6PDX mice (Table 2.3). Thus, G6PD deficiency resulted in adverse diet induced metabolic effects.

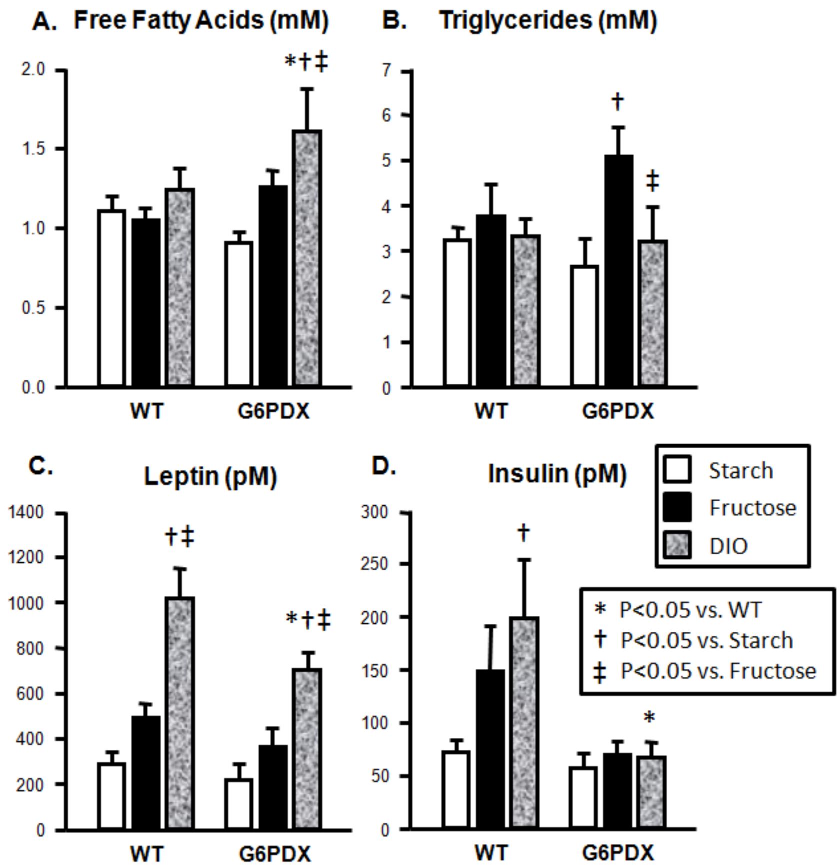

Figure 2.4. *Serum Metabolic Parameters*. **A**. DIO increased free fatty acids in G6PDX mice, but not in WT mice. **B**. High fructose intake increased triglycerides in G6PDX mice. **C**. DIO increased leptin in G6PDX and WT mice, but to a lesser extent in G6PDX mice. **D**. DIO increased insulin in WT mice, but failed to increase insulin in G6PDX mice. Data were obtained using blood serum from mice at 31 weeks. DIO, Diet Induced Obesity; G6PDX, glucose 6-phosphate dehydrogenase deficient mice; WT, wild type; n=6-10/group.

Table 2.3.

Parameter	Wild Type Starch	Fructose	DIO	G6PD Deficient Starch	Fructose	DIO
12 weeks						
Glucose (mM)	*12.8±0.5*	*13.9±0.7*	*13.2±0.4*	*14.0±1.9*	*14.3±0.4*	*13.0±0.5*
Triglycerides (mM)	*1.91±0.31*	*1.53±0.27*	*2.23±0.34*	*1.95±0.31*	*2.02±0.20*	*1.78±0.17*
Free Fatty Acids (mM)	*1.30±0.12*	*1.18±0.09*	*1.53±0.17*	*1.22±0.12*	*1.11±0.11*	*1.50±0.16*
Insulin (pM)	*33.4±3.2*	*41.5±8.5*	*48.2±13.7*	*33.7±3.4*	*36.2±4.9*	*35.1±3.8*
Leptin (pM)	*115±22*	*165±57*	*567±70†‡*	*121±20*	*176±20*	*526±87†‡*
Adiponectin (mg/mL)	*10.0±1.0*	*8.2±1.7*	*16.1±3.1*	*13.6±4.4*	*7.8±1.2*	*12.8±2.7*
31 weeks						
Glucose (mM)	*11.9±0.5*	*13.5±0.6*	*13.4±1.1*	*11.7±0.4*	*13.5±0.7*	*11.8±0.7*
Adiponectin (mg/mL)	*9.1±1.2*	*11.3±1.5*	*10.4±1.6*	*12.8±3.4*	*9.4±1.7*	*10.3±1.5*
Creatinine (μM)	*35.1±20.2*	*50.0±21.5*	*50.8±21.5*	*60.0±22.9*	*81.0±21*	*121±25**

Values are means ± SE; *P <0.05 vs. WT; †P <0.05 vs. Starch; ‡P<0.05 vs Fructose; n=6-10/group. DIO, Diet Induced Obesity.

Obesity often corresponds with changes in liver triglycerides and glycogen[204]. DIO decreased glycogen and increased triglycerides in the liver in both WT and G6PDX mice at 31 weeks, but to a lesser extent in G6PDX mice, consistent with a decrease in obesity in response to a high fat/high sugar diet (Table 2.2). At 12 weeks, DIO resulted in increased liver triglycerides and decreased glycogen only in G6PDX mice. These results suggest that G6PD deficiency confers earlier sensitivity to metabolic changes.

Finally, glucose tolerance has been used to assess metabolic dysfunction, and may be decreased in response to obesity and insulin resistance[202]. Previous investigators observed a decreased glucose tolerance in G6PDX mice compared to WT mice[13]. In our study, also expected to this effect, and hypothesized that dietary stress would further exacerbate glucose intolerance in G6PDX mice. However, we did not see this effect. Rather, blood glucose after glucose challenge was identical between WT and G6PDX mice among all diet groups (Figure 2.5). DIO decreased glucose tolerance, but to the same degree in both G6PDX and WT mice, indicating a similar degree of diet induced metabolic dysfunction in both strains. Thus, G6PD deficiency did not affect metabolic function as assessed by glucose challenge.

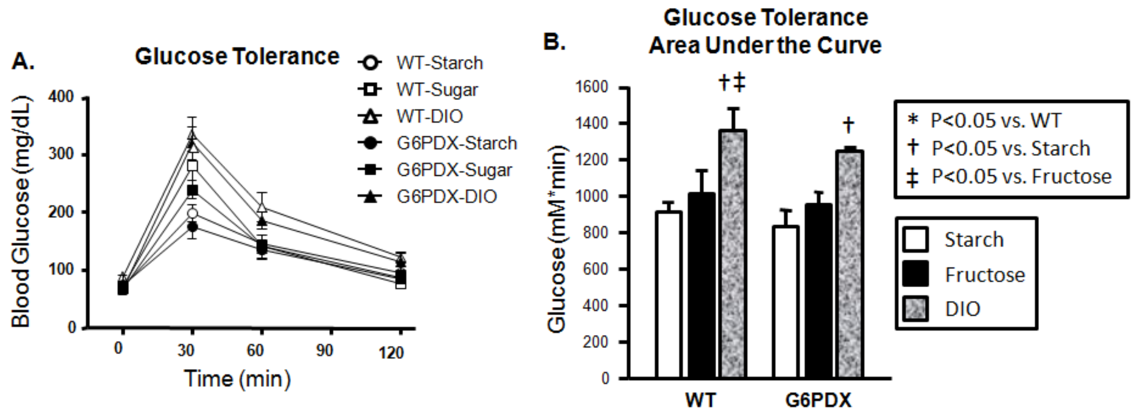

Figure 2.5. *Glucose Tolerance*. Intraperitoneal glucose tolerance tests indicated decreased glucose tolerance with obesity, and no effect of G6PD deficiency. Data were obtained from mice after 25 weeks of dietary treatment (28 weeks of age). DIO, Diet Induced Obesity; G6PDX, glucose 6-phosphate dehydrogenase deficient mice; WT, wild type; n=5-10/group.

Cardiovascular Data

G6PD deficiency increased left ventricular mass by 7% at 12 weeks (Table 2.4) ($p<0.001$ for main effect). This corresponded with a 15% increase in diastolic volume ($p=0.003$ for main effect), a 16% increase in systolic volume ($p=0.012$ for main effect), an 8% decrease in absolute wall thickness ($p=0.028$ for main effect), and a 13% decrease in relative wall thickness ($p=0.012$ for main effect) in response to G6PD deficiency, indicating modest left ventricular dilation in young G6PDX mice. These effects resulted in a 13% increase in stroke volume in young G6PDX mice compared to WT mice ($p=0.008$ for main effect), and independent of any change in blood pressure. However, these effects were not observed in older mice at 31 weeks. Thus, G6PD deficiency modestly increased myocardial dilation and hypertrophy in young animals.

Table 2.4.

Parameter	Wild Type Starch	Fructose	DIO	G6PD Deficient Starch	Fructose	DIO
11-12 weeks						
Cardiovascular Function						
Systolic Blood Pressure (mmHg)	*117±3*	*114±4*	*114±5*	*113±3*	*113±4*	*118±4*
Heart Rate (BPM)	*573±11*	*553±12*	*563±10*	*543±7*	*540±12*	*565±9*
Diastolic Volume (μL)	*40.5±2.8*	*40.5±2.5*	*42.1±2.0*	*47.0±2.3*	*47.4±2.6**	*46.6±2.5*
Systolic Volume (μL)	*21.4±1.9*	*21.8±1.6*	*21.7±1.7*	*25.6±1.3*	*25.2±1.8*	*24.3±1.6*
Stroke Volume (μL)	*19.2±1.1*	*18.7±1.4*	*20.4±1.0*	*21.4±1.3*	*22.2±1.1**	*22.3±1.3*
Ejection Fraction %	*48.8±1.9*	*46.3±2.5*	*49.2±2.1*	*45.5±1.3*	*47.9±1.6*	*48.4±1.6*
Absolute Wall Thickness (mm)	*1.73±0.08*	*1.77±0.10*	*1.73±0.07*	*1.62±0.08*	*1.61±0.07*	*1.61±0.06*
Relative Wall Thickness	*0.533±0.039*	*0.539±0.040*	*0.523±0.029*	*0.465±0.031*	*0.463±0.030*	*0.464±0.03*
Heart Mass						
Left Ventricular Mass (mg)	*59.1±1.4*	*59.6±1.6*	*65.4±1.6†‡*	*63.4±1.3**	*66.6±1.3**	*67.4±1.6*
Right Ventricular Mass (mg)	*18.2±0.8*	*16.4±0.8*	*18.9±0.8*	*17.1±1.2*	*17.4±1.2*	*18.4±0.9*
Atrial Mass (mg)	*3.78±0.23*	*4.14±0.29*	*5.02±0.29†*	*4.46±0.24*	*4.53±0.33*	*4.57±0.24*
23-24 weeks						
Cardiovascular Function						
Systolic Blood Pressure (mmHg)	*96±2*	*94±3*	*99±4*	*100±3*	*100±3*	*97±4*
Heart Rate (BPM)	*634±13*	*617±25*	*652±21*	*564±17**	*594±22*	*638±20†*
Diastolic Volume (μL)	*44.8±3.5*	*53.9±3.1*	*39.7±4.8‡*	*50.3±4.1*	*50.0±2.9*	*42.0±3.7*
Systolic Volume (μL)	*25.0±2.7*	*28.9±2.4*	*19.9±3.1‡*	*27.1±2.5*	*27.7±2.6*	*19.4±2.3*
Stroke Volume (μL)	*19.9±1.2*	*25.0±1.0*	*19.8±2.1*	*23.2±2.2*	*22.4±0.9*	*22.6±1.5*
Ejection Fraction %	*45.2±2.1*	*46.9±1.7*	*50.7±2.3*	*46.5±2.4*	*45.6±2.4*	*54.6±1.8†‡*
Absolute Wall Thickness (mm)	*1.84±0.13*	*1.79±0.08*	*2.21±0.20*	*1.67±0.14*	*1.77±0.16*	*1.84±0.14*
Relative Wall Thickness	*0.538±0.051*	*0.486±0.029*	*0.699±0.099‡*	*0.476±0.059*	*0.494±0.05*	*0.549±0.050*
31 weeks						
Heart Mass						
Left Ventricular Mass (mg)	*75.8±1.7*	*77.4±0.9*	*79.4±2.2*	*72.1±2.8*	*72.7±2.2*	*74.7±3.2*
Right Ventricular Mass (mg)	*19.6±0.9*	*21.0±0.8*	*21.8±1.2*	*18.7±1.9*	*19.6±0.9*	*20.8±1.0*
Atrial Mass (mg)	*4.63±0.39*	*4.79±0.40*	*5.20±0.28*	*4.11±0.17*	*4.56±0.14*	*4.60±0.18*

Values are means ± SE; *P <0.05 vs. WT; †P <0.05 vs. Starch; ‡P<0.05 vs Fructose; n=19-20/group at 12 weeks for blood pressure and echocardiography, n=9-10/group for all other parameters at 31 weeks of age. BPM, beats per minute; DIO, Diet Induced Obesity.

Although G6PD deficiency led to ventricular dilation and hypertrophy, G6PDX mice were insensitive to adverse dietary remodeling effects. On the other hand, in WT mice, DIO increased left ventricular mass by 11%, and increased atrial mass by 33% at 12 weeks, indicative of diet induced hypertrophy in young WT animals (Table 2.4). In older animals, DIO increased relative wall thickness by 44% compared to the high fructose diet in WT mice, indicating concentric hypertrophy in WT mice but not G6PDX mice. Rather, DIO resulted in an increased ejection fraction in older G6PDX mice. Thus, while DIO resulted in cardiac hypertrophy in WT mice, there was no hypertrophic response of diet in G6PDX mice.

Oxidative Stress

Aconitase is a mitochondrial oxidative enzyme whose activity is decreased in response to oxidative stress[205]. Thus, aconitase has been used as an indicator of oxidative damage. MDA and 4HA are lipid peroxidation breakdown products, and are also indicative of oxidative damage. Therefore, we assayed lipid peroxidation products (MDA+4HA) and aconitase activity as indices of oxidative stress (Table 2.5). There were no differences in liver aconitase activity. However, high fructose intake decreased lipid peroxidation products in the liver of older WT mice, but not G6PDX mice. This decrease in lipid peroxidation products in response to high fructose corresponded with increased G6PD activity intake in WT mice (Figure 2.1), suggesting that an increase in G6PD activity may decrease hepatic oxidative stress.

Table 2.5.

Parameter	Wild Type Starch	Fructose	DIO	G6PD Deficient Starch	Fructose	DIO
12 weeks						
Liver						
PKC Activity (ng·ml^{-1}·min^{-1})	*1.85±0.02*	*1.73±0.01†*	*1.73±0.02†*	*1.75±0.02**	*1.76±0.02*	*1.73±0.02*
Caspase 3 Activity (AU/g)	*230±15*	*262±16*	*241±14*	*263±14*	*235±14*	*203±14†*
GAPDH Activity (AU/g Protein)	*132±25*	*183±85*	*632±127‡†*	*1010±167**	*437±253†*	*742±129*
MCAD (μmol·gww^{-1}·min^{-1})	*2.54±0.23*	*2.91±0.37*	*2.93±0.28*	*2.51±0.35*	*2.99±0.35*	*2.86±0.32*
CS (μmol·gww^{-1}·min^{-1})	*33.8±2.5*	*45.4±4.0*	*32.8±3.8*	*34.3±2.0*	*49.1±6.6†*	*36.5±4.4*
Aconitase (mmol·gww^{-1}·min^{-1})	*2.99±0.19*	*3.10±0.22*	*3.28±0.28*	*2.73±0.15*	*3.43±0.33*	*2.77±0.29*
MDA+4HA (pmoles/mg Protein)	*276±21*	*262±20*	*257±20*	*264±21*	*219±20*	*273±20*
Skeletal Muscle						
CS (μmol·gww^{-1}·min^{-1})	*14.8±1.1*	*15.5±1.1*	*19.2±1.2*	*14.5±1.1*	*15.1±1.1*	*15.5±1.1*
Aconitase (mmol·gww^{-1}·min^{-1})	*1.30±0.14*	*1.45±0.14*	*1.57±0.14*	*1.22±0.14*	*1.26±0.14*	*1.18±0.14*
MDA+4HA (pmoles/mg Protein)	*2.42±0.62*	*1.39±0.39*	*2.82±0.44*	*2.98±0.81*	*3.18±0.83*	*4.83±1.86**
Left Ventricle						
PKC Activity (ng·ml^{-1}·min^{-1})	*1.93±0.16*	*1.33±0.16†*	*2.20±0.20‡*	*1.68±0.16*	*2.23±0.13*†*	*2.13±0.20*
Caspase 3 Activity (AU/g)	*138±7*	*134±7*	*142±6*	*140±8*	*147±6*	*158±8*
CS (μmol·gww^{-1}·min^{-1})	*157±12*	*150±12*	*198±12*	*173±12*	*186±13*	*176±14*
Aconitase (mmol·gww^{-1}·min^{-1})	*10.7±2.0*	*10.2±2.3*	*13.7±2.0*	*11.5±2.0*	*12.7±2.5*	*14.7±1.9*
MDA+4HA (pmoles/mg Protein)	*1768±479*	*2690±455*	*1623±455*	*1939±455*	*2962±455*	*2306±455*
31 weeks						
Liver						
PKC Activity (ng·ml^{-1}·min^{-1})	*1.78±0.04*	*1.75±0.01*	*1.75±0.02*	*1.75±0.03*	*1.91±0.01*	*1.89±0.01*
Caspase 3 Activity (AU/g)	*242±10*	*241±9*	*259±10*	*217±12*	*203±9**	*200±13**
GAPDH Activity (AU/g Protein)	*0.087±5*	*1.213±89†*	*0.086±4‡*	*0.096±15*	*0.078±7**	*0.087±10*
MCAD (μmol·gww^{-1}·min^{-1})	*2.70±0.28*	*2.39±0.27*	*3.22±0.55*	*2.35±0.38*	*2.20±0.35*	*3.07±0.38*
CS (μmol·gww^{-1}·min^{-1})	*34.1±5.3*	*39.8±5.5*	*43.4±15.6*	*30.7±3.4*	*42.4±7.8*	*34.9±1.1*
Aconitase (mmol·gww^{-1}·min^{-1})	*3.30±0.40*	*3.12±0.40*	*3.15±0.96*	*3.19±0.26*	*2.86±0.22*	*3.08±0.18*
MDA+4HA (pmoles/mg Protein)	*328±16*	*252±17†*	*336±17‡*	*315±19*	*309±19**	*292±19*
Skeletal Muscle						
CS (μmol·gww^{-1}·min^{-1})	*12.5±1.1*	*12.3±1.3*	*11.2±1.3*	*13.7±1.4*	*14.2±1.2*	*14.3±1.4*
Aconitase (mmol·gww^{-1}·min^{-1})	*1.23±0.12*	*1.01±0.13*	*0.66±0.13†*	*1.36±0.14*	*1.21±0.13*	*1.10±0.14**
MDA+4HA (pmoles/mg Protein)	*3.32±1.05*	*3.28±1.17*	*5.30±1.05*	*4.84±1.25*	*3.91±1.10*	*2.44±1.25*
Left Ventricle						
PKC Activity (ng·ml^{-1}·min^{-1})	*2.17±0.26*	*2.61±0.23*	*2.45±0.20*	*1.87±0.23*	*2.73±0.23†*	*2.51±0.23*
Caspase 3 Activity (AU/g)	*156±23*	*160±19*	*189±21*	*227±23**	*245±23**	*254±23**
CS (μmol·gww^{-1}·min^{-1})	*130±12*	*146±13*	*179±12†*	*179±14**	*154±12*	*146±15*
Aconitase (mmol·gww^{-1}·min^{-1})	*20.2±1.5*	*19.4±1.7*	*15.9±1.5*	*24.2±1.8*	*21.8±1.6*	*22.6±1.9**
MDA+4HA (pmoles/mg Protein)	*1167±227*	*1299±254*	*920±227*	*1293±271*	*1573±239*	*830±271*

Values are means ± SE; *P <0.05 vs. WT; †P <0.05 vs. Starch; ‡P<0.05 vs Fructose; n=4-10/group. 4HA, 4-hydroxyalkenals; AU, arbitrary units; DIO, Diet Induced Obesity; CS, citrate synthase activity; GAPDH, glyceraldehyde-3-phosphate dehydrogenase; gww, grams of wet tissue weight; MCAD, medium chain acyl CoA dehydrogenase activity; MDA, malondialdehyde; PKC, protein kinase C.

Skeletal muscle aconitase activity was decreased by DIO in older WT mice, indicative of increased ROS in response to DIO (Table 2.5). However, this effect of diet on decreasing aconitase activity was absent in G6PDX mice. No differences were observed in skeletal muscle citrate synthase activity, indicating that changes in aconitase activity were not due to decreased mitochondria. At 12 weeks, there were more lipid peroxidation products in response to DIO in G6PDX mice compared to WT mice, indicative of increased ROS in obese G6PDX mice at this time point. Thus, there was a temporal change, in which G6PD deficiency increased ROS in response to short term DIO, but prevented oxidative damage in the long term. The preservation of aconitase activity in the skeletal muscle of older G6PDX mice may have to do with the decreased level of obesity found in these animals (Figure 2.3).

Left ventricular aconitase activity was higher in G6PDX mice compared to WT mice at 31 weeks, indicative of decreased myocardial ROS in G6PDX mice compared to WT mice and similar to the skeletal muscle results (Table 2.5). We observed this effect despite an increase in myocardial citrate synthase activity by DIO in WT mice.

Additional Non-Oxidative Glucose Pathways

The HBP and polyol pathways were both upregulated in the livers of WT mice after 12 weeks of high fructose intake and DIO (Figure 2.6). There was a modest decrease in PKC activity, and no changes for AGE and GAPDH activity in WT livers, but (Table 2.5). These findings were generally paralleled in the heart, except that the fructose diet decreased PKC activity (Figure 2.7). Thus, induction of the HBP and polyol pathways in the heart and livers of WT mice at the early time point is likely an adaptation in response to increased fuel substrate supply. Although previous studies showed that increased oxidative stress may also increase flux through these pathways, this is unlikely here since we found no significant differences for MDA at the 12-week time point for all the diets employed in this study.

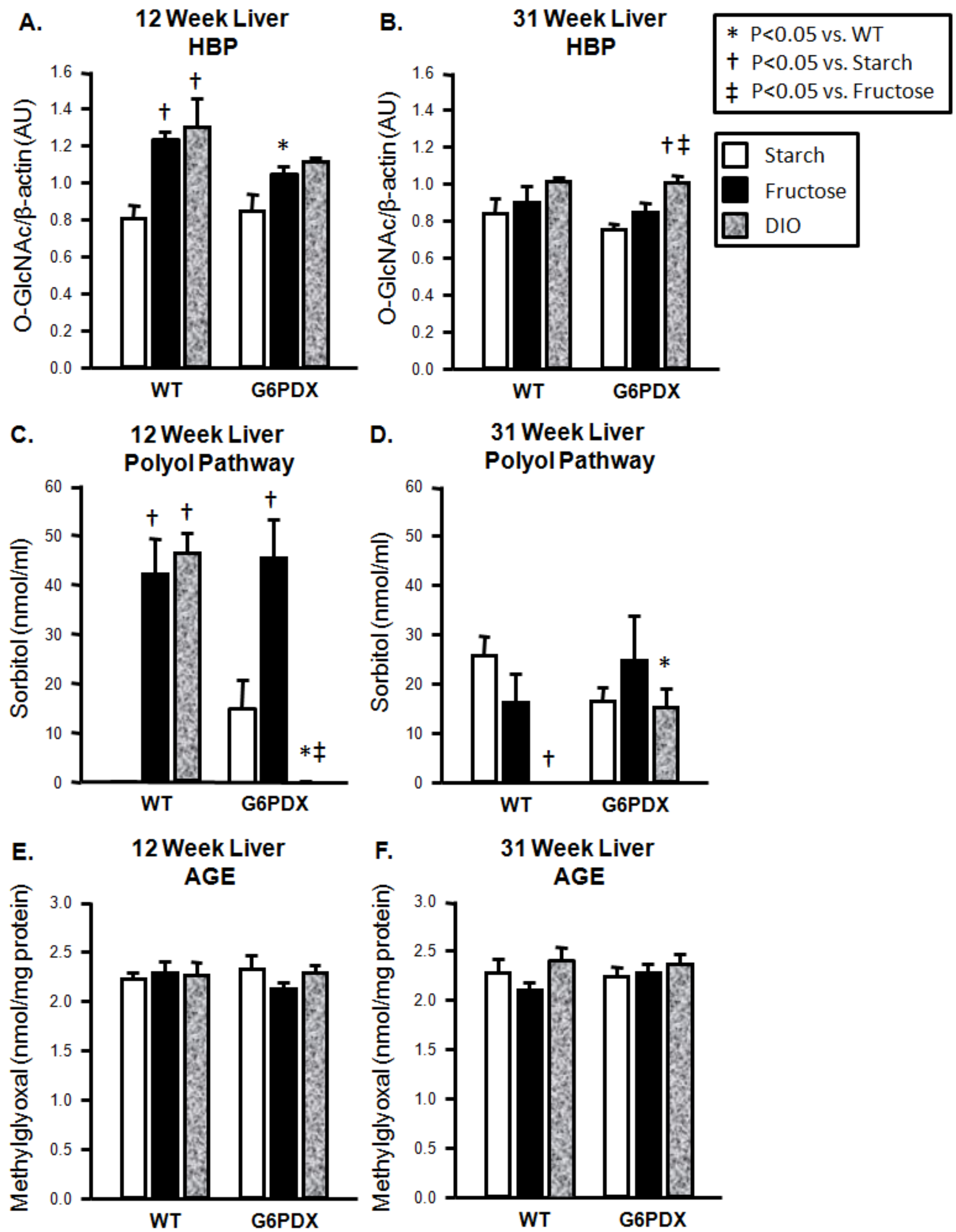

Figure 2.6. *Effects of dietary intervention on metabolic pathways in the liver*. **A-B**. Hexosamine biosynthetic pathway (HBP) activation as assessed by *O*-GlcNAc levels. **C-D**. Polyol pathway activation as assessed by sorbitol levels. **E-F**. Advanced glycation end

product (AGE) formation as assessed by methylglyoxal concentration. DIO, Diet Induced Obesity; G6PDX, glucose 6-phosphate dehydrogenase deficient mice; WT, wild type; n=4-10/group.

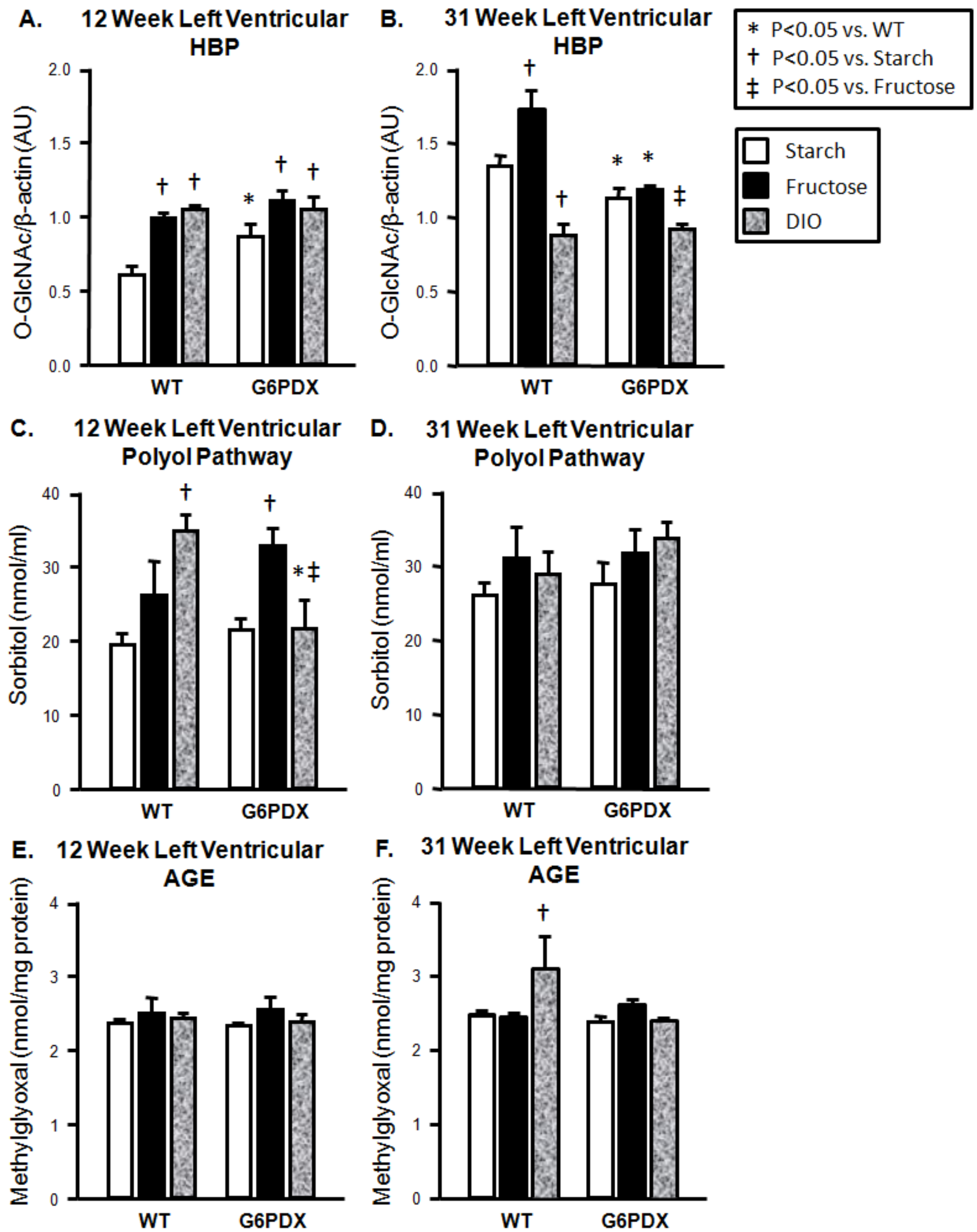

Figure 2.7. *Effects of dietary intervention on metabolic pathways in the heart*. **A-B**. Hexosamine biosynthetic pathway (HBP) activation as assessed by *O*-GlcNAc levels. **C-**

D. Polyol pathway activation as assessed by sorbitol levels. **E-F**. Advanced glycation end product (AGE) formation as assessed by methylglyoxal concentration. DIO, Diet Induced Obesity; G6PDX, glucose 6-phosphate dehydrogenase deficient mice; WT, wild type; n=4-9/group.

The induction of the HBP and polyol pathways was no longer present after 31 weeks in WT livers (fructose and DIO diets), with polyol pathway activation markedly decreased in the DIO group (Figure 2.6). The decreased induction of the HBP and polyol pathways was paralleled by an increase in AGE in DIO hearts at 31 weeks (Figure 2.7). Thus, our data suggest a biphasic response with early induction of the HBP and polyol pathways in the liver, followed by later AGE formation in the heart in response to DIO.

We further examined the activation of these pathways in the G6PDX mice. Early liver HBP activation was blunted in G6PDX mice (Figure 2.6). However, polyol pathway activation remained high in response to fructose feeding, while it sharply decreased in response to DIO. G6PDX hearts exhibited a more robust response with HBP, PKC and the polyol pathway activated to varying extents for the DIO and fructose diets (Figure 2.7; Table 2.5). Thus our data at the earlier time point (12 weeks) indicate that there was a general decrease in activation of non-oxidative glucose pathways. The data further indicate that high fructose intake elicited the greatest changes in livers and hearts of G6PDX mice. After long term feeding, the HBP was significantly increased in G6PDX livers (Figure 2.6). Fructose feeding increased PKC and decreased HBP activation, respectively, in older G6PDX mouse hearts (Figure 2.7; Table 2.5). However, the DIO diet did not significantly induce the PKC and AGE pathways as it did for the WT mice.

Discussion

We tested the hypothesis that G6PD deficiency exacerbates diet induced metabolic dysfunction by decreasing antioxidant defenses and thus increasing oxidative stress throughout the body, and that G6PD deficiency prevents myocardial oxidative stress and diet induced cardiac dysfunction by decreasing NADPH dependant superoxide production in the myocardium. We found G6PD deficiency resulted in increased sensitivity to other diet induced metabolic abnormalities including increased serum triglycerides and free fatty acids, and that G6PD deficiency reduced obesity but that this decrease in obesity did not beneficially affect metabolism. We further found that G6DP deficiency resulted in early modest cardiac defects, but that these cardiac effects were not exacerbated by DIO. We found that G6PD deficiency preserved left ventricular and skeletal muscle aconitase activity compared to WT mice with DIO, suggesting that G6PD deficiency decreased oxidative stress in these tissues, but not in liver tissue. In liver tissue, increased G6PD activity in WT mice corresponded with decreased lipid peroxidation products in response to long term fructose intake, but that G6PDX mice failed to decrease lipid peroxidation products in response to long term dietary fructose. Finally, we uncovered a diverse array of effects of G6PD deficiency on the induction of other non-oxidative glucose pathways.

The results indicate that G6PD deficiency decreased weight gain in response to a high fat/high sugar diet. Other investigators saw that treatment with DHEA, an inhibitor of G6PD, had an anti-obesity effect in genetically obese rats[206]. This makes sense considering that the NADPH produced by the PPP is in high demand for fatty acid synthesis in adipose tissue, and that a decrease in G6PD activity may decrease NADPH production and thus decrease fatty acid synthesis[207].

G6PD is required for fatty acid and cholesterol synthesis, and G6PD knockdown attenuates adipocyte differentiation[168]. Normally a decrease in body mass confers beneficial cardiometabolic effects, but a decrease in adipocyte differentiation and prevention of normal fat mass expansion may result in increased circulating lipids and ectopic fat deposition[208]. In our study, G6PD deficiency decreased obesity, fat pad mass, and leptin, and increased circulating free fatty acids. However, this corresponded with decreased ectopic fat buildup in the liver, rather than an increase in ectopic fat, indicating that the decrease in fat mass in our study may have had neutral effects.

Because G6PD normally consumes a portion of the glucose within a cell, one would expect G6PD deficiency to route increased glucose through alternative pathways. Thus, we expected to see a general increase in HBP and polyol pathway activation, and in AGE formation in response to G6PD deficiency. However, our data suggest that this was not generally the case. Rather, there was a general decrease in activation of metabolic pathways in response to G6PD deficiency with short term feeding. With longer term feeding, G6PD deficiency increased the HBP, and prevented an increase in AGE formation. Thus, our data suggest a more complex regulatory nature to these other alternative glucose pathways than expected.

Based on our observation that the HBP and polyol pathways were upregulated by short term DIO or high fructose intake in WT mice, induction of the HBP and polyol pathways may be an adaptation in response to increased substrate abundance. This early induction of the HBP and polyol pathways may contribute to metabolic dysfunction over time. Interestingly, prolonged feeding resulted in downregulation of these pathways (likely by feedback inhibition) which was followed by the induction of AGE formation in the WT hearts. Early activation of the HBP and polyol pathways, and later cardiac AGE formation may contribute to increased diet induced cardiometabolic stress in WT mice, while increased hepatic HBP activation may contribute to LV remodeling found in G6PDX mice[185, 209, 210]. Although previous studies showed that increased oxidative stress may also increase flux through these pathways, this is unlikely here since we found no evidence for oxidative stress in WT mice at 12-weeks when the HBP and polyol pathways were already activated.

Our studies examined the effects of G6PD deficiency in young mice. Although we did not observe adverse effects of obesity or G6PD deficiency on blood pressure or cardiac hypertrophy and failure, it would be of interest for further studies to investigate longer-term obesity. Jain, et al, observed a minor ventricular hypertrophy at 9 months in G6PDX mice[27]. The interaction between this minor hypertrophy with obesity on cardiometabolic health would be of interest for further investigations to pursue.

In summary, G6PD deficient mice had decreased obesity compared to WT mice in response to long-term dietary challenge, but showed increased sensitivity toward metabolic abnormalities such as increased circulating free fatty acids and triglycerides. We also saw diverse changes in alternative glucose pathway activation in response to G6PD deficiency. Overall, these changes did not affect diet induced glucose intolerance in G6PDX mice. These results indicate that despite decreasing obesity, G6PD deficiency did not confer a protective effect against diet induced metabolic dysfunction in mice.

Summary of Major Findings

1. *G6PD deficiency decreased obesity in response to a long-term high fat/high sugar diet in mice.*
2. *Despite resulting in decreased obesity, G6PD deficiency was not protective against the development of diet-induced metabolic abnormalities.*

Chapter 3 – Adverse Effects of Glucose 6-Phosphate Dehydrogenase Deficiency on the Development of Heart Failure

Chapter Abstract

Glucose 6-phosphate dehydrogenase (G6PD) deficiency is the most common enzyme deficiency in the world, and its impact on the development of heart failure is unclear. G6PD generates NADPH to be used by the glutathione pathway to remove reactive oxygen species (ROS), but also to produce ROS via NADPH dependent mechanisms. Cardiac G6PD activity and ROS are increased in heart failure, suggesting that G6PD deficiency may protect against heart failure by decreasing NADPH and ROS production. We assessed this hypothesis in an established mouse model of human G6PD deficiency (G6PDX mice, ~40% of normal G6PD activity). Myocardial infarction with 3 months follow-up resulted in LV dilation and dysfunction in both WT and G6PDX mice, but significantly greater end diastolic volume and wall thinning in G6PDX mice. Similarly, pressure overload induced by transverse aortic constriction (TAC) for 6 weeks caused greater LV dilation in G6PDX mice than WT. We further stressed TAC mice by feeding a high fructose diet to increase flux through G6PD and ROS production, and again observed worse LV remodeling and a lower ejection fraction in G6PDX than WT mice. Tissue content of lipid peroxidation products was increased in G6PDX mice in response to infarction, and aconitase activity was decreased with TAC, suggesting that G6PD deficiency increases myocardial oxidative stress and subsequent myocardial damage. In summary, G6PD deficiency increased redox stress and accelerated LV remodeling in response to infarction or aortic pressure overload, suggesting that people with G6PD

deficiency may be at greater risk for developing heart failure when there is concurrent hypertension or infarction.

Introduction

Glucose 6-phosphate dehydrogenase (G6PD) controls the flux into the pentose phosphate pathway, and is the main cytoplasmic source of NADPH[3, 29]. Generation of NADPH by G6PD fuels antioxidant systems through conversion of oxidized glutathione back to the reduced form and thus decreases reactive oxygen species (ROS)[27, 180]. G6PD deficiency is the most common enzyme deficiency in the world, affecting over 400 million people and conferring resistance to malaria[15 2]. It is prevalent in sub-Saharan Africa, Mediterranean countries and in Southeastern Asia. Alleles for mild to moderate severity deficiency result in 10-60% of normal G6PD activity[14]. The effects of G6PD deficiency on the risk for cardiovascular disease and subsequent outcomes are unclear. The limited available evidence suggests that G6PD deficiency may reduce the risk of heart disease and cardiovascular associated death, though a thorough evaluation in a large patient cohort has not been conducted[164, 165].

At present, how the impact of G6PD deficiency on the development and progression of heart failure is unclear. Depending on the circumstances, G6PD has both pro- and anti-oxidant effects. Bing, et al, found a remarkable increase in G6PD activity in post-infarct surviving myocardium, but the significance of this phenomenon was not further queried[211]. More recently, we found that dogs and patients with heart failure have elevated myocardial G6PD activity and [NADPH][3, 6], which might we interpreted as a compensatory mechanism necessary to oppose the increased generation of reactive oxygen species (ROS) in failing myocardium. In fact, G6PD inhibition in cardiomyocytes compromises antioxidant capacity and increases sensitivity to ROS induced cell death[9, 10, 27]. G6PD deficient (G6PDX) mice develop normally, but present with moderate cardiac dysfunction at around 9 months of age[27]. Myocardial ischemia/reperfusion causes greater oxidative stress and injury in G6PD compared to WT mice[27, 180]. On the other hand, pharmacological inhibition of G6PD decreased ROS generation in myocardial homogenates from failing hearts, suggesting that G6PD fuels NADPH dependent oxidant enzymes in advanced heart failure[3, 6]. Potential benefits of G6PD deficiency have also been reported on the vasculature[169, 170], however no studies have addressed the effects of chronic suppression of G6PDH on the development and/or progression of heart failure[164, 165].

The goal of the present investigation was to assess the effects of G6PD deficiency on the development of heart failure in myocardium subjected to injury or to chronic, severe stress. G6PDX mice, which have approximately 40% residual G6PD activity and recapitulates key aspects of clinical deficiency[44], were subjected to myocardial infarction caused by left coronary artery ligation, or to transverse aortic constriction (TAC) to induce pressure overload. Alterations in LV mass, chamber remodeling, ROS production and lipid peroxidation were assessed. We hypothesized that G6PD deficiency would protect against the development of heart failure by decreasing NADPH and ROS production in chronically stressed myocardium. We further stressed these mice with a high fructose diet to increase flux through pro-oxidant NADPH dependant enzymes[146, 154, 157, 212]. Recent studies from our lab and others have found that high fructose intake exacerbated the development of heart failure and accelerated mortality compared to a complex carbohydrate diet in salt-induced hypertension[151, 152], TAC[154, 213], and volume overload[155] models of heart failure. Thus, we further hypothesized that G6PD deficiency would prevent the adverse effects of high fructose intake in mice subjected to TAC.

Experimental Design.

Infarct Experimental Design.

Sixteen week-old male mice underwent permanent coronary occlusion or sham surgery. Cardiac function was assessed by echocardiography at 7 and 11 weeks, and by intraventricular catheterization during euthanization at 12 weeks after surgery.

TAC Experimental Design.

Ten week-old male mice underwent TAC or sham surgery. TAC was performed using a 28 gauge needle. Echocardiography was performed 1-2 days prior to euthanization at 6 weeks after surgery.

Fructose/TAC Experimental Design.

Eight week-old male mice underwent sham or TAC surgery with a 27 gauge needle, and were placed on a high starch diet or high fructose diet which consisted of 60% of energy intake from fructose on the following day. Blood pressure was measured by tail cuff plethysmography at 10 weeks after surgery, echocardiography was performed at 4, 8, 12 and 16 weeks, and mice were euthanized at 17 weeks for biochemical analysis.

Statistical Analysis.

Values are shown as mean ± standard error. Comparisons between strain and treatment groups were made using a two-way ANOVA with the Holm-Sidak correction. Recovery from surgery was assessed by a Chi-square analysis. Post-surgery survival was assessed by Log-Rank Kaplan Meier analysis. A two tailed t-test was used to compare the difference between WT and G6PDX infarct size. $P<0.05$ was considered significant.

Myocardial Infarction Results

Recovery and Survival after Myocardial Infarction

A total of 32 WT and 46 G6PDX mice underwent LAD ligation to produce an infarct, while 10 WT and 10 G6PDX mice underwent sham surgery. Post-infarct 24 hour survival was 63% for WT and 61% for G6PDX mice (p=0.93 for difference). There was minimal mortality from 1 day to 12 weeks after infarction, with no differences among groups (Figure 3.1, 95% survival for WT mice and 96% survival for G6PDX mice). There were no differences in body mass over the course of the study (Table 3.1).

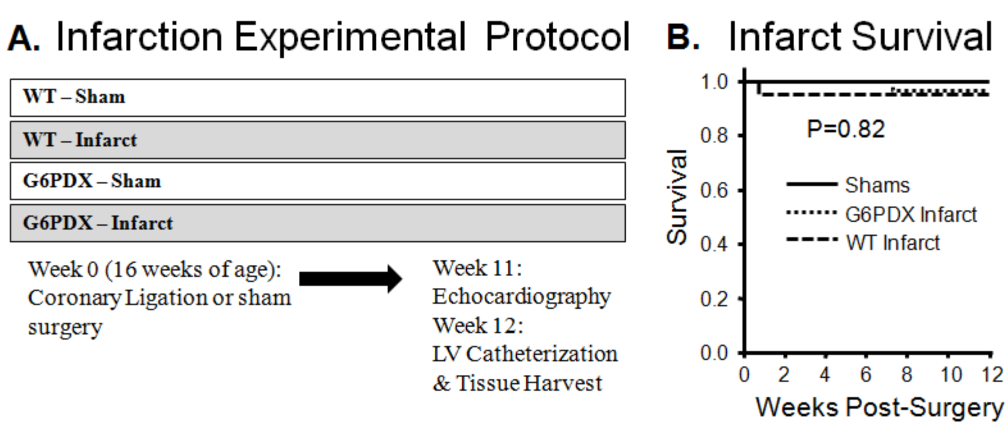

Figure 3.1. **A**, *Infarction Experimental Protocol*. Sixteen week-old mice underwent permanent coronary occlusion or sham surgery. Cardiac function was assessed by echocardiography at 11 weeks, and by intraventricular catheterization during euthanization at 12 weeks after surgery. **B**, *Post-infarct survival*. Neither surgery nor G6PD deficiency affected post-infarct survival over the course of the study (p=0.82). Time 0 of the survival curve begins 1 day after TAC, so the data are representative of survival after complete recovery from the surgery. Survival was assessed by Log-Rank Kaplan Meier analysis; Sham n=10/group, WT infarct n=20/group, G6PDX infarct n=29/group.

Table 3.1.

Parameter	Wild Type		G6PD Deficient	
	Sham	Infarct	Sham	Infarct
Beginning Body Mass (g)	*31.9±0.8*	*31.4±0.6*	*31.6±0.8*	*30.8±0.5*
Terminal Body Mass (g)	*37.0±1.2*	*35.4±0.8*	*35.2±1.2*	*33.9±0.7*
Body Mass Increase %	*16.1±2.6*	*12.5±1.9*	*11.4±2.6*	*10.3±1.5*
Tibia Length (mm)	*20.14±0.10*	*20.08±0.08*	*20.40±0.10*	*20.34±0.06#*
Heart Mass/Tibia Length (mg/mm)	*6.73±0.43*	*8.12±0.32**	*6.66±0.43*	*8.70±0.26**
Heart Mass/Body Mass (mg/g)	*3.68±0.38*	*4.63±0.28**	*3.88±0.38*	*5.37±0.23*#*
Wet/Dry Lung Weight Ratio	*4.64±0.06*	*4.61±0.05*	*4.68±0.06*	*4.67±0.04*
Kidney Mass (mg)	*325±12*	*296±8**	*304±012*	*270±7*#*
Liver Mass (g)	*1.88±0.071*	*1.68±0.051**	*1.72±0.071*	*1.63±0.042*
Epididymal Fat Mass (g)	*1.53±0.14*	*1.43±0.10*	*1.28±0.14*	*1.18±0.08*

Data were obtained using mice at 12 weeks after LAD ligation or sham surgery; *P <0.05 vs. Sham; #P <0.05 vs. WT; Sham n=10/group, WT Infarct n=19, G6PDX n=28.

G6PD Deficiency Increases LV dilation after Myocardial Infarction

G6PD mRNA and G6PD activity were decreased in G6PDX mice compared to WT mice, and infarction increased myocardial G6PD mRNA and G6PD activity in WT mice, but not in G6PDX mice (Figure 3.2A-B). Heart mass was increased by LAD ligation, indicating cardiac hypertrophy in both WT and G6PDX mice (Figure 3.2C; Table 3.1). Infarct size was not different between strains (WT: 14.2±1.4%, G6PDX: 16.8±1.2%, p=0.17). Myocardial infarction caused eccentric hypertrophy as seen in the increase in LV end diastolic volume, in both WT and G6PDX mice, however LV dilation was significantly greater with G6PD deficiency (Figure 3.2D-E; Tables 3.2-3.3), reflected by a greater LV end diastolic volume in G6PDX mice compared to WT mice. G6PDX mice also displayed a decrease in relative wall thickness in G6PDX mice, further indicating that G6PD deficiency increased susceptibility to LV dilation (Figure 3.2F). The decrease in wall thickness corresponded with a decrease in capillary density in G6PDX mice (Table 3.4). Myocardial infarction decreased systolic and diastolic function, as indicated by decreased ejection fraction and dP/dt min, and increased MPI and LV end diastolic pressure (Figure 3.2G-I; Figure 3.3). Taken together, G6PD deficiency exacerbated LV dilation, but did not accelerate systolic or diastolic dysfunction after myocardial infarction.

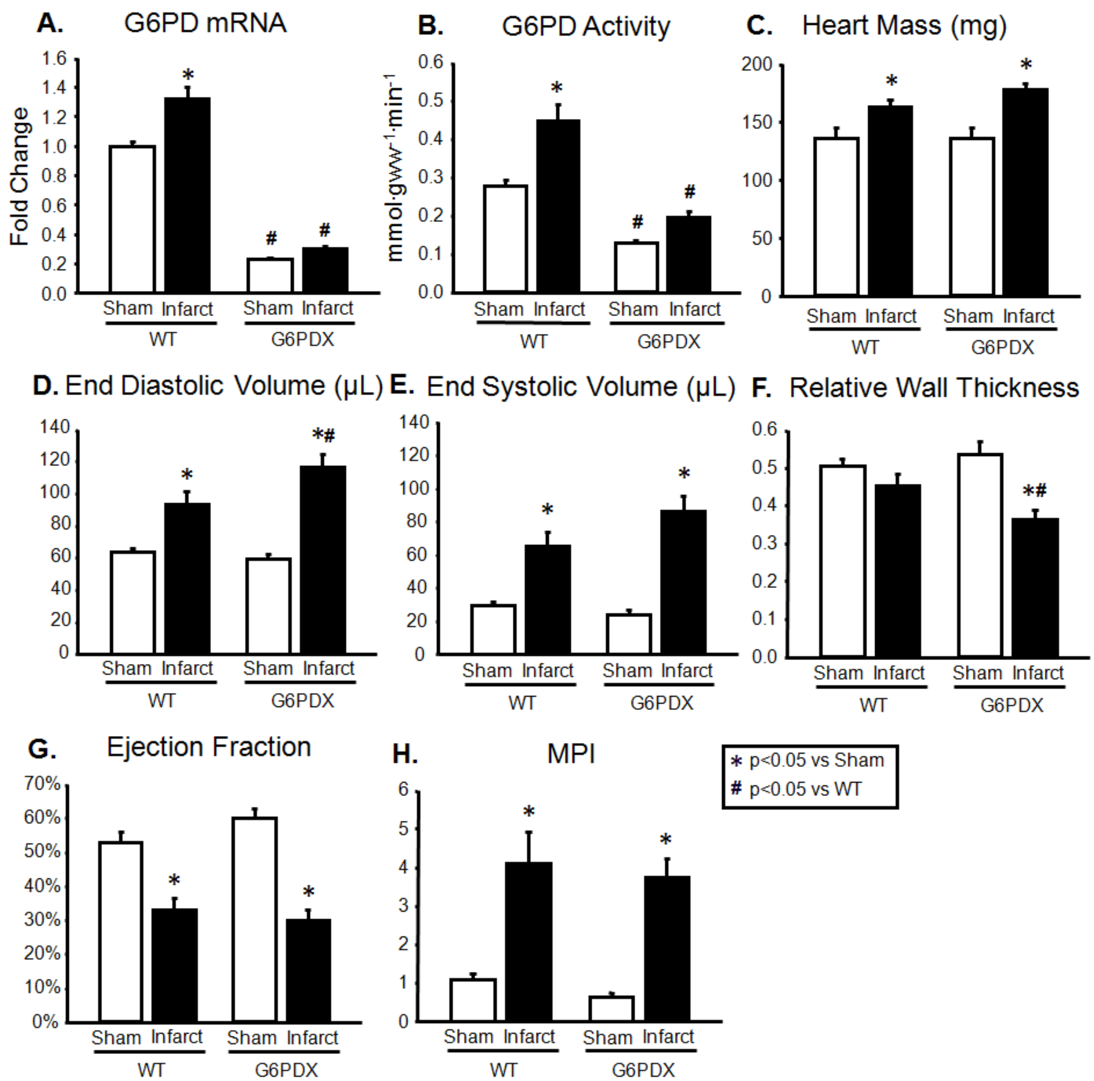

Figure 3.2. **G6PD deficiency exacerbates LV hypertrophy and dilation, but does not affect function after myocardial infarction**. **A-B**. Myocardial G6PD mRNA expression and enzymatic activity were increased by LAD ligation in WT mice, but not in G6PD deficient mice. **C**. Myocardial infarction increased heart mass indicating myocardial hypertrophy. **D-E**. Myocardial infarction increased LV end diastolic and end systolic volume. LV end diastolic volume was increased further by G6PD deficiency, further indicating that G6PD deficiency increased susceptibility to LV dilation. **F**. Myocardial infarction resulted in decreased relative wall thickness in G6PDX mice, indicating that G6PD deficiency increased susceptibility to dilation. **G-I**. Myocardial infarction led to adverse cardiac function, as indicated decreased ejection fraction indicating systolic dysfunction, and increased MPI and LV end diastolic pressure indicating diastolic dysfunction. These functional parameters were unaffected by G6PD deficiency. Data were obtained using mice at 12 weeks after LAD ligation or sham surgery; *P <0.05 vs. Sham; #P <0.05 vs. WT; Sham n=9-10/group, WT infarct n=19, G6PDX infarct n=27-28.

Table 3.2.

Parameter	Wild Type		G6PD Deficient	
	Sham	Infarct	Sham	Infarct
Fractional Shortening %	*27.0±2.3*	*16.0±1.7**	*31.7±2.3*	*14.6±1.4**
Stroke Volume (µL)	*34.0±2.4*	*27.9±1.7**	*35.5±2.4*	*30.0±1.4**
AWT;d (mm)	*0.97±0.08*	*0.92±0.06*	*1.03±0.08*	*0.75±0.05*#*
AWT;s (mm)	*1.37±0.10*	*1.14±0.07*	*1.40±0.10*	*0.93±0.06*#*
End Diastolic Diameter (mm)	*3.85±0.20*	*4.46±0.15**	*3.73±0.20*	*4.90±0.12*#*
End Systolic Diameter (mm)	*2.81±0.26*	*3.78±0.19**	*2.56±0.26*	*4.24±0.15**
PWT;d (mm)	*0.97±0.06*	*1.02±0.04*	*0.96±0.06*	*0.98±0.04*
PWT;s (mm)	*1.26±0.07*	*1.24±0.05*	*1.37±0.07*	*1.19±0.04*
Absolute Wall Thickness (mm)	*1.94±0.09*	*1.94±0.07*	*1.99±0.09*	*1.73±0.06*
End Diastolic Area (mm^2)	*11.2±1.4*	*16.3±1.0**	*10.7±1.4*	*17.6±0.9**
End Systolic Area (mm^2)	*7.2±1.5*	*12.8±1.1**	*6.3±1.5*	*14.5±0.9**
Area Fractional Shortening %	*35.7±3.0*	*23.9±2.2**	*41.1±3.0*	*19.3±1.8**
E/A Ratio	*1.91±0.18*	*1.58±0.14*	*1.73±0.18*	*1.65±0.11*
Isovolumetric Contraction Time (ms)	*16.7±4.0*	*26.1±3.0*	*11.1±4.0*	*26.3±2.5**
Isovolumetric Relaxation Time (ms)	*26.3±3.3*	*34.4±2.4*	*17.2±3.2*	*37.0±2.0**
Ejection Time (ms)	*40.7±3.2*	*21.9±2.3**	*44.4±3.2*	*22.2±1.9**
Myocardial Performance Index	*1.11±0.74*	*4.12±0.55**	*0.67±0.74*	*3.75±0.45**
Aortic Root Diameter (mm)	*1.40±0.04*	*1.40±0.03*	*1.43±0.04*	*1.38±0.02*
Heart Rate (bpm)	*445±16*	*458±12*	*489±16*	*471±10*

Data were obtained using mice anesthetized with 1.5% isoflurane at 11 weeks after LAD ligation or sham surgery; *P <0.05 vs. Sham; #P <0.05 vs. WT; Sham n=10/group, WT Infarct n=19, G6PDX n=28. AWT;d, anterior wall thickness at diastole; AWT;s, anterior wall thickness at systole; PWT;d, posterior wall thickness at diastole; PWT;s, anterior wall thickness at systole; bpm, beats per minute.

Table 3.3.

Parameter	Wild Type		G6PD Deficient	
	Sham	Infarct	Sham	Infarct
Ejection Fraction %	*46.9±3.7*	*32.1±2.9**	*53.3±3.7*	*29.6±2.2**
Fractional Shortening %	*19.6±1.7*	*12.5±1.3**	*22.7±1.7*	*11.3±1.0**
Stroke Volume (µL)	*27.4±3.2*	*27.2±2.4*	*32.6±3.2*	*31.1±1.9*
End Diastolic Volume (µL)	*61.7±9.3*	*90.1±7.1**	*62.3±9.3*	*110.8±5.5*#*
End Systolic Volume (µL)	*34.4±8.5*	*63.0±6.6**	*29.7±8.5*	*79.7±5.1*#*
AWT;d (mm)	*1.19±0.07*	*1.01±0.05**	*1.08±0.07*	*0.90±0.04**
AWT;s (mm)	*1.44±0.08*	*1.21±0.06**	*1.39±0.08*	*1.04±0.05*#*
End Diastolic Diameter (mm)	*3.87±0.14*	*4.35±0.11**	*3.87±0.14*	*4.69±0.09*#*
End Systolic Diameter (mm)	*3.13±0.17*	*3.82±0.13**	*3.00±0.17*	*4.18±0.10*#*
PWT;d (mm)	*0.81±0.07*	*0.90±0.05*	*0.86±0.07*	*0.92±0.04*
PWT;s (mm)	*0.93±0.08*	*1.01±0.06*	*1.07±0.08*	*1.08±0.05*
Absolute Wall Thickness (mm)	*2.00±0.11*	*1.91±0.08*	*1.94±0.11*	*1.83±0.06*
Relative Wall Thickness (mm)	*0.53±0.04*	*0.45±0.03*	*0.52±0.04*	*0.39±0.02**
End Diastolic Area (mm^2)	*11.0±1.0*	*15.1±0.7**	*11.0±1.0*	*17.3±0.6*#*
End Systolic Area (mm^2)	*8.0±1.0*	*13.0±0.8**	*8.0±1.0*	*14.8±0.6**
Area Fractional Shortening %	*27.9±2.2*	*15.0±1.7**	*28.2±2.2*	*15.3±1.3**
Isovolumetric Contraction Time (ms)	*25.5±4.7*	*34.6±3.7*	*19.6±5.2*	*36.6±2.9**
Isovolumetric Relaxation Time (ms)	*16.5±3.1*	*29.4±2.4**	*17.3±3.5*	*25.2±1.9**
Ejection Time (ms)	*41.5±3.1*	*34.8±2.5*	*36.8±3.5*	*36.9±1.9*
Myocardial Performance Index	*1.03±0.28*	*2.05±0.23**	*1.03±0.32*	*1.98±0.17**
Aortic Root Diameter (mm)	*1.30±0.04*	*1.17±0.03**	*1.21±0.04*	*1.18±0.02*
Body Mass (g)	*34.7±1.0*	*34.2±0.8*	*33.1±1.0*	*32.7±0.6*
Heart Rate (bpm)	*530±16*	*489±12*	*534±16*	*497±10*

Data were obtained using mice anesthetized with 2.5% isoflurane at 7 weeks after LAD ligation or sham surgery; *P <0.05 vs. Sham; #P <0.05 vs. WT; Sham n=10/group, WT Infarct n=17, G6PDX n=28. AWT;d, anterior wall thickness at diastole; AWT;s, anterior wall thickness at systole; PWT;d, posterior wall thickness at diastole; PWT;s, anterior wall thickness at systole; BPM, beats per minute.

Table 3.4.

Parameter	Wild Type		G6PD Deficient	
	Sham	Infarct	Sham	Infarct
Myocyte Cross Sectional Area (μm^2)	*633±18*	*660±13*	*635±18*	*655±11*
Volume Fraction Interstitial Fibrosis %	*12.4±0.7*	*12.3±0.5*	*11.2±0.7*	*12.0±0.4*
Capillaries/mm^2	*2275±109*	*2111±79*	*2256±109*	*1928±68**

Data were obtained using myocardium from mice at 12 weeks after LAD ligation or sham surgery; *P <0.05 vs. Sham; #P <0.05 vs. WT; Sham n=10/group, WT Infarct n=19, G6PDX n=26.

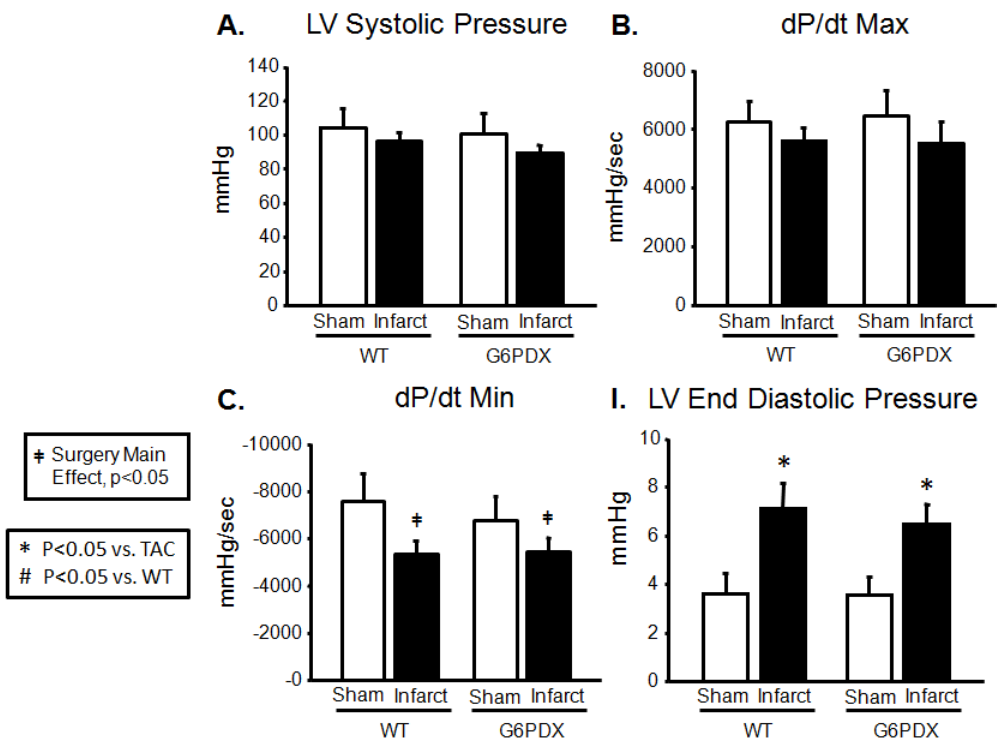

Figure 3.3. **Effect of infarction on LV Pressure**. **A-B**. LV end systolic pressure and dp/dt max were unaffected by G6PD deficiency or myocardial infarction. **C**. Myocardial infarction decreased dp/dt min (p=0.030 for main effect), but this parameter not affected by G6PD deficiency. **D**. Myocardial infarction increased end LV diastolic pressure in WT and G6PDX mice to the same extent. Data were obtained using mice at 12 weeks after LAD ligation or sham surgery; ǂ main effect of surgery, *P <0.05 vs. Sham; #P <0.05 vs. WT; Sham n=7-10/group, Infarct n=14-18/group. dP/dt, change in pressure over time.

Effects of G6PD Deficiency on Biochemical Parameters after Myocardial Infarction

Myocardial [NADPH] is increased in severe heart failure[3, 6], and we saw an increase in myocardial [NADPH] in infarcted G6PDX mice (Figure 3.4A). Although myocardial superoxide production was unaffected by infarction or G6PD deficiency, infarction increased myocardial lipid peroxidation products in G6PDX mice suggesting increased oxidative stress with G6PD deficiency (Figure 3.4B-C). Heart failure decreases the capacity for oxidative metabolism in myocardium, as reflected in a decrease in the activities of aconitase, citrate synthase, and MCAD. The activities of these enzymes were decrease by myocardial infarction but were unaffected by G6PD deficiency (Figure 3.4D-F). Heart failure increases myocardial mRNA expression of the fetal genes ANP and MHCβ, and expression of these genes was increased by infarction but unaffected by G6PD deficiency (Figure 3.4G-H; Table 3.5). Taken together, these results suggest that G6PD deficiency increased oxidative stress, but not other indicators of heart failure in response to myocardial infarction.

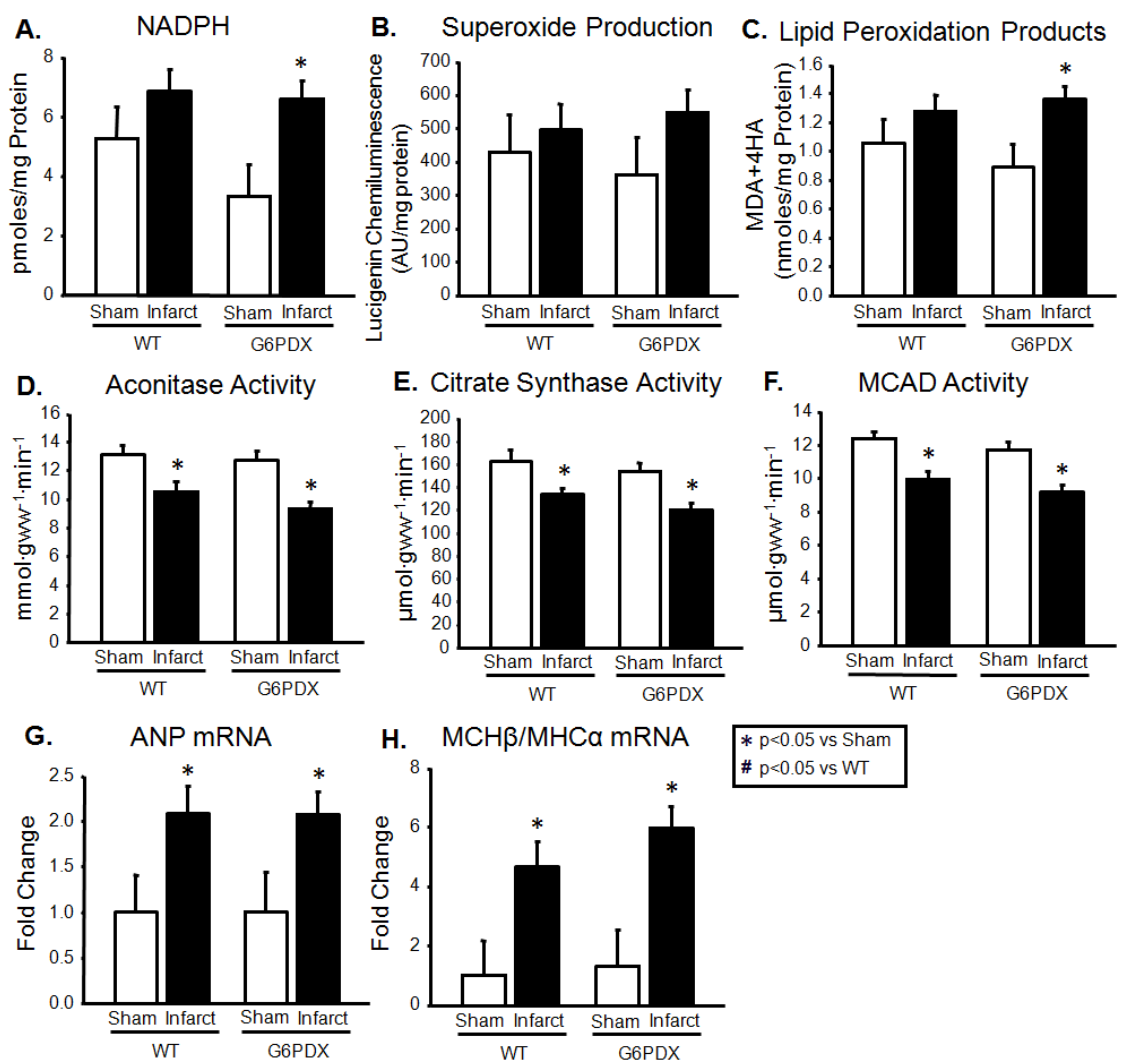

Figure 3.4. **Infarction - Biochemical Data**. **A**. Infarction increased myocardial [NADPH] in G6PDX mice. **B**. Myocardial superoxide production was unaffected by infarction or G6PD deficiency. **C**. Infarction increased myocardial lipid peroxidation

products in G6PDX mice. **D-F**. Infarction decreased myocardial aconitase activity, citrate synthase activity, and MCAD activity. The activities of these enzymes were unaffected by G6PD deficiency. **G-H**. Myocardial ANP and MHCβ/MHCα mRNA were also increased by infarction and unaffected by G6PD deficiency. Data were obtained using myocardium from mice at 12 weeks after LAD ligation or sham surgery; *P <0.05 vs. Sham; #P <0.05 vs. WT; Sham n=9-10/group, WT infarct n=19, G6PDX infarct n=27-28. 4HA, 4-hydroxyalkenals; ANP, atrial natriuretic peptide; gww, grams of wet weight tissue; MCAD, medium chain acyl-coenzyme A dehydrogenase; MHC, myosin heavy chain; NADPH, nicotinamide adenine dinucleotide phosphate; MDA, malondialdehyde.

Table 3.5.

Parameter	Wild Type		G6PD Deficient	
	Sham	Infarct	Sham	Infarct
ANP (Ct)	*18.0±0.3*	*17.2±0.2**	*17.9±0.3*	*17.0±0.2**
MHCβ (Ct)	*22.7±0.3*	*21.2±0.2**	*22.3±0.3*	*20.9±0.2**
MHCα (Ct)	*14.3±0.2*	*14.7±0.1*	*14.3±0.2*	*14.9±0.1**
G6PD (Ct; Exons 1-2)	*25.9±0.1*	*25.6±0.1*	*28.7±0.1#*	*28.4±0.1#*
G6PD (Fold Change; Exons 1-2)	*1.00±0.07*	*1.27±0.05**	*0.15±0.07#*	*0.18±0.04#*
G6PD (Ct; Exons 12-13)	*25.3±0.1*	*25.0±0.1**	*27.5±0.1#*	*27.1±0.1#*
18s (Ct)	*6.03±0.23*	*6.15±0.17*	*6.11±0.24*	*6.15±0.14*

Data were obtained using myocardium from mice at 12 weeks after LAD ligation or sham surgery; *P <0.05 vs. Sham; #P <0.05 vs. WT; Sham n=9-10/group, WT Infarct n=19, G6PDX n=27. 18s, ribosomal RNA; ANP, atrial natriuretic peptide; Ct, cycle at which threshold is crossed; MHC, myosin heavy chain; G6PD, glucose 6-phosphate dehydrogenase.

Transverse Aortic Constriction Results

Recovery and Survival after TAC

A total of 28 WT mice and 24 G6PDX mice underwent TAC with a 28 gauge needle, while 7 WT mice and 7 G6PDX mice underwent sham surgery. TAC 24 hour survival was 39% for WT mice and 54% for G6PDX mice (p=0.43 for difference). Minimal mortality was again observed from 1 day to 6 weeks after TAC, with no differences among groups (Figure 3.5, 91% survival for WT mice and 92% survival for G6PDX mice). There were no differences in body mass (Table 3.6).

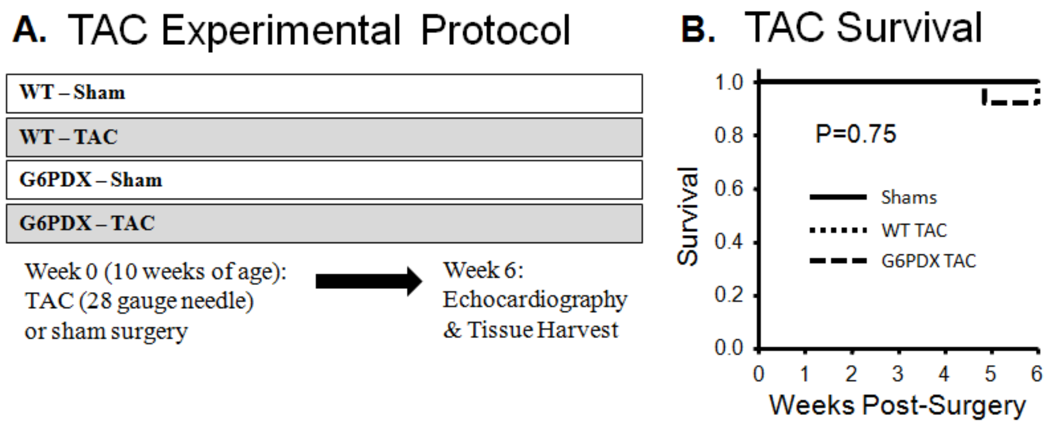

Figure 3.5. **A**, *TAC Experimental Protocol*. Ten week-old mice underwent TAC or sham surgery. TAC was performed using a 28 gauge needle. Echocardiography and euthanization were performed at 6 weeks. **B**, *Post-TAC Survival*. Neither surgery nor G6PD deficiency affected post-TAC survival over the course of the study (p=0.75). Time 0 of the survival curve begins 1 day after TAC, so the data are representative of survival after complete recovery from the surgery. Survival was assessed by Log-Rank Kaplan Meier analysis; n=38 total mice, Sham n=7/group, TAC n=11-13/group.

Table 3.6.

Parameter	Wild Type		G6PD Deficient	
	Sham	TAC	Sham	TAC
Beginning Body Mass (g)	*25.5±0.4*	*25.6±0.4*	*25.6±0.4*	*25.5±0.3*
Terminal Body Mass (g)	*29.4±0.5*	*29.5±0.5*	*29.9±0.5*	*28.4±0.4*
Body Mass Increase %	*15.4±2.5*	*15.2±2.1*	*17.1±2.5*	*11.6±1.9*
Tibia Length (mm)	*19.4±0.1*	*19.5±0.1*	*19.7±0.1*	*19.7±0.1*
LV Mass (mg)	*87±4*	*131±4**	*88±4*	*137±3**
LV Mass/Body Mass (mg/g)	*2.96±0.18*	*4.46±0.15**	*2.94±0.18*	*4.85±0.14**
RV Mass (mg)	*20.4±3.6*	*29.2±3.0*	*21.2±3.6*	*30.6±2.8**
RV Mass/Tibia Length (mg/mm)	*1.05±0.18*	*1.49±0.15*	*1.08±0.18*	*1.55±0.14**
Atrial Mass (mg)	*4.9±2.4*	*11.9±2.0**	*5.5±2.4*	*15.8±1.8**
Atrial Mass/Tibia Length (µg/mm)	*250±119*	*609±99**	*280±119*	*800±91**
Wet/Dry Lung Weight Ratio	*4.91±0.12*	*4.86±0.10*	*4.73±0.12*	*4.83±0.09*
Liver Mass (g)	*1.55±0.05*	*1.47±0.04*	*1.53±0.05*	*1.41±0.04**
Kidney Mass (mg)	*250±10*	*233±8*	*246±10*	*212±8**
Epididymal Fat Mass (mg)	*798±68*	*702±57*	*908±68*	*587±52**

Data were obtained using mice at 6 weeks after Sham or TAC surgery with a 28 gauge needle; *P <0.05 vs. Sham; #P <0.05 vs. WT; Sham n=7/group, TAC=10-12/group. LV, left ventricle; RV, right ventricle.

G6PD Deficiency Increases Propensity for LV Dilation after TAC

TAC increased LV mass to the same extent in WT and G6PDX mice (Figure 3.6C), however only G6PDX mice had a statistically significant increase in LV end diastolic and end systolic volumes, and absolute wall thickness, (Figure 3.6D-F; Table 3.7). This indicates that G6PD deficiency increased the propensity for LV dilation. TAC decreased systolic function, as indicated by decreased ejection fraction, but with no effect of G6PD deficiency (Figure 3.6G). TAC increased G6PD mRNA and G6PD activity in WT mice, but not in G6PDX mice (Figure 3.6A-B). G6PD deficiency may increase the propensity for wasting, or cachexia. Cachexia, which indicates poor prognosis in heart failure[214], and TAC resulted in decreased epididymal fat mass, liver mass, and kidney mass in G6PDX mice but not WT animals (Table 3.6). These changes were observed despite no change in overall body mass.

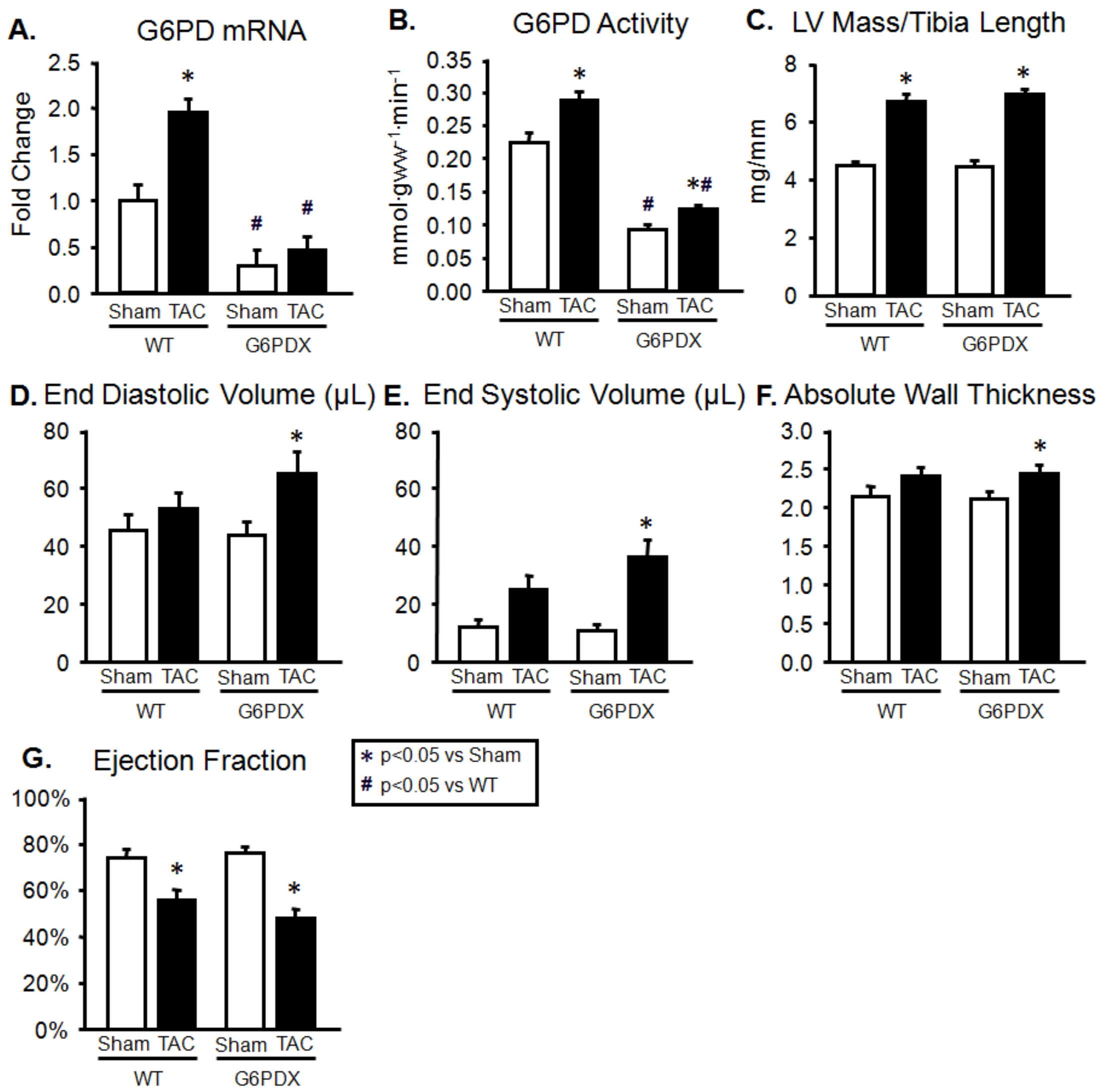

Figure 3.6. **G6PD deficiency increases propensity for LV dilation after TAC**. **A-B**. TAC increased G6PD mRNA and G6PD activity in WT mice, but not in G6PDX mice. **C**. TAC increased LV mass to the same extent in WT and G6PDX mice. **D-F**. TAC increased LV end diastolic volume, end systolic volume, and absolute wall thickness in G6PDX mice. **G**. TAC decreased systolic function to the same extent in G6PDX and WT mice. Data were obtained using mice at 6 weeks after Sham or TAC surgery with a 28 gauge needle; *P <0.05 vs. Sham; #P <0.05 vs. WT; Sham n=7/group, TAC=10-12/group.

Table 3.7.

Parameter	Wild Type		G6PD Deficient	
	Sham	TAC	Sham	TAC
Fractional Shortening %	*42.8±2.8*	*29.0±2.4**	*44.0±2.8*	*24.2±2.2**
Stroke Volume (μL)	*33.4±2.2*	*27.9±1.8*	*32.8±2.2*	*29.1±1.7*
AWT;d (mm)	*1.07±0.07*	*1.18±0.06*	*1.03±0.07*	*1.15±0.06*
AWT;s (mm)	*1.48±0.09*	*1.62±0.07*	*1.47±0.09*	*1.57±0.07*
End Diastolic Diameter (mm)	*3.32±0.19*	*3.53±0.16*	*3.26±0.19*	*3.83±0.14**
End Systolic Diameter (mm)	*1.92±0.22*	*2.54±0.18**	*1.85±0.22*	*2.94±0.17**
PWT;d (mm)	*1.08±0.07*	*1.22±0.06*	*1.10±0.07*	*1.29±0.06**
PWT;s (mm)	*1.55±0.09*	*1.51±0.08*	*1.53±0.09*	*1.53±0.07*
Relative Wall Thickness	*0.66±0.07*	*0.70±0.06*	*0.67±0.07*	*0.67±0.05*
End Diastolic Area (mm^2)	*8.27±1.03*	*9.89±0.86*	*8.40±1.03*	*10.21±0.79*
End Systolic Area (mm^2)	*4.34±0.93*	*6.62±0.78*	*4.58±0.93*	*7.24±0.71**
Area Fractional Shortening %	*47.9±4.3*	*35.2±3.6**	*46.3±4.3*	*30.2±3.3**
E/A Ratio	*1.20±0.13*	*1.57±0.11*	*1.19±0.13*	*1.23±0.10*
Isovolumetric Contraction Time (ms)	*14.2±2.9*	*10.3±2.5*	*10.1±2.9*	*17.0±2.3*
Isovolumetric Relaxation Time (ms)	*22.0±4.3*	*23.4±3.6*	*20.7±4.3*	*22.1±3.4*
Ejection Time (ms)	*30.6±3.0*	*36.6±2.5*	*30.3±3.0*	*36.5±2.4*
Myocardial Performance Index	*1.25±0.33*	*1.16±0.28*	*1.13±0.33*	*1.23±0.27*
Aortic Root Diameter (mm)	*1.33±0.03*	*1.32±0.02*	*1.31±0.03*	*1.33±0.02*
Heart Rate (bpm)	*632±17*	*611±14*	*609±17*	*585±13*

Data were obtained using mice anesthetized with 1% isoflurane at 6 weeks after Sham or TAC surgery with a 28 gauge needle; *P<0.05 vs. Sham; #P<0.05 vs. WT; Sham n=7/group, TAC=10-12/group. AWT;d, anterior wall thickness at diastole; AWT;s, anterior wall thickness at systole; PWT;d, posterior wall thickness at diastole; PWT;s, anterior wall thickness at systole; bpm, beats per minute.

Effects of G6PD Deficiency on Biochemical Parameters after TAC

As with myocardial infarction, [NADPH] was increased in G6PDX mice in response to TAC (Figure 3.7A). G6PD deficiency decreased superoxide production (Figure 3.7B). There was no effect of G6PD deficiency or TAC on lipid peroxidation products (Figure 3.7C). TAC decreased myocardial aconitase activity, citrate synthase activity, and MCAD activity to the same extent in G6PDX and WT mice (Figure 3.7D-F), and these changes corresponded with an increase in ANP and MHCβ/MHCα mRNA (Figure 3.7G-H; Table 3.8).

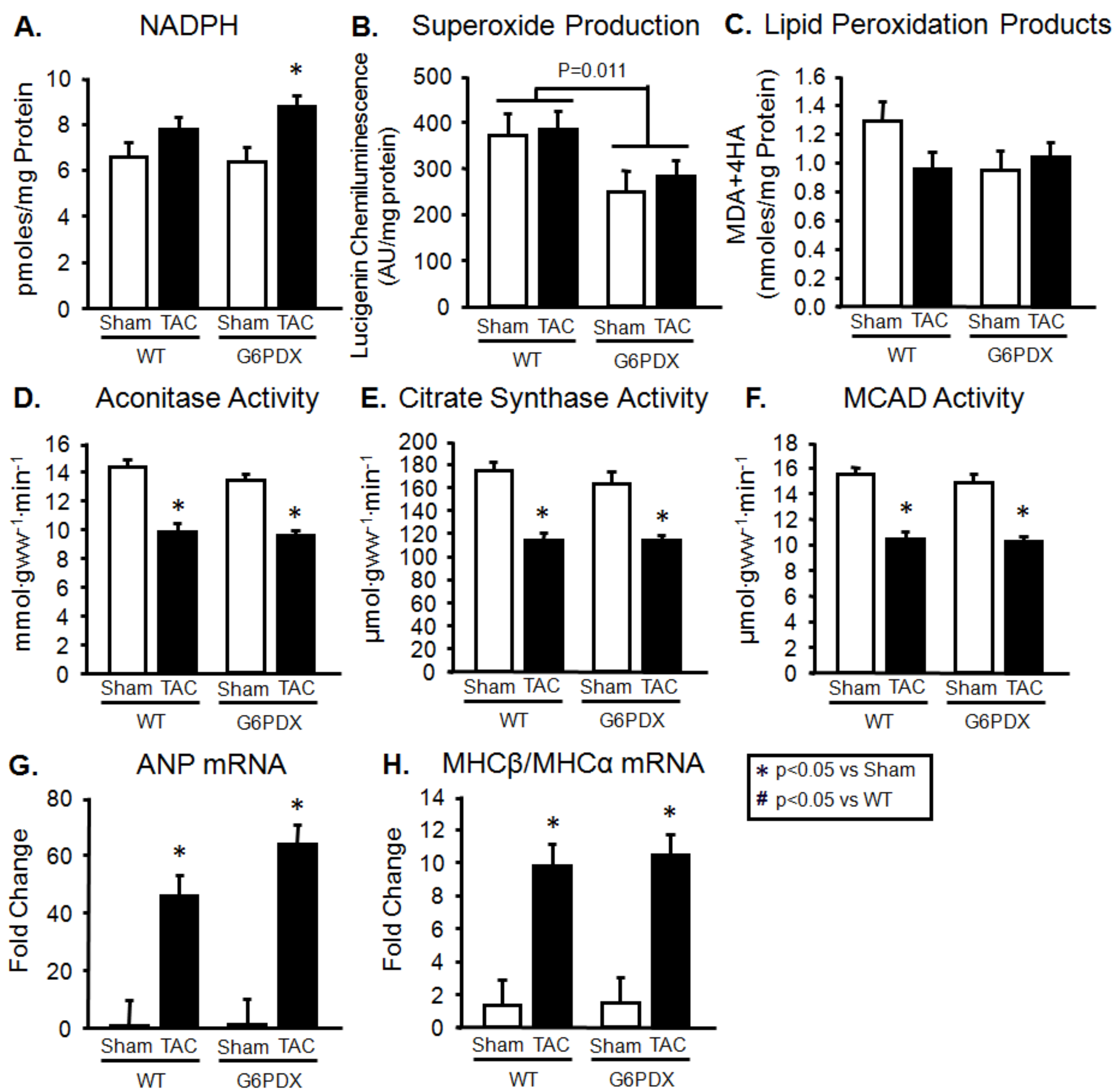

Figure 3.7. **TAC - Biochemical Data**. **A**. LV NADPH was increased by TAC in G6PDX mice. **B**. Superoxide production was decreased by G6PD deficiency. **C**. Lipid peroxidation products were unaffected by G6PD deficiency or TAC. **D-F**. TAC decreased myocardial aconitase activity, citrate synthase activity, and MCAD activity to the same extent in G6PDX and WT mice **G-H**. TAC increased ANP and MHCβ/MHCα in WT and G6PDX mice to the same extent. Data were obtained using left ventricular myocardium from mice at 6 weeks after Sham or TAC surgery with a 28 gauge needle; *P <0.05 vs. Sham; #P <0.05 vs. WT; Sham n=7/group, TAC=10-12/group. 4HA, 4-hydroxyalkenals; ANP, atrial natriuretic peptide; gww, grams of wet weight tissue; MCAD, medium chain acyl-coenzyme A dehydrogenase; MHC, myosin heavy chain; NADPH, nicotinamide adenine dinucleotide phosphate; MDA, malondialdehyde.

Table 3.8.

Parameter	Wild Type		G6PD Deficient	
	Sham	TAC	Sham	TAC
ANP (Ct)	*22.6±0.4*	*17.2±0.4**	*22.2±0.4*	*16.8±0.3**
MHCβ (Ct)	*23.5±0.2*	*20.3±0.2**	*23.0±0.2*	*20.0±0.2**
MHCα (Ct)	*16.6±0.3*	*16.4±0.2*	*16.4±0.3*	*16.3±0.2*
G6PD (Ct)	*28.6±0.3*	*27.5±0.3**	*30.6±0.3#*	*29.6±0.3*#*
18s (Ct)	*8.34±0.30*	*7.43±0.25*	*7.52±0.30*	*7.31±0.24*

Data were obtained using left ventricular myocardium from mice at 6 weeks after Sham or TAC surgery with a 28 gauge needle; *P<0.05 vs. Sham; #P<0.05 vs. WT; Sham n=7/group, TAC=10-11/group. 18s, ribosomal RNA; ANP, atrial natriuretic peptide; Ct, cycle at which threshold is crossed; MHC, myosin heavy chain; G6PD, glucose 6-phosphate dehydrogenase.

High Fructose Intake and Transverse Aortic Constriction Results

Recovery and Survival after Fructose/TAC

A total of 55 WT mice and 47 G6PDX mice underwent moderate TAC with a 27 gauge needle, while 28 WT mice and 29 G6PDX mice underwent sham surgery. Immediately following surgery, mice were assigned to either a high starch or a high fructose diet (Table 3.9). TAC 24 hour survival was 65% for WT mice and 72% for G6PDX mice (p=0.59 for difference). There was minimal mortality from 1 day to 17 weeks after TAC, with no differences among groups (Figure 3.8). G6PDX mice consumed a greater amount of energy on the high fructose diet compared to the high starch diet, but this did not affect body or fat pad mass, and there were no differences in body mass throughout the 17 weeks following surgery (Table 3.10-3.11).

Table 3.9.

	Fat		Carbohydrate			Protein
Diet	Soy Oil	Lard	Cornstarch	Maltodextrin	Fructose	Casein
Starch	6	4	57	12	0	20
Fructose	6	4	9	0	60	20

Values are energy contribution to the diet (% of total). Diets were matched for vitamin and mineral content.

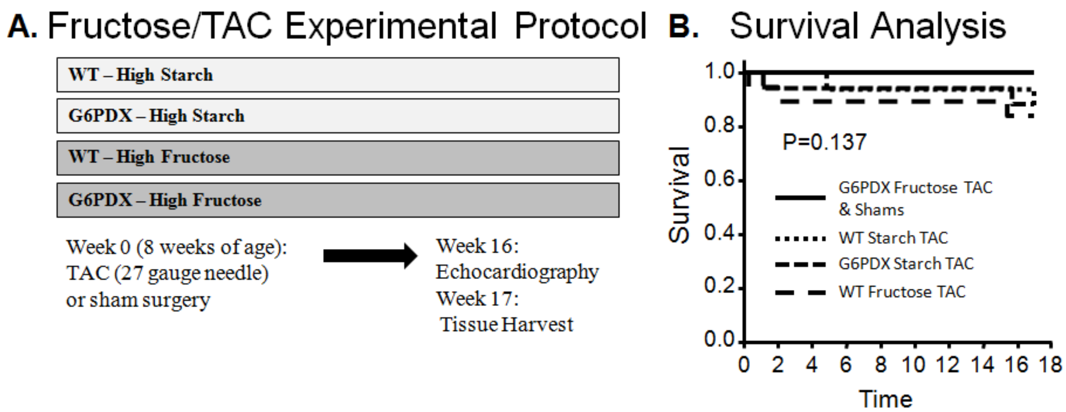

Figure 3.8. **A**, *Fructose/TAC Experimental Protocol*. Eight week-old mice underwent sham or TAC surgery with a 27 gauge needle, and were placed on a high starch or high fructose diet on the following day. Echocardiography was performed at 16 weeks, and mice were euthanized at 17 weeks for biochemical analysis. **B**, *Post-TAC survival*. Post-TAC survival was unaffected by surgery, G6PD deficiency, or diet over the course of the study (p=0.137). Time 0 of the survival curve begins 1 day after TAC, so the data are representative of survival after complete recovery from the surgery. Survival was assessed by Log-Rank Kaplan Meier analysis; n=126 total mice, n=14-19/group.

Table 3.10.

Parameter	Wild Type		G6PD Deficient	
	Starch	Fructose	Starch	Fructose
Food Intake ($g \cdot mouse^{-1} \cdot day^{-1}$)	*2.94±0.14*	*3.11±0.09*	*2.80±0.11*	*3.16±0.13**
Energy Intake ($Calories \cdot mouse^{-1} \cdot day^{-1}$)	*11.3±0.5*	*12.0±0.4*	*10.8±0.4*	*12.2±0.5**

Data were obtained using mice over a course of 17 weeks following Sham or TAC surgery with a 27 gauge needle; *P <0.05 vs. Starch; #P <0.05 vs. WT; n=6-7 cages/group.

Table 3.11.

Parameter	Wild Type Sham	Wild Type TAC	G6PD Deficient Sham	G6PD Deficient TAC
High Starch Diet				
Initial Body Mass (g)	*24.0±0.4*	*24.1±0.2*	*24.1±0.3*	*24.1±0.4*
Terminal Body Mass (g)	*33.6±1.0*	*32.4±1.0*	*33.8±1.0*	*32.5±1.0*
Tibia Length (mm)	*20.0±0.1*	*20.2±0.1*	*20.3±0.1*	*20.2±0.1*
LV Mass (mg)	*91±5*	*127±5**	*90±5*	*115±5**
LV/Body Mass (mg/g)	*2.71±0.20*	*4.00±0.18**	*2.67±0.20*	*3.58±0.19**
RV Mass (mg)	*22.5±2.3*	*31.4±2.1**	*22.9±2.3*	*22.8±2.1#*
RV/Tibia (mg/mm)	*1.12±0.12*	*1.56±0.10*	*1.13±0.12*	*1.13±0.11*
Atrial Mass (mg)	*6.7±2.1*	*16.4±1.9**	*6±2.1*	*8.6±1.9#*
Atria/Tibia (µg/mm)	*335±105*	*815±97**	*295±105*	*422±97#*
Liver Mass (g)	*1.72±0.05*	*1.60±0.05*	*1.62±0.05*	*1.61±0.05*
Kidney Mass (mg)	*257±8*	*237±7*	*256±8*	*239±7*
Epididymal Fat Mass (mg)	*1.10±0.11*	*0.88±0.10*	*1.08±0.11*	*0.91±0.11*
High Fructose Diet				
Initial Body Mass (g)	*24.0±0.4*	*23.9±0.3*	*24.0±0.3*	*24.2±0.3*
Terminal Body Mass (g)	*34.3±0.8*	*34.8±0.8*	*34.3±0.8*	*32.4±0.8*
Tibia Length (mm)	*20.2±0.1*	*20.1±0.1*	*20.2±0.1*	*20.2±0.1*
LV Mass (mg)	*92±4*	*123±4**	*90±5*	*137±4*#*
LV/Body Mass (mg/g)	*2.70±0.16*	*3.53±0.16**	*2.62±0.17*	*4.30±0.16*#*
RV Mass (mg)	*23.0±2.2*	*25.8±2.1*	*23.2±2.3*	*31.6±2.1**
RV/Tibia (mg/mm)	*1.14±0.11*	*1.28±0.10*	*1.15±0.11*	*1.57±0.10*#*
Atrial Mass (mg)	*6.5±1.1*	*10.2±1.1**	*6.2±1.2*	*12.9±1.1**
Atria/Tibia (µg/mm)	*323±54*	*506±52**	*309±57*	*642±52**
Liver Mass (g)	*1.93±0.06*	*1.88±0.06*	*1.88±0.07*	*1.82±0.06*
Kidney Mass (mg)	*267±8*	*252±8*	*247±9*	*229±8#*
Epididymal Fat Mass (mg)	*1.16±0.09*	*1.28±0.08*	*1.22±0.09*	*0.91±0.08*#*

Data were obtained using mice at 17 weeks after Sham or TAC surgery with a 27 gauge needle; *P <0.05 vs. TAC; #P <0.05 vs. WT; Sham n=12-13/group, TAC n=14-15/group. LV, left ventricle; RV, right ventricle.

G6PD Deficiency Exacerbates the Cardiac Effects of Pressure Overload with High Fructose Intake

TAC increased LV mass in all groups, but to a greater extent in G6PDX mice compared to WT mice after high fructose intake (Figure 3.9B). Atrial and right ventricular mass were also increased by TAC, with a greater increase in right ventricular mass in G6PDX mice compared to WT mice after high fructose intake (Table 3.11). Caudal systolic blood pressure was unaffected by TAC or G6PD deficiency (Table 3.12).

TAC resulted in decreased stroke volume and concentric hypertrophy indicated by increased absolute and relative wall thickness (Table 3.13). G6PD deficient animals displayed systolic dysfunction, as seen by an increase in LV end systolic volume and a decrease in ejection fraction in response to TAC after high fructose intake (Figure 3.9C). TAC increased LV fetal gene expression, as indicated by increased MHCβ/MHCα and ANP mRNA in all groups (Figure 3.9D; Table 3.14). The greatest ANP expression was in G6PDX mice with the high fructose diet. TAC also increased left ventricular G6PD activity in WT mice on the high starch diet (Figure 3.9A). G6PD activity was unaffected by TAC in WT mice fed the high fructose diet, and decreased in G6PDX mice. Taken together, the results indicate G6PD deficiency exacerbates cardiac hypertrophy and dysfunction in response to pressure overload after high fructose intake.

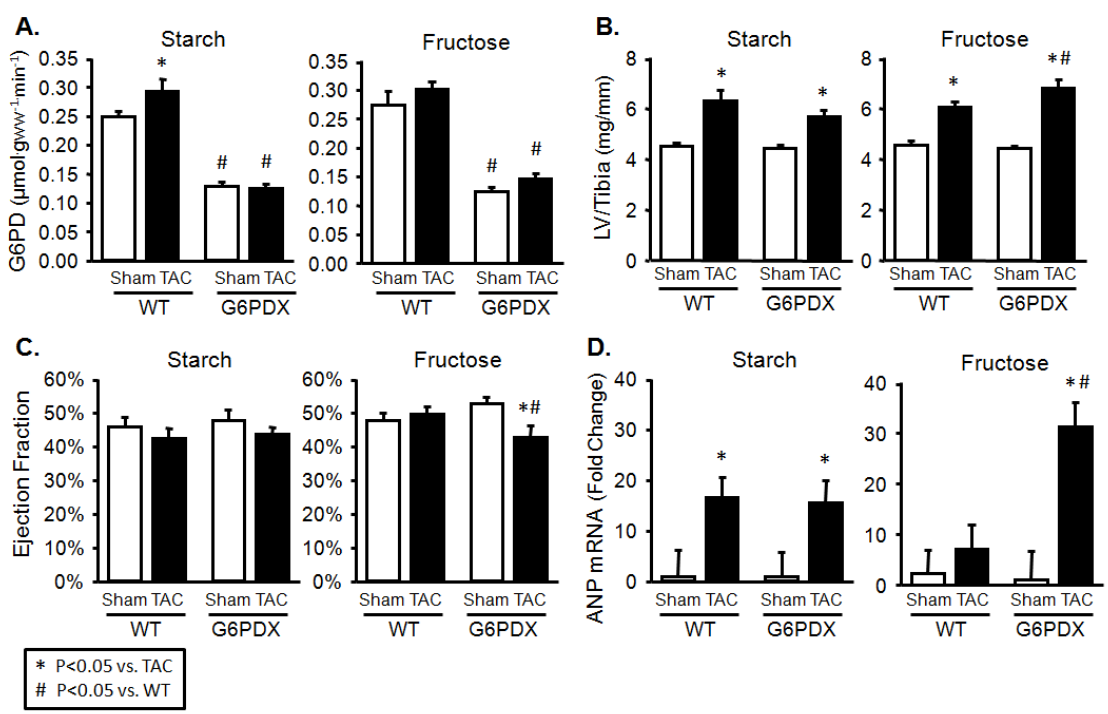

Figure 3.9. **G6PD deficiency exacerbates the cardiac effects of pressure overload with high fructose intake**. **A**. LV G6PD activity was increased by TAC in the high

starch diet, and was decreased in G6PDX mice. **B**. LV mass was increased by TAC in all groups, and was increased to the greatest extent in G6PDX mice with high fructose intake. **C**. Ejection Fraction was decreased in G6PDX mice with the high fructose diet. **D**. LV ANP mRNA expression was increased by TAC to the greatest extent in G6PD deficient animals with high fructose intake. Data were obtained 16-17 weeks post-TAC *P <0.05 vs. TAC; #P <0.05 vs. WT; Sham n=9-16/group, TAC n=12-16/group. ANP, atrial natriuretic peptide.

Table 3.12.

Parameter	Wild Type		G6PD Deficient	
	Sham	TAC	Sham	TAC
High Starch Diet				
Systolic Blood Pressure (mmHg)	*101±4*	*102±3*	*107±3*	*106±3*
Heart Rate (bpm)	*599±14*	*559±12*	*579±13*	*568±13*
High Fructose Diet				
Systolic Blood Pressure (mmHg)	*108±3*	*101±3*	*111±3*	*103±3*
Heart Rate (bpm)	*603±11*	*587±11*	*593±12*	*558±10**

Data were obtained using mice at 10 weeks after Sham or TAC surgery with a 27 gauge needle; *P <0.05 vs. TAC; #P <0.05 vs. WT; Sham n=13-16/group, TAC n=15-17/group; bpm, beats per minute.

Table 3.13.

Parameter	Wild Type		G6PD Deficient	
	Sham	TAC	Sham	TAC
16 Weeks - High Starch Diet				
Fractional Shortening %	*18.9±0.01.4*	*17.3±0.01.2*	*19.9±0.01.3*	*17.6±0.01.3*
Stroke Volume (µL)	*27.8±1.8*	*23.7±1.6*	*29.9±1.7*	*20.6±1.7**
End Diastolic Volume (µL)	*60.4±5.1*	*60.0±4.5*	*64.7±4.8*	*47.7±4.8*
End Systolic Volume (µL)	*32.6±4.2*	*36.3±3.6*	*34.8±3.9*	*27.1±3.9*
AW;d (mm)	*1.08±0.10*	*1.22±0.09*	*0.98±0.09*	*1.19±0.09*
AW;s (mm)	*1.32±0.11*	*1.49±0.09*	*1.29±0.10*	*1.46±0.10*
End Diastolic Diameter (mm)	*3.85±0.11*	*3.77±0.10*	*3.93±0.11*	*3.53±0.11**
End Systolic Diameter (mm)	*3.12±0.13*	*3.15±0.11*	*3.16±0.12*	*2.92±0.12*
PW;d (mm)	*0.77±0.08*	*1.16±0.07**	*0.82±0.07*	*1.14±0.07**
PW;s (mm)	*0.96±0.08*	*1.34±0.07**	*1.02±0.07*	*1.30±0.07**
Absolute Wall Thickness (mm)	*1.84±0.15*	*2.39±0.13**	*1.80±0.14*	*2.33±0.14**
Relative Wall Thickness	*0.48±0.06*	*0.66±0.05**	*0.47±0.05*	*0.68±0.05**
End Diastolic Area (mm^2)	*10.9±0.4*	*10.7±0.3*	*10.7±0.4*	*9.9±0.4*
End Systolic Area (mm^2)	*8.5±0.5*	*8.4±0.4*	*8.2±0.4*	*7.5±0.4*
Area Fractional Shortening %	*16.8±1.3*	*15.8±1.1*	*18.4±1.2*	*15.9±1.2*
Ejection Time (ms)	*43.1±2.4*	*48.4±2.1*	*46.2±2.3*	*44.7±2.3*
IVRT+IVCT (ms)	*48.8±5.5*	*57.5±4.8*	*43.8±5.1*	*51.2±5.2*
Myocardial Performance Index	*1.14±0.23*	*1.30±0.20*	*0.97±0.21*	*1.33±0.21*
Aortic Outflow VTI (cm)	*0.31±0.04*	*0.25±0.04*	*0.36±0.04*	*0.32±0.04*
Peak Aortic Outflow Velocity (mm/s)	*89±10*	*67±9*	*101±9*	*89±9*
Peak Mitral Inflow Velocity(mm/s)	*976±56*	*794±49*	*885±52*	*905±52*
Aortic Root Diameter (mm)	*1.18±0.039*	*1.20±0.034*	*1.20±0.036*	*1.15±0.036*
Heart Rate (bpm)	*475±13*	*466±12*	*496±12*	*491±12*
16 Weeks - High Fructose Diet				
Fractional Shortening %	*19.7±1.2*	*20.7±1.2*	*22.3±1.3*	*17.5±1.2**
Stroke Volume (µL)	*29.5±1.6*	*23.7±1.6**	*31.1±1.7*	*23.5±1.5**
End Diastolic Volume (µL)	*63.3±4.2*	*48.4±4.3*	*59.7±4.5*	*58.9±4.0*
End Systolic Volume (µL)	*33.8±3.4*	*24.7±3.5*	*28.6±3.6*	*35.5±3.3**
AW;d (mm)	*0.97±0.07*	*1.27±0.08**	*1.03±0.08*	*1.17±0.07*
AW;s (mm)	*1.23±0.08*	*1.60±0.08**	*1.31±0.08*	*1.48±0.07*
End Diastolic Diameter (mm)	*3.90±0.09*	*3.56±0.09**	*3.83±0.10*	*3.78±0.09*
End Systolic Diameter (mm)	*3.14±0.11*	*2.83±0.11**	*2.98±0.11*	*3.14±0.10#*
PW;d (mm)	*0.80±0.06*	*1.23±0.06**	*0.82±0.06*	*1.21±0.06**
PW;s (mm)	*1.03±0.06*	*1.42±0.06**	*1.06±0.06*	*1.40±0.06**
Absolute Wall Thickness (mm)	*1.77±0.10*	*2.50±0.10**	*1.84±0.11*	*2.38±0.10**
Relative Wall Thickness	*0.46±0.04*	*0.71±0.04**	*0.49±0.04*	*0.65±0.04**
End Diastolic Area (mm^2)	*10.5±0.4*	*10.0±0.4*	*10.7±0.4*	*11.1±0.3*
End Systolic Area (mm^2)	*8.2±0.4*	*7.2±0.4*	*7.5±0.4*	*8.7±0.4*#*
Area Fractional Shortening %	*19.9±±1.1*	*20.3±±1.1*	*22.2±±1.2*	*16.7±±1.1*#*
Ejection Time (ms)	*45.3±1.9*	*49.3±1.9*	*42.7±2.0*	*50.0±1.8**
IVRT+IVCT (ms)	*47.7±4.3*	*42.5±4.5*	*43.6±4.6*	*48.8±4.2*
Myocardial Performance Index	*1.07±0.09*	*0.88±0.09*	*1.02±0.09*	*0.98±0.09*
Aortic Outflow VTI (cm)	*0.32±0.04*	*0.34±0.04*	*0.33±0.05*	*0.31±0.04*
Peak Aortic Outflow Velocity (mm/s)	*93±11*	*86±11*	*103±12*	*85±11*

Table 3.13. Continued

Peak Mitral Inflow Velocity (mm/s)	*913±62*	*898±64*	*893±66*	*858±60*
Aortic Root Diameter (mm)	*1.19±0.023*	*1.19±0.023*	*1.25±0.024*	*1.23±0.022*
Heart Rate (bpm)	*493±12*	*494±13*	*498±13*	*492±12*
12 Weeks - High Starch Diet				
Ejection Fraction %	*54.0±3.1*	*45.1±2.7*	*46.7±3.0*	*44.6±2.8*
Fractional Shortening %	*25.2±2.4*	*18.4±2.1*	*19.3±2.3*	*18.0±2.1*
Stroke Volume (µL)	*29.9±1.9*	*21.1±1.7**	*26.4±1.8*	*20.5±1.7**
End Diastolic Volume (µL)	*57.0±4.2*	*48.2±3.7*	*58.4±4.0*	*46.7±3.8**
End Systolic Volume (µL)	*27.0±3.4*	*27.2±3.0*	*32.0±3.3*	*26.2±3.1*
AW;d (mm)	*1.23±0.12*	*1.24±0.10*	*1.00±0.11*	*1.07±0.11*
AW;s (mm)	*1.58±0.13*	*1.51±0.12*	*1.28±0.13*	*1.35±0.12*
End Diastolic Diameter (mm)	*3.77±0.10*	*3.54±0.09*	*3.80±0.10*	*3.50±0.09**
End Systolic Diameter (mm)	*2.83±0.14*	*2.90±0.12*	*3.07±0.13*	*2.88±0.12*
PW;d (mm)	*0.83±0.10*	*1.19±0.09**	*0.80±0.10*	*1.12±0.09**
PW;s (mm)	*0.94±0.10*	*1.38±0.09**	*1.01±0.09*	*1.29±0.09**
Absolute Wall Thickness (mm)	*2.06±0.19*	*2.43±0.16*	*1.80±0.18*	*2.19±0.17*
Relative Wall Thickness	*0.56±0.07*	*0.71±0.06*	*0.49±0.07*	*0.65±0.06*
End Diastolic Area (mm^2)	*10.0±0.5*	*10.0±0.4*	*10.6±0.5*	*9.4±0.4*
End Systolic Area (mm^2)	*7.4±0.5*	*7.5±0.4*	*7.9±0.5*	*7.0±0.4*
Area Fractional Shortening %	*26.7±2.1*	*26.4±1.9*	*25.6±2.1*	*25.6±1.9*
Ejection Time (ms)	*44.2±2.5*	*44.7±2.1*	*46.6±2.3*	*48.0±2.2*
IVRT+IVCT (ms)	*54.4±4.3*	*54.1±3.6*	*47.5±4.0*	*48.4±3.8*
Myocardial Performance Index	*1.26±0.13*	*1.29±0.11*	*1.05±0.12*	*1.06±0.11*
Aortic Outflow VTI (cm)	*0.38±0.05*	*0.25±0.04*	*0.35±0.04*	*0.36±0.04*
Peak Aortic Outflow Velocity (mm/s)	*103±12*	*71±10*	*100±11*	*99±10*
Peak Mitral Inflow Velocity (mm/s)	*1009±61*	*788±51**	*957±57*	*884±53*
Aortic Root Diameter (mm)	*1.17±0.03*	*1.19±0.03*	*1.19±0.03*	*1.14±0.03*
Heart Rate (bpm)	*472±12*	*447±10*	*481±11*	*478±11*
12 Weeks - High Fructose Diet				
Ejection Fraction %	*48.0±3.4*	*47.4±3.2*	*48.1±3.4*	*41.1±3.1*
Fractional Shortening %	*19.8±2.0*	*20.6±1.8*	*19.9±2.0*	*16.7±1.8*
Stroke Volume (µL)	*26.4±1.9*	*20.4±1.8**	*28.0±1.9*	*21.3±1.8**
End Diastolic Volume (µL)	*55.6±4.8*	*47.8±4.5*	*59.7±4.8*	*52.7±4.4*
End Systolic Volume (µL)	*29.1±3.9*	*27.4±3.6*	*31.7±3.9*	*31.4±3.5*
AW;d (mm)	*1.09±0.09*	*1.30±0.09*	*1.00±0.09*	*1.09±0.08*
AW;s (mm)	*1.32±0.10*	*1.61±0.09**	*1.24±0.10*	*1.38±0.09*
End Diastolic Diameter (mm)	*3.74±0.11*	*3.50±0.11*	*3.82±0.11*	*3.64±0.10*
End Systolic Diameter (mm)	*3.00±0.14*	*2.81±0.13*	*3.07±0.14*	*3.04±0.12*
PW;d (mm)	*0.92±0.09*	*1.24±0.08**	*0.81±0.09*	*1.35±0.08**
PW;s (mm)	*1.14±0.09*	*1.43±0.09**	*1.02±0.09*	*1.50±0.08**
Absolute Wall Thickness (mm)	*2.00±0.14*	*2.54±0.13**	*1.81±0.14*	*2.44±0.13**
Relative Wall Thickness	*0.54±0.06*	*0.76±0.06**	*0.49±0.06*	*0.69±0.05**
End Diastolic Area (mm^2)	*10.4±0.4*	*10.1±0.4*	*10.2±0.4*	*10.4±0.4*
End Systolic Area (mm^2)	*7.8±0.4*	*7.2±0.4*	*7.4±0.4*	*8.1±0.4*
Area Fractional Shortening %	*25.5±2.4*	*29.0±2.2*	*26.6±2.4*	*22.2±2.2*
Ejection Time (ms)	*48.0±1.9*	*47.7±1.7*	*47.9±1.9*	*49.4±1.7*
IVRT+IVCT (ms)	*46.8±4.1*	*49.8±3.8*	*38.8±4.1*	*48.6±3.8*

Table 3.13. Continued

Myocardial Performance Index	*0.99±0.10*	*1.09±0.09*	*0.84±0.10*	*1.02±0.09*
Aortic Outflow VTI (cm)	*0.44±0.05*	*0.43±0.05*	*0.41±0.05*	*0.36±0.05*
Peak Aortic Outflow Velocity (mm/s)	*115±13*	*118±13*	*114±13*	*91±13*
Peak Mitral Inflow Velocity(mm/s)	*1002±48*	*910±45*	*1016±48*	*911±45*
Aortic Root Diameter (mm)	*1.18±0.03*	*1.17±0.03*	*1.22±0.03*	*1.19±0.03*
Heart Rate (bpm)	*481±14*	*453±13*	*518±14*	*489±13*
8 Weeks - High Starch Diet				
Ejection Fraction %	*44.8±3.1*	*50.4±2.8*	*46.5±2.9*	*48.1±2.8*
Fractional Shortening %	*18.6±1.6*	*21.2±1.5*	*19.1±1.5*	*19.9±1.5*
Stroke Volume (µL)	*24.3±2.1*	*19.2±1.9*	*23.0±1.9*	*19.7±1.9*
End Diastolic Volume (µL)	*57.1±4.91*	*39.6±4.43**	*52.3±4.58*	*41.9±4.43*
End Systolic Volume (µL)	*32.8±3.8*	*20.5±3.4**	*29.3±3.5*	*22.2±3.4*
AW;d (mm)	*1.03±0.10*	*1.18±0.09*	*1.06±0.09*	*1.16±0.09*
AW;s (mm)	*1.27±0.10*	*1.48±0.09*	*1.29±0.09*	*1.47±0.09*
End Diastolic Diameter (mm)	*3.76±0.13*	*3.29±0.12**	*3.61±0.12*	*3.37±0.12*
End Systolic Diameter (mm)	*3.07±0.14*	*2.61±0.13**	*2.94±0.13*	*2.71±0.13*
PW;d (mm)	*0.84±0.11*	*1.31±0.10**	*0.91±0.10*	*1.28±0.10**
PW;s (mm)	*1.02±0.11*	*1.55±0.10**	*1.12±0.10*	*1.44±0.10**
Absolute Wall Thickness (mm)	*1.87±0.17*	*2.49±0.16**	*1.96±0.16*	*2.44±0.16**
Relative Wall Thickness	*0.51±0.08*	*0.81±0.07**	*0.58±0.07*	*0.75±0.07*
End Diastolic Area (mm^2)	*9.9±0.4*	*9.2±0.4*	*10.2±0.4*	*9.2±0.4*
End Systolic Area (mm^2)	*7.4±0.5*	*6.9±0.4*	*7.5±0.4*	*6.7±0.4*
Area Fractional Shortening %	*19.5±2.19*	*22.8±1.8*	*21.4±2.0*	*23.3±1.9*
Ejection Time (ms)	*46.7±2.5*	*54.3±2.1**	*47.1±2.3*	*54.3±2.3**
IVRT+IVCT (ms)	*61.3±5.2*	*58.1±4.4*	*54.2±5.0*	*60.9±4.6*
Myocardial Performance Index	*1.30±0.10*	*1.07±0.08*	*1.13±0.10*	*1.18±0.09*
Aortic Outflow VTI (cm)	*0.31±0.04*	*0.33±0.03*	*0.31±0.04*	*0.37±0.04*
Peak Aortic Outflow Velocity (mm/s)	*88.9±8*	*77.2±7*	*85.0±8*	*85.8±7*
Peak Mitral Inflow Velocity(mm/s)	*985±47*	*813±39**	*988±43*	*862±43**
Aortic Root Diameter (mm)	*1.12±0.04*	*1.13±0.03*	*1.19±0.03*	*1.13±0.03*
Heart Rate (bpm)	*478±15*	*445±13*	*465±14*	*457±14*
8 Weeks - High Fructose Diet				
Ejection Fraction %	*43.4±2.7*	*45.5±2.6*	*48.8±2.8*	*46.8±2.6*
Fractional Shortening %	*17.5±1.4*	*18.4±1.4*	*20.2±1.5*	*19.8±1.4*
Stroke Volume (µL)	*23.8±2.2*	*21.9±2.1*	*26.3±2.2*	*19.8±2.0*
End Diastolic Volume (µL)	*54.6±4.6*	*49.3±4.5*	*54.8±4.8*	*44.8±4.4*
End Systolic Volume (µL)	*30.8±3.1*	*27.5±3.0*	*28.5±3.2*	*24.0±2.9*
AW;d (mm)	*1.00±0.08*	*1.02±0.07*	*1.01±0.08*	*1.04±0.07*
AW;s (mm)	*1.23±0.08*	*1.25±0.08*	*1.26±0.08*	*1.34±0.08*
End Diastolic Diameter (mm)	*3.68±0.12*	*3.55±0.12*	*3.71±0.13*	*3.42±0.12*
End Systolic Diameter (mm)	*3.03±0.12*	*2.91±0.12*	*2.97±0.13*	*2.77±0.12*
PW;d (mm)	*1.00±0.09*	*1.15±0.09*	*0.86±0.09*	*1.24±0.09**
PW;s (mm)	*1.17±0.09*	*1.33±0.09*	*1.09±0.09*	*1.41±0.08**
Absolute Wall Thickness (mm)	*2.01±0.14*	*2.17±0.14*	*1.87±0.15*	*2.29±0.14**
Relative Wall Thickness	*0.58±0.07*	*0.64±0.07*	*0.52±0.07*	*0.71±0.06*
End Diastolic Area (mm^2)	*9.8±0.3*	*10.4±0.3*	*10.2±0.3*	*9.5±0.3*
End Systolic Area (mm^2)	*7.1±0.4*	*7.7±0.4*	*7.5±0.4*	*6.8±0.4*
Area Fractional Shortening %	*27.5±2.3*	*26.7±2.1*	*27.3±2.3*	*28.9±2.1*
Ejection Time (ms)	*48.7±2.4*	*55.0±2.3*	*47.9±2.6*	*50.0±2.3*

Table 3.13. Continued

IVRT+IVCT (ms)	*58.7±4.7*	*57.8±4.5*	*60.0±5.0*	*56.3±4.5*
Myocardial Performance Index	*1.21±0.13*	*1.05±0.13*	*1.24±0.14*	*1.27±0.13*
Aortic Outflow VTI (cm)	*0.34±0.04*	*0.42±0.04*	*0.31±0.05*	*0.31±0.04*
Peak Aortic Outflow Velocity (mm/s)	*91±17*	*123±17*	*82±19*	*79±17*
Peak Mitral Inflow Velocity(mm/s)	*941±49*	*844±48*	*916±53*	*827±48*
Aortic Root Diameter (mm)	*1.14±0.03*	*1.21±0.03*	*1.24±0.03#*	*1.13±0.03*#*
Heart Rate (bpm)	*441±11*	*476±10**	*471±11*	*454±10*
4 Weeks - High Starch Diet				
Ejection Fraction %	*41.9±3.3*	*46.7±2.8*	*45.1±3.1*	*40.3±3.0*
Fractional Shortening %	*16.9±1.9*	*20.1±1.6*	*18.4±1.8*	*16.0±1.7*
Stroke Volume (μL)	*24.2±2.0*	*16.1±1.7**	*24.8±1.9*	*17.3±1.8**
End Diastolic Volume (μL)	*59.0±4.3*	*37.6±3.6**	*55.2±4.0*	*42.9±3.8**
End Systolic Volume (μL)	*34.8±3.0*	*21.5±2.6**	*30.4±2.8*	*25.6±2.7*
AW;d (mm)	*1.00±0.08*	*1.13±0.07*	*0.94±0.08*	*1.01±0.07*
AW;s (mm)	*1.20±0.09*	*1.36±0.07*	*1.18±0.08*	*1.25±0.08*
End Diastolic Diameter (mm)	*3.76±0.12*	*3.22±0.10**	*3.74±0.11*	*3.42±0.11**
End Systolic Diameter (mm)	*3.13±0.13*	*2.61±0.11**	*3.05±0.12*	*2.87±0.12*
PW;d (mm)	*0.83±0.09*	*1.22±0.08**	*0.83±0.08*	*1.09±0.08**
PW;s (mm)	*1.01±0.09*	*1.39±0.08**	*1.02±0.08*	*1.23±0.08*
Absolute Wall Thickness (mm)	*1.83±0.14*	*2.34±0.12**	*1.77±0.13*	*2.10±0.13*
Relative Wall Thickness	*0.53±0.07*	*0.77±0.06**	*0.48±0.07*	*0.62±0.07*
End Diastolic Area (mm^2)	*9.8±0.4*	*8.3±0.3**	*10.3±0.4*	*9.3±0.4*
End Systolic Area (mm^2)	*7.3±0.5*	*6.2±0.4*	*7.5±0.4*	*7.1±0.4*
Area Fractional Shortening %	*26.1±2.7*	*26.1±2.3*	*26.6±2.5*	*24.4±2.4*
Ejection Time (ms)	*51.0±2.3*	*56.9±2.0*	*49.5±2.2*	*57.0±2.1**
IVRT+IVCT (ms)	*59.0±6.0*	*61.0±5.2*	*57.7±5.5*	*58.1±5.4*
Myocardial Performance Index	*1.15±0.12*	*1.08±0.10*	*1.14±0.11*	*1.08±0.11*
Aortic Outflow VTI (cm)	*0.40±0.04*	*0.46±0.03*	*0.37±0.04*	*0.42±0.03*
Peak Aortic Outflow Velocity (mm/s)	*102±9*	*104±7*	*96±8*	*92±8*
Peak Mitral Inflow Velocity(mm/s)	*939±48*	*860±42*	*949±44*	*799±43**
Aortic Root Diameter (mm)	*1.04±0.04*	*1.16±0.03**	*1.19±0.04#*	*1.14±0.04*
Heart Rate (bpm)	*446±19*	*430±16*	*469±18*	*460±17*
4 Weeks - High Fructose Diet				
Ejection Fraction %	*40.6±2.5*	*43.0±2.4*	*43.3±2.8*	*45.9±2.3*
Fractional Shortening %	*16.2±1.2*	*17.4±1.2*	*17.3±1.4*	*18.8±1.1*
Stroke Volume (μL)	*23.4±1.5*	*17.5±1.4**	*26.3±1.7*	*18.5±1.4**
End Diastolic Volume (μL)	*57.7±3.4*	*42.7±3.3**	*61.9±3.8*	*41.9±3.2**
End Systolic Volume (μL)	*34.3±2.6*	*25.2±2.5**	*35.6±2.9*	*23.3±2.4**
AW;d (mm)	*0.90±0.06*	*1.01±0.06*	*0.88±0.07*	*1.04±0.06*
AW;s (mm)	*1.08±0.06*	*1.23±0.06*	*1.09±0.07*	*1.34±0.06**
End Diastolic Diameter (mm)	*3.79±0.09*	*3.39±0.09**	*3.88±0.11*	*3.37±0.09**
End Systolic Diameter (mm)	*3.18±0.10*	*2.82±0.10**	*3.21±0.12*	*2.75±0.10**
PW;d (mm)	*0.86±0.09*	*1.16±0.09**	*0.82±0.10*	*1.20±0.08**
PW;s (mm)	*1.06±0.09*	*1.34±0.08**	*1.01±0.10*	*1.37±0.08**
Absolute Wall Thickness (mm)	*1.76±0.11*	*2.18±0.11**	*1.70±0.13*	*2.24±0.11**

Table 3.13. Continued

Relative Wall Thickness	*0.47±0.05*	*0.67±0.05**	*0.44±0.06*	*0.69±0.05**
End Diastolic Area (mm^2)	*10.8±0.3*	*9.4±0.3**	*10.6±0.4*	*9.3±0.3**
End Systolic Area (mm^2)	*8.4±0.3*	*6.9±0.3**	*7.8±0.4*	*6.7±0.3**
Area Fractional Shortening %	*22.0±02.1*	*27.7±02.1*	*26.6±02.4*	*28.6±02.0*
Ejection Time (ms)	*49.7±2.0*	*54.2±2.0*	*48.1±2.3*	*59.0±1.9**
IVRT+IVCT (ms)	*58.5±3.6*	*55.3±3.6*	*54.2±4.0*	*56.0±3.4*
Myocardial Performance Index	*1.18±0.07*	*1.04±0.07*	*1.14±0.08*	*0.96±0.07*
Aortic Outflow VTI (cm)	*0.36±0.04*	*0.39±0.04*	*0.34±0.04*	*0.44±0.04*
Peak Aortic Outflow Velocity (mm/s)	*89±8*	*93±8*	*90±9*	*96±8*
Peak Mitral Inflow Velocity(mm/s)	*911±46*	*868±46*	*973±51*	*916±43*
Aortic Root Diameter (mm)	*1.11±0.04*	*1.16±0.04*	*1.13±0.04*	*1.22±0.04*
Heart Rate (bpm)	*468±15*	*456±15*	*482±17*	*463±14*

Data were obtained using mice anesthetized with 2.5% isoflurane at the given times after Sham or TAC surgery with a 27 gauge needle*P <0.05 vs. TAC; #P <0.05 vs. WT; Sham n=12-16/group, TAC n=15-17/group. AWT;d, anterior wall thickness at diastole; AWT;s, anterior wall thickness at systole; bpm, beats per minute; PWT;d, posterior wall thickness at diastole; PWT;s, anterior wall thickness at systole; bpm, beats per minute.

Table 3.14.

Parameter	Wild Type		G6PD Deficient	
	Sham	TAC	Sham	TAC
High Starch Diet				
ANP (Ct)	*22.2±0.5*	*19.0±0.4**	*22.5±0.5*	*19.2±0.5**
MHCβ/MHCα (Fold Change)	*1.3±2.9*	*12.0±2.2**	*1.8±2.6*	*10.0±2.4**
MHCβ (Ct)	*23.5±0.4*	*21.7±0.3**	*23.6±0.4*	*21.2±0.3**
MHCα (Ct)	*15.6±0.3*	*16.4±0.2*	*15.9±0.3*	*16.0±0.3*
PPIA (Ct)	*21.5±0.2*	*21.4±0.2*	*21.6±0.2*	*21.7±0.2*
CS (μmol·gww^{-1}·min^{-1})	*218±8*	*182±7**	*227±9*	*211±8#*
MCAD (μmol·gww^{-1}·min^{-1})	*13.4±0.5*	*11.2±0.4**	*14.1±0.5*	*12.9±0.5#*
MDA+4HA (pmoles/mg Protein)	*945±78*	*782±68*	*649±78#*	*757±75*
High Fructose Diet				
ANP (Ct)	*22.3±0.4*	*20.0±0.4**	*22.3±0.5*	*18.2±0.4*#*
MHCβ/MHCα (Fold Change)	*1.5±1.6*	*5.2±1.7*	*3.1±1.9*	*13.3±1.7*#*
MHCβ (Ct)	*23.7±0.3*	*22.1±0.4*	*22.4±0.4*	*20.6±0.4*
MHCα (Ct)	*15.8±0.2*	*15.7±0.2*	*15.6±0.2*	*15.9±0.2*
PPIA (Ct)	*21.8±0.3*	*21.6±0.3*	*21.8±0.3*	*21.5±0.3*
CS (μmol·gww^{-1}·min^{-1})	*227±8*	*196±8**	*222±9*	*176±8**
MCAD (μmol·gww^{-1}·min^{-1})	*13.2±0.5*	*11.6±0.4**	*14.4±0.5*	*10.6±0.4**
MDA+4HA (pmoles/mg Protein)	*825±137*	*793±137*	*1086±149*	*707±132*

Data were obtained using left ventricular myocardium from mice at 17 weeks after Sham or TAC surgery with a 27 gauge needle; *P <0.05 vs. TAC; #P <0.05 vs. WT; Sham n=9-13/group, TAC n=12-16/group. 4HA, 4-hydroxyalkenals; ANP, atrial natriuretic peptide; CS, citrate synthase; gww, grams of wet weight tissue; Ct, cycle at which threshold is crossed; MCAD, medium chain acyl-coenzyme A dehydrogenase; MDA, malondialdehyde; MHC, myosin heavy chain; PPIA, peptidylprolyl isomerase A.

Effects of G6PD Deficiency on Metabolic Parameters after TAC and High Fructose

We hypothesized that a combination of pressure overload and high fructose increases flux through G6PD in WT mice to increase [NADPH], superoxide production and oxidative stress. In accordance with this hypothesis, [NADPH] was increased in response to TAC in WT mice with high fructose intake (Figure 3.10A). However, contrary to our hypothesis, this increase in [NADPH] did not correspond with increases in superoxide production or lipid peroxidation (Figure 3.10B; Table 3.14). On the other hand, decreased aconitase activity may indicate oxidative stress[205], and aconitase activity was decreased in response to TAC in G6PDX mice after high fructose intake (Figure 3.10C). These results suggest that G6PD deficiency may increase rather than decreases oxidative stress in response to high fructose intake and TAC.

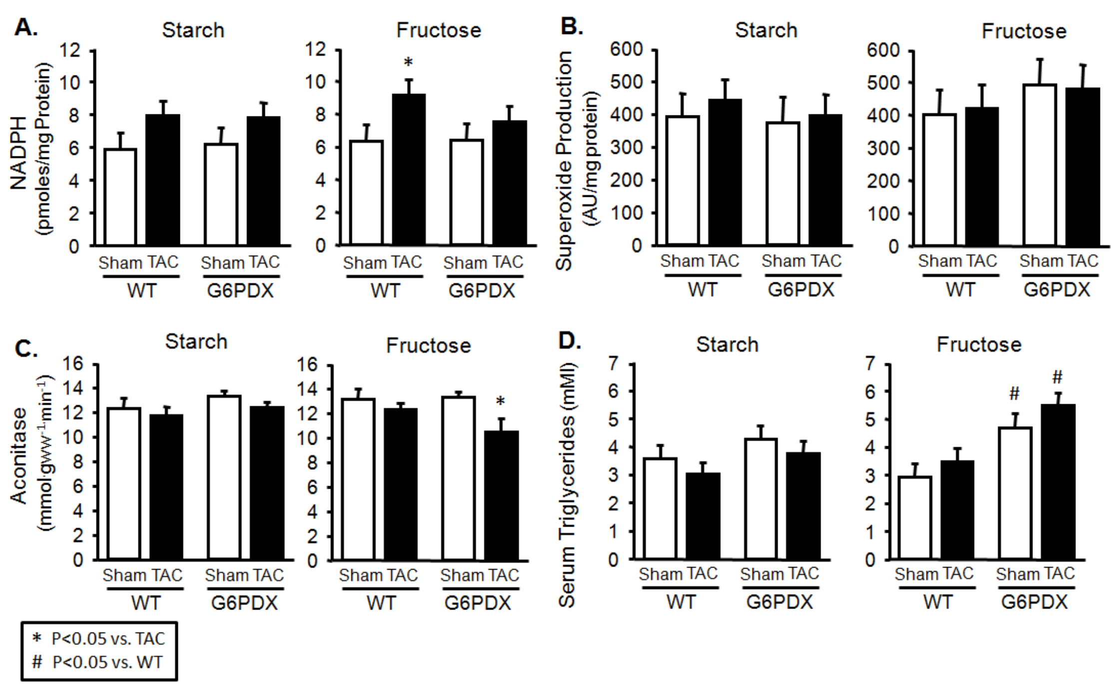

Figure 3.10. **Fructose/TAC - Biochemical and Metabolic Data**. **A**. TAC increased LV [NADPH] after high fructose intake in WT mice, but not in G6PDX mice. **B**. Superoxide production was unchanged by TAC or G6PD deficiency among animals that received the

high fructose diet or the high starch diet. **C**. Aconitase activity, an index of oxidative stress, was decreased by TAC in G6PDX mice after high fructose intake. **D**. G6PD deficiency increased serum triglycerides compared to WT mice with high fructose intake. Data were obtained 17 weeks post-TAC *P <0.05 vs. TAC; #P <0.05 vs. WT; Sham n=9-16/group, TAC n=12-16/group. gww, grams of wet weight tissue; NADPH, nicotinamide adenine dinucleotide phosphate.

High sugar intake is associated with increased circulating triglycerides, and adverse metabolic effects may interact with pressure overload to adversely affect heart failure[141]. G6PDX mice had increased serum triglycerides after high sugar intake, indicating that G6PD deficiency increases propensity for hypertriglceridemia (Figure 3.10D). G6PD deficiency also decreased serum insulin in animals with high fructose intake, consistent with a decrease in β-cell function as reported by others (Table 3.15)[13]. Serum glucose and free fatty acids were unaffected by G6PD deficiency or TAC. G6PDX mice had decreased epididymal fat mass and kidney mass after TAC with high fructose intake, suggesting that G6PD deficiency increases the propensity toward cachexia (Table 3.11). This was observed despite an increase in energy intake by G6PDX mice with the high fructose diet compared to diet high starch diet (Table 3.10). The adverse effects of increased LV hypertrophy and dysfunction in response to G6PD deficiency are evidenced by cachexia in G6PDX mice. These results indicate that G6PD deficiency adversely affects the systemic condition and compounds the adverse effects of pressure overload.

Table 3.15.

Parameter	Wild Type		G6PD Deficient	
	Sham	TAC	Sham	TAC
High Starch Diet				
Glucose (mM)	*11.0±0.7*	*11.4±0.6*	*11.4±0.7*	*11.5±0.7*
Free Fatty Acids (mM)	*1.17±0.13*	*1.14±0.11*	*1.22±0.13*	*1.19±0.12*
Insulin (pM)	*0.75±0.19*	*0.68±0.17*	*0.96±0.19*	*0.52±0.18*
High Fructose Diet				
Glucose (mM)	*12.5±0.579*	*12.5±0.579*	*12.1±0.603*	*11.2±0.558*
Free Fatty Acids (mM)	*1.09±0.095*	*1.30±0.095*	*1.07±0.099*	*1.16±0.091*
Insulin (pM)	*1.07±0.16*	*0.71±0.16*	*0.56±0.17#*	*0.88±0.15*

Data were obtained using blood serum from mice at 17 weeks after Sham or TAC surgery with a 27 gauge needle; *P <0.05 vs. TAC; #P <0.05 vs. WT; Sham n=12-13/group, TAC n=13-15/group.

Discussion

The main novel finding of this study is that the progression of heart failure was modestly accelerated by a clinically relevant level of moderate G6PD deficiency. Thus contrary to our hypothesis, G6PD deficiency does not attenuate myocardial damage in response to injury or severe stress. After myocardial infarction or chronic pressure overload, G6PDX displayed moderate, albeit statistically significant worsening of LV dilation and/or contractile dysfunction, associated with increased lipid peroxidation products in cardiac tissue.

Our apparently paradoxical hypothesis was based on solid evidence that pharmacological inhibition of G6PD decreases ROS generation in myocardial homogenates from canine and human failing hearts, suggesting that G6PD fuels NADPH dependent oxidant enzymes in advanced heart failure[3, 6]. Alternatively, it may be argued that, given the critical role attributed to the oxidative pentose phosphate pathway in the maintenance of redox homeostasis, G6PD deficiency should cause a very rapid deterioration of cardiac muscle subjected to stresses such as infarction and pressure overload. In fact, the inhibition of G6PD increases the sensitivity of cells to oxidative damage and death, while G6PD overexpression protects cells against oxidative damage[10]. Further, the activity of G6PD in isolated cardiomyocytes is enhanced in response to oxidative stress, and inhibition of G6PD increased oxidative stress and impairs cardiomyocyte calcium handling and contractility[3].

Our results indicate that although LV dilation was significantly enhanced in response to G6PD deficiency, accelerated contractile dysfunction was not evident. There may be a complex and evolving balance between negative and positive effects of G6PD deficiency during the progression of heart failure, whose net result is a pathophysiological condition not excessively different from that observed in wild type mice. Previous studies have shown that G6PDX mice display worse contractile recovery of an acute bout of myocardial ischemia, and that this may have been mediated by accelerated oxidative stress[4]. Nonetheless, this might be a transient detrimental consequence of G6PD deficiency, not affecting the long-term outcome.

G6PD enzyme activity in our study was ~40% of WT. This was somewhat higher than the ~20% activity reported by other investigators using the same mice. This discrepancy may be due to some effect of inbreeding of the mice in our laboratory. When we initially started breeding our colony in 2010, the G6PDX mice had 21% residual G6PD activity (200±15 $\mu mol \cdot gww^{-1} \cdot min^{-1}$ in WT mice vs. 42±11 $\mu mol \cdot gww^{-1} \cdot min^{-1}$ in G6PDX mice, n=5/group), but the myocardial activity has been consistently higher (~40%) since that time.

The measurement of [NADPH] determines the NADPH setpoint, rather than the production of NADPH over time. Further, the G6PD enzyme assay, determines the maximal G6PD activity, rather than the actual flux through G6PD which is dependent on cellular location and glucose 6-phosphate concentration. Despite this limitation, we expected G6PD deficiency to decrease [NADPH], as seen by Xu, et al, and others in the kidneys of G6PDX mice and in cardiomyocytes with pharmacological inhibition of G6PD[9, 11]. However, NADPH levels were not significantly different in G6PDX compared to WT mice, and we were surprised to see that in G6PDX mice there was a significant increase in [NADPH] in response to either myocardial infarction or TAC. The reason for the increase is unclear, but suggests that there is a compensatory mechanism for increasing NADPH.

The compensation for increasing NADPH in G6PDX mice is of interest for further studies. Possible mechanisms include the upregulation of other NADPH-producing enzymes in the mitochondria. These enzymes include malic enzyme, isocitrate dehydrogenase, and glutamate dehydrogenase. Alternatively, the production of NADPH may be unchanged in response to heart failure or G6PD deficiency, and just the [NADPH] set-point is changed. Our measurement of NADPH assessed this set-point. To assess actual flux through G6PD, and thus the production of NADPH by this enzyme, one would need to use more sophisticated analysis than the measures we performed. This analysis would include the use of radiolabeled glucose 6-phosphate to determine flux. Finally, the long-term compensation by G6PDX mice for increasing NADPH seems to exacerbate heart failure in G6PDX mice in our studies. To examine the effect of G6PD deficiency without compensation, one would need to perform studies in an inducible model of G6PD deficiency. It would also be of interest to examine the cardiac-specific effects of G6PD deficiency by making a cardiac-specific model.

Previous investigators reported that NADPH oxidase adversely affected the development of heart failure after mice received a high fat/high sugar diet to induce obesity[138]. In cultured adipose cells, high glucose increased [NADPH], NADPH oxidase activity, and ROS, and the glucose-induced increase in ROS was prevented by G6PD knockdown[215]. Thus, we hypothesized that high fructose intake would exacerbate heart failure by increasing flux through G6PD to increase [NADPH] and superoxide production, and predicted that G6PD deficiency would have a beneficial effect on the heart in the context of a high fructose diet. In support of the hypothesis that high sugar intake increases flux through the pentose phosphate pathway, we saw an increase in [NADPH] in WT mice with TAC and high fructose, but not in G6PDX mice. However, this increase in [NADPH] did not correspond to any changes in superoxide production, and G6PD deficiency was not beneficial. Rather, G6PD deficiency resulted in a decrease in aconitase activity, and established marker of oxidative stress, corresponding with greater LV hypertrophy and dysfunction with TAC and high fructose intake. Our results are similar to those seen by Zhang, et al, who reported that in cultured endothelial cells, high glucose decreased G6PD activity and increased oxidative stress[12]. Thus, G6PD deficiency made the myocardium more sensitive to adverse effects of high sugar intake.

Our studies examined the effects of G6PD deficiency in young mice. It would be of interest for further studies to investigate heart failure in older G6PDX mice. Jain, et al, observed a minor ventricular hypertrophy at 9 months in G6PDX mice[27]. This minor hypertrophy may affect the outcome of heart failure, and this interaction would be of interest to pursue in future studies.

In summary, we assessed the impact of G6PD deficiency on the development of heart failure using an established genetic mouse model G6PD deficiency and pressure overload or infarct-induced failure. There was worse cardiac dysfunction and/or LV remodeling with G6PD deficiency which was associated with greater redox stress. These findings suggest that individuals with G6PD deficiency may be at greater risk for developing heart failure when they have concurrent hypertension or myocardial infarction. Thus further investigation into the effects of G6PD deficiency on the development and progression of heart failure in humans is warranted.

Summary of Major Findings

1. *G6PD deficiency increased cardiac oxidative stress, and ventricular dilation, but did not affect cardiac function after myocardial infarction in mice*.
2. *G6PD deficiency increased ventricular dilation but did not affect cardiac function in response to severe TAC in mice*.
3. *G6PD deficiency adversely affected the outcome of pressure overload induced heart failure with a high fructose diet in mice*.

Chapter 4 – High Sugar Intake Does Not Exacerbate Metabolic Abnormalities or Cardiac Dysfunction in Genetic Cardiomyopathy

Nutrition. Epub 2012 Feb 2.

Chapter Abstract

Objective*:** High sugar intake increases heart disease risk in humans. In animals, sugar intake accelerates heart failure development via increased reactive oxygen species (ROS). Glucose 6-phosphate dehydrogenase (G6PD) can fuel ROS production by providing NADPH for superoxide generation by NADPH oxidase. On the other hand, G6PD also facilitates ROS scavenging via the glutathione pathway. We hypothesized that high sugar intake would increase flux through G6PD to increase myocardial [NADPH] and ROS, and accelerate cardiac dysfunction and death. ***Research Methods & Procedures: Six-week old TO-2 hamsters, a nonhypertensive model of genetic cardiomyopathy caused by a δ-sarcoglycan mutation, were fed a long-term diet of either high starch or high sugar (57% of energy from sucrose+fructose). ***Results***: After 24 weeks, δ-sarcoglycan deficient animals displayed expected decreases in survival and cardiac function associated with cardiomyopathy (ejection fraction: control=68.7±4.5%; TO-2 starch=46.1±3.7, p<0.05 TO-2 starch vs control; TO-2 sugar=58.0±4.2%, N.S. vs TO-2 starch or control; median survival: TO-2 starch=278 days, TO-2 sugar=318 days, P=0.133). Although we expected high sugar intake to exacerbate cardiomyopathy, surprisingly there was no further decrease in ejection fraction or survival with high sugar compared to starch in cardiomyopathic animals. Cardiomyopathic animals had systemic and cardiac metabolic abnormalities (elevated serum lipids and glucose, and decreased

myocardial oxidative enzymes) which were unaffected by diet. High sugar intake increased myocardial superoxide, but [NADPH] and lipid peroxidation were unaffected. ***Conclusions***: Despite increased superoxide production, high sugar intake did not adversely affect cardiac function or survival in genetic cardiomyopathy.

Introduction

Clinical studies show that high sugar intake is associated with dyslipidemia and that high dietary glycemic load may increase the risk for coronary heart disease[120, 141, 148-150]; however, little is known about the effects of sugar intake on the development and progression of heart failure. A recent epidemiological study found that hospitalization or death from new onset heart failure was not related to sugar intake over a 9 year follow-up in middle age and elderly women[156]. There is less information regarding effects of sugar intake in populations that are at high risk for developing heart failure, such as patients with hypertension, ischemic heart disease or inherited cardiomyopathies.

Recent studies from our group and others have found that high intake of fructose or sucrose accelerated the development of heart failure and mortality compared to a complex carbohydrate diet in rats with salt-induced hypertension[151, 152], rats with volume overload[155], and mice with transverse aortic constriction (TAC)[154, 216]. High fructose intake increases the generation of superoxide in myocardium, suggesting that cardiac function is decreased by accelerated formation of reactive oxygen species (ROS) and subsequent oxidative damage[154, 157]. Support for this comes from the observation the accelerated development of heart failure by high fructose intake was prevented by tempol, a superoxide dismutase mimetic, in mice with aortic constriction[154]. There is greater oxidative stress in heart failure, as evidenced by increased lipid peroxidation products and a decreased ratio of reduced/oxidized glutathione (GSH/GSSG)[217]. Recent studies show glucose 6-phosphate dehydrogenase (G6PD) expression is increased in failing myocardium, and that superoxide generation is fueled by increased production of NADPH by G6PD in humans and animal models of heart failure[3, 6-8]. Consumption of a high sugar diet may further increase flux through G6PD and accelerate production of NADPH and subsequent ROS production in heart failure[3, 6, 7, 117, 169].

Evidence for acceleration of cardiac pathology with high sugar intake comes from animal models that employed an increase in cardiac after load induced by aortic constriction or hypertension, which increases cardiac mass, myocardial oxygen consumption, and ROS generation. However, the majority of heart failure patients do not have this type of extreme uncontrolled hypertension. Thus, pressure overload models have limited relevance to many forms of human heart failure. In the present investigation, we examine the potential cardiotoxic effects of sugar intake in a model of heart failure that does not involve cardiac hypertrophy or an increase in myocardial workload and oxygen consumption. Studies were performed in cardiomyopathic hamsters which have a mutation in δ-sarcoglycan that results in progressive cardiac dysfunction and a shortened life span (~40-50 weeks compared to 2 to 3 years for normal strains). These animals have systemic and cardiac metabolic abnormalities (defects in cardiac mitochondria, and elevated circulating glucose and triglycerides and low insulin), and increased myocardial oxidative stress[117, 217, 218]. We hypothesized that long-term consumption of a high sugar diet would accelerate cardiac dysfunction due to greater oxidative stress via accelerated NADPH generation by G6PD. Dietary treatments were initiated at six weeks of age and survival was assessed out to 78 weeks. A subgroup was assessed at 29 weeks for cardiac function, and at 30 weeks for metabolic parameters, and myocardial ROS formation and oxidative damage. We hypothesized that in cardiomyopathic hamsters, a high sugar diet (57% of energy intake) would increase ROS formation and lipid peroxidation, impair cardiac and systemic metabolism, and decrease cardiac function and survival compared to the starch diet.

Experimental Methods & Design

Experimental Design

Six-week old male hamsters that were either normal healthy controls (Bio F1B strain) or cardiomyopathic due to a mutation in δ-sarcoglycan (Bio TO-2 strain) were purchased from Bio Breeders Inc (Watertown, MA). The healthy control animals were fed a standard high starch diet, and the cardiomyopathic animals were either maintained on the standard high starch diet or on a high sugar diet. The aim of this study was to assess the role of high sugar intake within the context of cardiomyopathy, therefore we did not include a high sugar diet group of healthy control F1B hamsters. Healthy controls (n=17) and cardiomyopathic animals (n=37 starch diet, n=30 high sugar diet) were assessed for mortality for 545 days. An additional subset (n=11-12/group) were assessed for cardiac function at 29 weeks and euthanized at 30 weeks of age for biochemical analysis.

Diets

Animals were fed ad libitum custom manufactured purified diets that derived 12% of energy from fat, 20% from protein (casein supplemented with L-cystine), and 68% from carbohydrate (Research Diets Inc, New Brunswick, NJ). The high starch diet (#D09103101) contained no sugar (12% of total energy from maltodextrin and 55% from corn starch). The high sugar diet (#D09103110, Research Diets) contained 5% of energy from corn starch, 5% from maltodextrin, 28.5% from fructose, and 28.5% from glucose.

Statistics

Values are shown as mean ± standard error. The three groups were compared using a one-way analysis of variance with the Holm-Sidak correction. Kaplan-Meier analysis was used to assess survival. $P<0.05$ was considered significant.

Results

Survival and Morphometric Parameters

There were no differences in body mass between the two diets, but the high sugar diet increased combined fat mass by 29% ($p<0.05$; Table 4.1). High sugar had no effect on LV mass, but it resulted in 17% lower right ventricular and 60% lower atrial masses. Cardiomyopathic hamsters had the expected high rate of mortality compared to healthy control animals (Figure 4.1). We expected to see an increase in mortality in response to high sugar intake, however there was not a significant difference in mortality for the high sugar diet compared to the high starch diet (Median survival: 278 days for the cardiomyopathic starch group vs 318 for the high sugar group, $p=0.133$).

Table 4.1.

Parameter	Healthy Control	Cardiomyopathic Starch	Cardiomyopathic Sugar
LV Mass (mg)	*417±10*	*339±11**	*328±9**
LV Mass/Tibia Length (mg/mm)	*15.7±0.3*	*13.5±0.4**	*13.1±0.3**
LV Mass/BodyMass (mg/g)	*2.47±0.09*	*2.62±0.05*	*2.49±0.06*
RV Mass (mg)	*104±5*	*86±5**	*71±3*#*
Combined Atrial Mass (mg)	*23.4±1.9*	*66.1±15.1**	*26.5±3.3#*
Tibia Length (mm)	*26.5±0.2*	*25.1±0.2**	*25.0±0.2**
Terminal Body Mass (g)	*170±5*	*130±4**	*132±3**
Liver Mass (g)	*6.82±0.20*	*4.99±0.19**	*5.32±0.09**
Retroperitoneal Fat (g)	*2.00±0.11*	*0.82±0.08**	*1.20±0.12*#*
Epididymal Fat (g)	*3.29±0.14*	*1.64±0.09**	*2.13±0.11*#*
Subcutaneous Fat (g)	*4.23±0.29*	*1.75±0.12**	*2.09±0.13**
Combined Fat Mass (g)	*9.51±0.53*	*4.20±0.28**	*5.42±0.35*#*

LV, left ventricle; RV, right ventricle; *P <0.05 vs. Control; #P <0.05 vs. Starch; n=11-12.

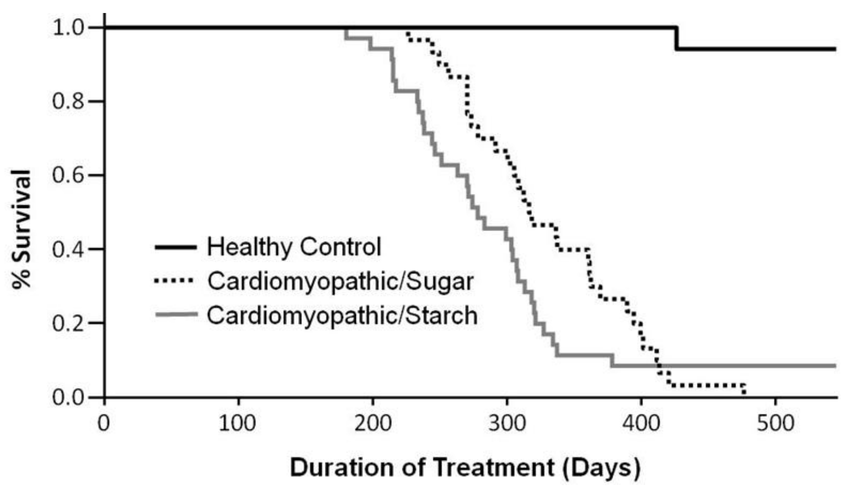

Figure 4.1. Survival of hamsters from initiation of the diet at 6 weeks of age. Cardiomyopathy resulted in the expected decrease in lifespan, but there was no effect of diet (p=0.133 high sugar vs. starch diets) (n=17 healthy controls, n=37 cardiomyopathic starch diet, n=30 cardiomyopathic high sugar diet).

Functional and Metabolic parameters

Ventricular dysfunction and wall thinning were evident in cardiomyopathic animals with high starch (Figure 4.2; Table 4.2). Ejection fraction, the percentage of blood that is pumped out of the heart with each beat, was decreased from 68.7% to 46.1%

in cardiomyopathy indicative of ventricular dysfunction. Contrary to our hypothesis which predicted that high sugar intake would result in a further decrease in ejection fraction compared to starch, the high sugar diet did not decrease ejection fraction in cardiomyopathic animals and may increase ejection fraction compared to starch (p=0.094 for trend).

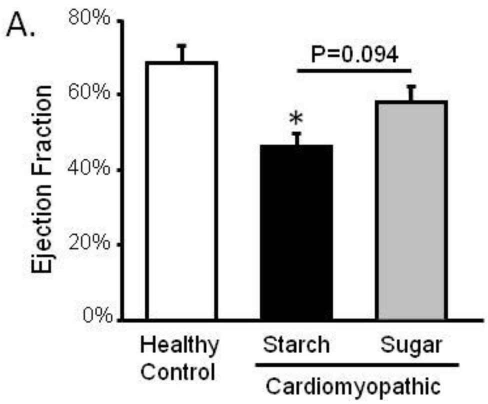

Figure 4.2. **Echocardiography**. Left ventricular ejection fraction at 29 weeks of age; *P <0.05 vs. Control; n=11-12.

Table 4.2.

Parameter	Healthy Control	Cardiomyopathic Starch	Cardiomyopathic Sugar
ESV/Tibia Length (µL/mm)	*1.58±0.35*	*3.39±0.43**	*2.72±0.55*
EDV/Tibia Length (µL/mm)	*4.69±0.66*	*6.08±0.65*	*5.79±0.96*
AWT/Tibia Length (µm/mm)	*142±3*	*117±5**	*121±4**
Relative Wall Thickness	*0.748±0.032*	*0.591±0.042**	*0.590±0.029**
Heart Rate (BPM)	*338±16*	*323±13*	*344±8*

ESV, end systolic volume; EDV, end diastolic volume; AWT, absolute wall thickness; BPM, beats per minute; *P <0.05 vs. Control; n=11-12.

Cardiomyopathic hamsters had high circulating glucose (cardiomyopathy: 206mg/dL vs control: 95mg/dL, p<0.05), triglycerides (cardiomyopathy: 581mg/dL vs control: 184mg/dL, p<0.05), and free fatty acids (cardiomyopathy: 1.67mM vs control: 0.68mM, p<0.05), and this corresponded with low plasma insulin (cardiomyopathy: 329pg/mL vs control: 540pg/mL, p<0.05) (Figure 4.3). However, none of these parameters were significantly affected by sugar intake.

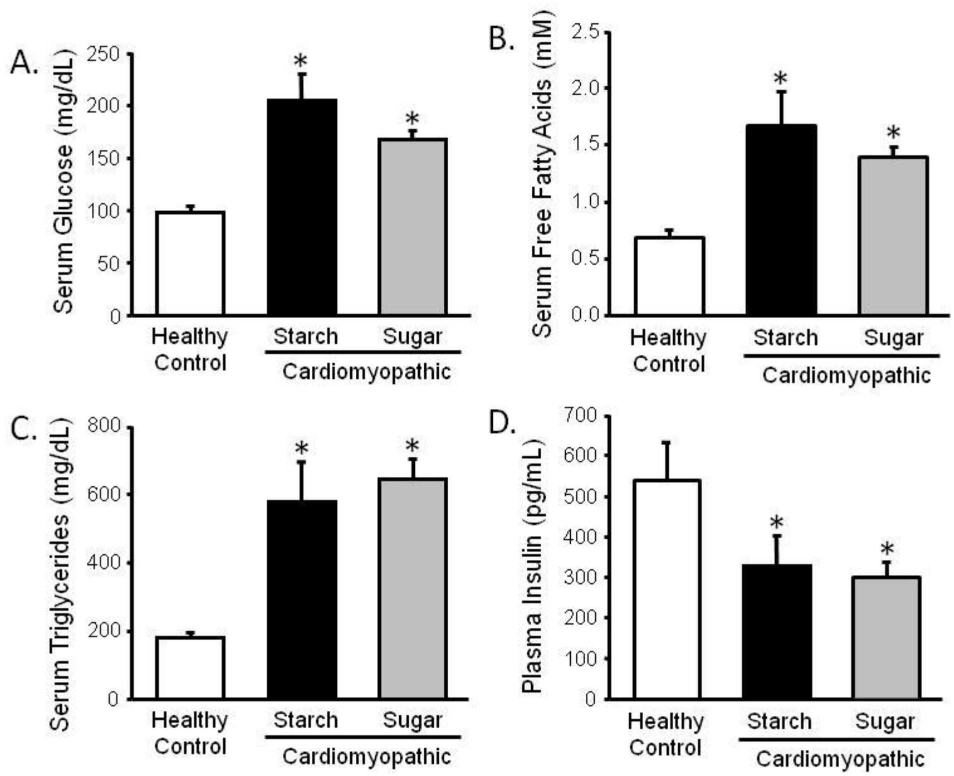

Figure 4.3. Serum glucose (**a**), free fatty acids (**b**), and triglycerides (**c**), and plasma insulin (**d**) taken at 30 weeks of age in the nonfasted state. *P <0.05 vs. Control; #P <0.05 vs. Starch; n=9-12.

Heart failure is accompanied by mitochondrial dysfunction and low myocardial ATP levels[74, 75], and disrupted mitochondria and decreased respiration rates have been reported in cardiomyopathic hamsters[76]. We observed a decrease in the activity of the mitochondrial oxidative enzymes CS (36% decrease), MCAD (37% decrease), and ICDH (29% decrease) in cardiomyopathic compared to control hamsters, with no significant differences between diets (Figure 4.4).

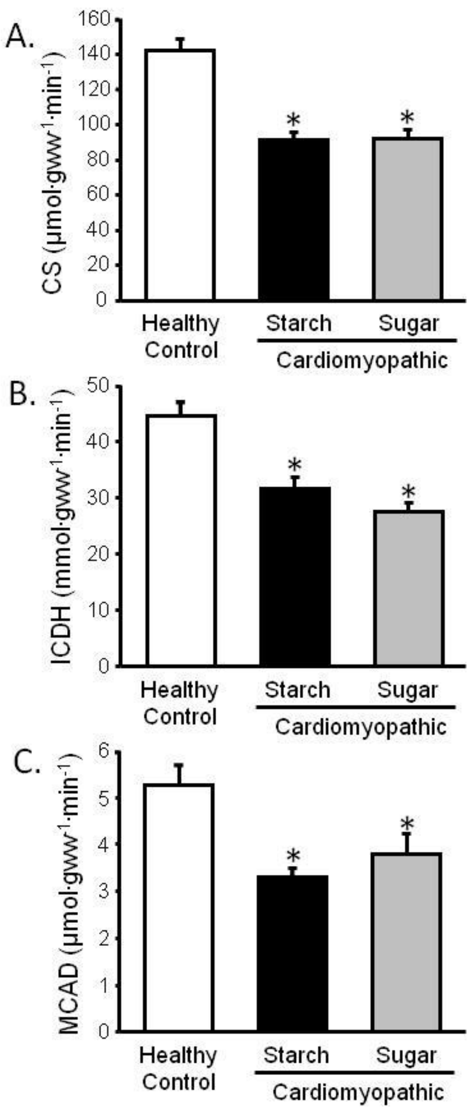

Figure 4.4. **Metabolic Enzyme Activity**. Left ventricular citrate synthase (CS) (**a**), isocitrate dehydrogenase (ICDH) (**b**), and medium-chain acyl coenzyme-A dehydrogenase (MCAD) enzyme activity (**c**); *P <0.05 vs. Control; n=11-12.

Indices of Oxidative Stress.

Cardiomyopathic hamsters fed the high starch diet had elevated myocardial G6PD activity (35% increase) compared to normal hamsters, however this was not observed with high sugar intake (Figure 4.5). The high sugar diet increased superoxide production by 39%, but there were no differences in myocardial NADPH concentration or lipid peroxidation products among the three groups.

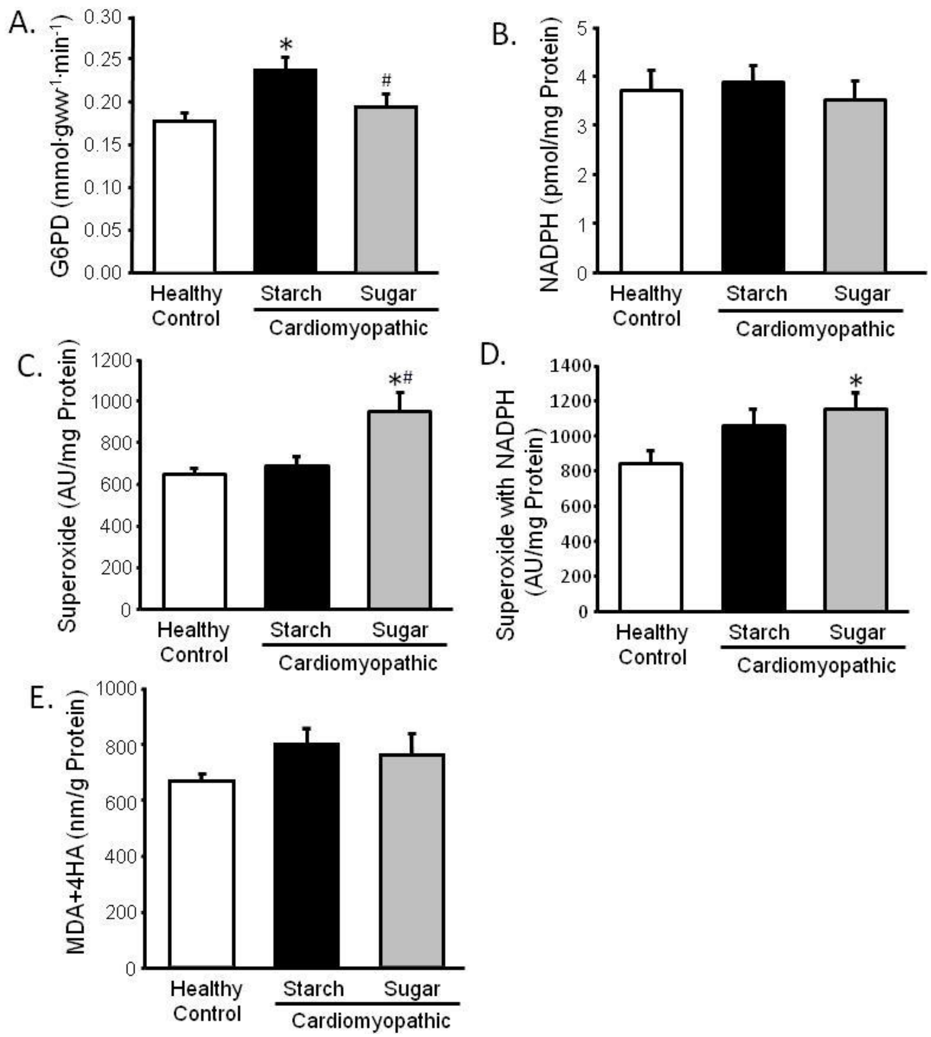

Figure 4.5. **Indices of Oxidative Stress**. Left ventricular glucose 6-phosphate dehydrogenase (G6PD) activity (**a**), NADPH content (**b**), superoxide production (**c**), superoxide production with NADPH included in the reaction mix (**d**), and lipid

peroxidation products, malondialdehyde and 4-hydroxyalkenals (MDA+4HA) (**e**); *P <0.05 vs. Control; #P <0.05 vs. Starch; n=11-12.

Discussion

Previous studies in pressure overload models of heart failure demonstrated that high intake of sugar accelerated the development of cardiac hypertrophy, contractile dysfunction, and death. Since this type of extreme afterload-induced heart failure has limited clinical relevance, it is important to also investigate if this effect occurs in a heart failure model that does not involve hypertension and the subsequent increase in cardiac workload. Here we used the well described cardiomyopathic TO-2 hamsters, and found that a high sugar diet increased myocardial superoxide production, but did not affect [NADPH] or lipid peroxidation products. Surprisingly, the high sugar diet did not exacerbate LV dysfunction or accelerate mortality. This was independent of systemic and cardiac metabolic abnormalities (elevated serum lipids and glucose, and decreased myocardial mitochondrial oxidative enzyme activities) which were unaffected by diet.

High sugar intake can accelerate heart failure, however this finding is not consistent[146]. In salt-sensitive hypertensive rats, high sugar intake increased fetal gene expression, apoptosis, contractile dysfunction, and mortality[151, 152]. Similarly, mortality, cardiac hypertrophy, and fetal gene expression were increased by high sugar intake in mice with TAC-induced pressure overload[154, 219]. In a volume overload model generated by an arterial-venous shunt in rats, a high fructose diet exacerbated chamber dilation and systolic dysfunction[155]. On the other hand, in a rat abdominal aortic banded model of heart failure, high sucrose intake attenuated LV hypertrophy and did not affect cardiac function or fetal gene expression compared to a high starch diet[220]. Finally, ischemia-reperfusion models have shown a benefit of fructose feeding[221, 222], as in both *in vivo* and isolated perfused hearts there is protection from ischemia-reperfusion injury by high sugar intake despite increased lipid peroxidation and oxidative stress. These studies indicate that the effects of high sugar intake are complex and require further study.

Patients with cardiac dysfunction often show signs of metabolic disturbances that may be affected by diet[223]. We observed metabolic defects in cardiomyopathic hamsters on the high starch diet, including high circulating glucose, triglycerides, and free fatty acids, as well as decreased insulin, which were not exacerbated by the high sugar diet. High sugar intake can result in metabolic dysfunction; however there were already metabolic defects in cardiomyopathic hamsters regardless of diet. The decreased plasma insulin in cardiomyopathic hamsters may indicate β-cell dysfunction, and was observed previously in young cardiomyopathic hamsters[224] . A previous report indicated that β-sarcoglycan deficient mice exhibited decreased tolerance to glucose, and that this corresponded with decreased fat pad mass[218]. In the present work, the combined fat pad mass was largely decreased in cardiomyopathic hamsters. However, with high sugar intake there was a partial-preservation of fat mass which may be beneficial[225]. These results indicate that although cardiomyopathic hamsters exhibited metabolic defects, these defects were not exacerbated by high sugar intake.

It has been proposed that an increase in NADPH generation by G6PD is a major contributor to ROS production in heart failure[3, 6, 169].Studies in patients and dogs with heart failure indicated that increased G6PD expression was associated with increased [NADPH] and ROS production that was prevented by G6PD inhibition. We therefore predicted that G6PD activity and [NADPH] would be increased in genetic cardiomyopathy. We further predicted that if high sugar intake increases the flux of glucose 6-phosphate through G6PD, then high sugar intake would elevate [NADPH] and further increase superoxide production. However, although high sugar intake increased superoxide production, [NADPH] was unaffected, suggesting that changes in [NADPH] and G6PD do not play a significant role in this model of cardiomyopathy.

The clinical implications of this study should be interpreted with caution. Although high sugar intake did not exacerbate cardiac dysfunction in a hamster model of cardiomyopathy, it should be stressed that this may or may not be the case in humans, particularly in patients with acquired forms of heart failure resulting from hypertension and/or ischemic heart disease. Although the effects of sugar intake on the progression and development of heart failure in humans has not been studied per se, high sugar intake does increase the risk of heart disease in humans, and this may lead to heart failure[148, 150]. Studies should examine the effects of diet on the progression of heart failure in humans.

Conclusion

We determined that high sugar intake did not exacerbate ventricular function, metabolic abnormalities, or survival. The results further indicate that NADPH and superoxide production do not play major roles in this model. These results warrant further investigation of sugar intake effects on humans with similar forms of genetic cardiomyopathy.

Summary of Major Findings

1. *A high sugar diet did not adversely affect the outcome of genetic cardiomyopathy in hamsters*.
2. *We found no evidence that G6PD and cytoplasmic ROS play a role in genetic cardiomyopathy in hamsters*.

Chapter 5 – Conclusion

Dissertation Summary

We have made the following novel findings:

1. *G6PD deficiency decreased obesity in response to a long-term high fat/high sugar diet in mice*. After 16 weeks of DIO, G6PDX mice stopped gaining weight despite eating the same amount of food intake as WT mice. The decrease in body mass corresponded with decreased fat pad mass, liver adiposity, and circulating leptin in response to G6PD deficiency.

2. *Despite resulting in decreased obesity, G6PD deficiency was not protective against the development of diet-induced metabolic abnormalities*. In response to long-term DIO, G6PDX mice exhibited the same degree of glucose intolerance as WT mice. G6PD deficiency led to additional metabolic abnormalities, including increased serum free fatty acids in response to long-term DIO, and increased serum triglycerides in response to high fructose intake.

3. *G6PD deficiency increased cardiac oxidative stress, and ventricular dilation, but did not affect cardiac function after myocardial infarction in mice*. After 11-12 weeks after LAD ligation, G6PD deficiency exacerbated LAD ligation-induced increases in LV end diastolic volume, and resulted in a decrease in relative wall thickness. Myocardial infarction decreased in LV ejection fraction, and increased

LV myocardial performance index and end diastolic pressure in G6PDX mice to the same extent as in WT mice.

4. *G6PD deficiency increased ventricular dilation but did not affect cardiac function in response to severe TAC in mice*. After 6 weeks after severe aortic constriction, G6PD deficient mice developed increased LV end diastolic and end systolic volumes, suggesting increased ventricular dilation in response to G6PD deficiency. TAC decreased ejection fraction to the same extent in G6PDX mice as in WT mice.

5. *G6PD deficiency adversely affected the outcome of pressure overload induced heart failure with a high fructose diet in mice*. After 16-17 weeks after TAC and high fructose intake, G6PD deficiency led to greater increases in LV mass and fetal gene expression, and led to a decrease in ejection fraction and aconitase activity, indicating that G6PD deficiency adversely affected the development of heart failure with a high fructose diet.

6. *A high sugar diet did not adversely affect the outcome of genetic cardiomyopathy in hamsters*. After 24 weeks of high sugar intake, indices of heart failure including decreases in LV ejection fraction, wall thickness, and oxidative enzyme capacity were not worsened by high sugar intake compared to a high starch diet in TO-2 hamsters. Over the course of 545 days, hamster mortality was not accelerated by high sugar intake.

7. *We found no evidence that G6PD and cytoplasmic ROS play a role in genetic cardiomyopathy in hamsters*. Although G6PD activity was increased by cardiomyopathy, we detected no concurrent changes in [NADPH] or lipid peroxidation products. Superoxide production was increased by high sugar intake, did not correspond with any worsening of heart failure in this model of cardiomyopathy.

Table 5.1 Summary of Adverse Cardiometabolic Effects of G6PD Deficiency

Source	**Effect**
Chapter 2	Susceptible to increased triglycerides and free fatty acids
Chapter 2	Susceptible to increased serum creatinine
Chapter 3	Increased LV dilation in response to heart failure stimuli
Chapter 3	Susceptible to increased lipid peroxidation
Chapter 3	Increased LV hypertrophy, fetal gene expression, and systolic dysfunction in response to high fructose intake and heart failure stimuli

Clinical Implications

The effects of G6PD deficiency on the heart remain largely unexplored despite its being the most common enzyme deficiency in the world[2]. Although previous studies suggested that G6PD may fuel superoxide production in failing myocardium and that G6PD deficiency may decrease the risk of developing coronary heart disease[165], the effects of G6PD deficiency on the development and progression of heart failure were never addressed. Our studies in mice indicate that G6PD deficiency adversely affects heart failure and diet induced cardiometabolic dysfunction. Thus, it is important to gain further insight into this common enzyme deficiency in the context of human disease, and to know of any potentially harmful effects of G6PD deficiency on human health.

Future Directions

Sugar Toxicity

Previous studies in our lab and others showed an acceleration of heart failure by high sugar intake[151, 152, 154, 226]. However, in the experiments presented in this dissertation, we did not observe any major adverse effects of high sugar intake on the outcome of heart failure in WT animals. Specifically, long term high sugar intake (57% sucrose + fructose) did not accelerate heart failure in a genetic model of cardiomyopathy in hamsters, and high fructose intake (60% fructose) did not decrease cardiac function or accelerate the progression of heart failure in WT animals. One reason for the lack of sugar cardiotoxicity in our studies may be due to differences in species and strain. We used mice with a mixed C3H/HeJ background strain. C57BL/6J mice were used in previous studies that indicated an adverse effect of sugar on the heart[146, 227]. Other investigators have reported that C57BL/6J mice develop metabolic abnormalities when faced with dietary stress, and that C3H mice are resistant to these effects[128, 228-230]. Additional information could be obtained by back-crossing G6PDX mice onto a C57BL/6J background. With this strain, we would likely see a greater effect of DIO and high fructose intake on cardiac and metabolic dysfunction. This back-cross is currently being performed by another laboratory at the University of Iowa, and these experiments can be performed with a C57BL/6J background strain in the future (Netanya Spencer, The University of Iowa, personal communication).

Mitochondrial ROS

G6PD is a largely cytoplasmic enzyme, and our studies determined the effects of G6PD on total ROS. However, it would be of interest to distinguish between effects on cytoplasmic ROS and mitochondrial ROS in our heart failure models. Emerging studies have increasing demonstrated a role of mitochondrial ROS in the development of heart failure. Specifically, mitochondrially-targeted catalase overexpression decreased the severity of heart failure in genetic models of heart failure and after pressure overload[118, 119]. To discover the individual roles of cytoplasmic and mitochondrial ROS, additional studies could be performed using mitochondria harvested from the TAC or infarct models of heart failure. One would then be able to assess the effect of G6PD deficiency on mitochondrial ROS, and possibly rule out its effects on total ROS. This would clarify whether or not any effects of G6PD deficiency on overall ROS are due to cytoplasmic or mitochondrial ROS.

Flux of Glucose 6-Phosphate through G6PD

Our studies examined the hypothesis that high sugar intake increases flux through G6PD to increase [NADPH] and superoxide production. Although we determined G6PD activity, [NADPH], and superoxide production in animals that received high sugar intake, we did not directly assess the flux of glucose 6-phosphate through G6PD. To directly determine the flux of glucose 6-phosphate through G6PD would require the use of glucose 6-phosphate that is isotopically labeled at the 1˚ carbon atom. The downstream enzyme, 6PGD, cleaves off the 1˚ carbon to produce ribulose-5-phosphate. The decrease in radiolabeled glucose 6-phosphate and the increase in radiolabeled CO_2 may then be measured to determine the flux through G6PD. We have discussed this possibility with investigators at the University of Montreal that are equipped for making such measurements, and this analysis may be performed in future studies (Christine Des Rosiers, Université de Montréal, personal communication).

G6PD Deficiency in Genetic Cardiomyopathy

In TO-2 hamsters, we report an increase in G6PD activity in response to cardiomyopathy. However, this increase in G6PD activity did not correspond with any increase in [NADPH] or superoxide production. Our results therefore do not support a role of G6PD activity in this hamster model of cardiomyopathy. However, this does not rule out a potential impact of G6PD on the outcome of cardiomyopathy in other models of cardiomyopathy or in other animals. For example, G6PD deficiency resulted in a decrease in protein aggregation and cardiac hypertrophy in model of genetic cardiomyopathy consisting of cardiac overexpression of mutant αB-crystallin in mice (CryAB mice)[7]. The affect of G6PD deficiency on genetic cardiomyopathy should be studied in additional models of genetic cardiomyopathy. Three commonly used genetic heart failure models include dystrophin deficient (mdx) mice, muscle lim protein (MLP)-KO mice, Gαq overexpressing mice. Dystrophin is essential for maintaining structural integrity of cardiac and muscle cells, and mdx mice develop muscular dystrophy and cardiomyopathy[231] . MLP is a z-disc interacting protein which is important in positive regulation of muscle development and is implicated in DCM[232]. Gαq is a signaling protein which can increase activation of NADPH oxidase, and whose overexpression of Gαq results in massive hypertrophy and early death[233-235]. Further studies may employ cross-breeding G6PDX mice with these genetic cardiomyopathy models to determine whether G6PD deficiency would be beneficial or adverse in these cases.

Heart Failure in G6PD Deficient Patients

In 2 small Sardinian studies, Cocco, et al, and Meloni, et al, determined that G6PD deficiency may lead to a decreased risk of cardiovascular-associated death and coronary heart disease respectively[164, 165]. Coronary heart disease may result from adverse vascular effects rather than a direct effect on the heart, and these investigators proposed that their results were due to a decrease in cholesterol synthesis and decreased circulating cholesterol in response to G6PD deficiency. HMG-CoA reductase, the first and rate determining enzyme involved in the synthesis of cholesterol, requires NADPH to convert its substrate, HMG-CoA, to mevalonic acid, and indeed G6PDX mice do have decreased circulating cholesterol (Sachin A. Gupte, University of South Alabama, unpublished data). Further studies are needed to validate the results of these studies using larger sample sizes, and should examine blood cholesterol levels in G6PD deficient humans.

Despite the reported beneficial effect of G6PD deficiency on heart disease risk, studies have not determined if G6PD deficiency affects the risk of developing heart failure. We determined that G6PD deficiency adversely affects the development and progression of heart failure in mice, and it is therefore of interest to determine the effects of G6PD deficiency on the development and progression of heart failure in human patients. This should be addressed by assessing hypertensive patients for G6PD deficiency, and then following these patients over an extended period to see if G6PD deficiency affects the risk of developing heart failure. Another study could examine

G6PD deficient patients who have already developed heart failure, to determine whether G6PD deficiency positively or negatively affects prognosis. Thus, studies could be performed which would determine whether G6PD deficiency positively or negatively affects heart failure risk and disease prognosis in humans.

We determined that G6PD deficiency increased oxidative stress and adversely affected the development of heart failure in mice. Because G6PD deficiency is commonly found in many human populations, it is possible to perform a mechanistic study using myocardium from human heart failure patients. Failing myocardium may be obtained from tissue banks and screened for G6PD deficiency. G6PD deficient individuals could easily be identified by common alleles such as the *G6PD A-* allele or the *Med* allele. Once G6PD deficient vs non-deficient individuals are identified, a number of important assays could then be performed with a small amount of tissue. A single 15-20mg tissue sample is sufficient to assess hydrogen peroxide and superoxide production via luminol and lucigenin chemiluminescence respectively[6]. NADPH oxidase activity is then determined via lucigenin chemiluminescence by adding an excess of NADPH to the superoxide assay. G6PD activity and [NADPH] can also be assessed in 10-15 mg tissue aliquots. Thus, one could determine whether G6PD deficiency positively or negatively affects G6PD activity, [NADPH], and ROS production in failing human myocardium.

G6PD Deficiency in Obese Patients

There are reports that G6PD deficiency may increase the risk of insulin resistance and diabetes[171-176]. However, a clear picture of the effects of G6PD deficiency on obesity and metabolic dysfunction in humans still remains to be determined. We characterized the cardiometabolic effects of G6PD deficiency in mice. Specifically, we determined that G6PDX mice gained less weight and became less obese compared to WT mice in response to a high fat/high sugar diet. Thus, it would be of interest to determine if G6PD deficiency affects the development of obesity, insulin resistance, and diabetes in human populations. Finally, because ROS production is implicated in obesity and metabolic dysfunction, the effect of G6PD deficiency on [NADPH] and ROS should also be determined in human populations[4, 8, 236].

Conclusion

G6PD deficiency remains the most common enzymopathy worldwide, and despite being so common, the effects of this deficiency are largely unexplored[2]. We set out to test whether or not G6PD deficiency would affect the heart and overall metabolic health in the context of obesity and high sugar intake. In our experiments, we determined that G6PD deficiency adversely affected heart failure and diet induced metabolic abnormalities. Because of its adverse cardiometabolic effects in mice, it important for us to study the effects of G6PD deficiency in human populations.

Appendix – Materials and Methods

Animal Treatment

All procedures were conducted in accordance with the Guidelines for the Care and Use of Laboratory Animals (NIH publication No. 85-23), and were approved by the University of Maryland Animal Care and Use Committee. Animals were fed ad libitum and maintained on a 12 hour light/dark cycle. Unless otherwise indicated, animals were fed a standard lab chow which consisted of 18% of energy from fat, 58% carbohydrate, and 24% protein (#2018SX, Teklad Diets, Indianapolis, IN).

Mouse Surgery

Myocardial Infarction.

Infarction was induced by permanent left anterior descending (LAD) occlusion, as follows: mice were anesthetized with 2% isoflurane in oxygen and ventilated at a tidal volume of 0.30 mL at 80 breaths / minute (Harvard Apparatus Inspira, Holliston, MA). Mice were placed in a position in which they were lying on their side on a warm heating pad. The ribs were separated, and a tapered 7-0 silk suture was used to tie off the LAD. The ribs and skin were then each closed with 6-0 silk. Sham animals were subjected to the same procedure except that the LAD was not occluded. Animals were allowed to recover for 3-5 minutes with 100% oxygen immediately after surgery, and then placed on a warm heating pad for full recovery.

Transverse Aortic Constriction

Pressure overload was induced by TAC. Anesthetized mice were placed in the supine position on a warm heating pad, and ventilated with 2% isoflurane in oxygen and ventilated at a tidal volume of 0.30 mL at 80 breaths / minute. A 27 gauge (17 week series) or 28 gauge needle (6 week series) was placed next to the transverse aorta, and a 6-0 silk suture was tied around both the aorta and the needle, and the needle was removed. The muscle and skin were then closed separately with 6-0 silk suture. Sham animals were subjected to the same surgical procedure except that the aorta was not constricted. Animals were allowed to recover for 3-5 minutes with 100% oxygen immediately after surgery, and then placed on a warm heating pad for full recovery.

Echocardiography

Cardiac function was assessed by echocardiography using a Vevo 2100 High-Resolution Imaging Systems (Visual Sonics, Toronto) with a 40MHz transducer or a Vevo 770 with a 30 MHz linear array transducer for mice or a 15 MHz linear array transducer for hamsters. Measurements taken with the Vevo 2100 were performed on animals anesthetized with 1-1.5% isoflurane in oxygen, and measurements with the Vevo 770 were performed on animals anesthetized 2-2.5% isoflurane. Anesthetized animals were shaved and placed in the supine position on a warming pad. M-mode frames were recorded from the parasternal short axis, and PW Doppler measurements were recorded from the apical view. Absolute wall thickness (AWT) and relative wall thickness (RWT) were calculated as: (PWTd + AWTd) and (PWTd + AWTd) / EDD, where PWTd is the diastolic posterior wall thickness, AWTd is the diastolic anterior wall thickness, and EDD is the end diastolic diameter. Ejection fraction was calculated as: (EDV - ESV) / EDV x 100%, where EDV is the end diastolic volume and ESV is the end systolic volume. From measurements taken from the Vevo 2100, EDV and ESV were calculated as: ((7.0 / (2.4 + EDD)) * EDD^3 and ((7.0 / (2.4 + ESD)) * ESD^3 respectively, where ESD is the end systolic diameter. From measurements taken from the Vevo 770, EDV and ESV were calculated as: 1.047 x EDD^3 and 1.047 x ESD^3 respectively. Myocardial performance index (MPI) was calculated as (isovolumetric contraction time + isovolumetric relaxation time) / ejection time.

Intraperitoneal Glucose Tolerance Test

Animals were fasted overnight for 15 hours, and injected with glucose (2 g/kg body mass). Blood was collected from the tail immediately before intraperitoneal injection (0 minutes) and then following injection at 30, 60, and 120 minutes. Glucose was measured with a Contour glucose meter (Bayer, Mishawaka, IN).

Terminal Procedure

Intraventricular Catheterization

Some animals underwent intraventricular catheterization prior to necropsy. Anesthetized mice were intubated and the thorax was opened. A high fidelity manomoner tipped catheter (SPR-1000 model, Millar, Houston, TX) was rapidly inserted through the apex into the LV, and pressure was recorded for 1-2 minutes, after which the terminal necropsy procedure was performed.

Necropsy

Animals were anesthetized, and the rib cage was opened. A small 20-30 mg piece of the LV free wall was cut free and snap frozen, weighed, and placed in liquid nitrogen for later NADPH or glutathione measurement. The remainder of the heart was dissected in ice-cold phosphate buffered saline, weighed, and frozen in liquid nitrogen. Blood was drawn from the thorax and centrifuged for 15 min at 1500 g to obtain serum. The liver, right kidney, and epididymal fat pads were weighed, and the tibia length was measured. All samples were stored at -80^{o}C until subsequent analysis.

Biochemical Measurements

Serum Measurements

All measurements were made with investigators blinded to strain and treatment. Serum glucose, triglycerides and free fatty acid concentrations were assayed spectrophotometrically (Wako Diagnostics, Richmond, VA). In plasma obtained from hamsters, insulin was measured with an enzyme-linked immunosorbent assay (Shibayagi Co., Shibukawa, Gunma, Japan). In serum obtained from mice leptin (#22-LEPMS-E01, Alpco Immunoassays, Salem, NH), insulin (#80-INSMSU-E01, Alpco Immunoassays, Salem, NH), and adiponectin (#EZMADP-60K, Millipore, St. Charles, MO) were also measured by enzyme-linked immunosorbent assays. All enzyme-linked immunosorbent assays were performed in duplicate for each sample, and other serum assays were performed in triplicate or quadruplicate for each sample.

Liver Glycogen

Tissue (25-35 mg) was homogenized in 3 M perchloric acid, after which homogenates were incubated for 2 hours with and without amyloglucosidase (50 µg/mL in 50 mM sodium acetate, 0.02% BSA, pH 5.5). Following this treatment, samples were centrifuged for 5 min at 2500 rpm, and 25 µL of the supernatant was used to determine the glucose concentration spectrophotometrically with a commercially available kit (Wako Diagnostics, Richmond, VA).

Liver Triglycerides

To measure triglycerides, 10-20 mg of tissue sample was homogenized in 1.5mL of 2:1 chloroform:methanol. After homogenization, 3.5 mL of 2:1 chloroform:methanol was added to samples, and samples were sonicated at 4 C for 1 hour and vortexed for 3 minutes. Vortexed samples were centrifuged at 1550 g for 15 minutes, and the supernatant was transferred to new glass vials. Pellets were resuspended in 5 mL of 2:1 chloroform:methanol, vortexed, centrifuged again, and the supernatants were transferred to the tubes containing the supernatants from the first centrifugation. The supernatants were allowed to dry and then assayed for triglycerides using a colorimetric assay kit (Wako Diagnostics, Richmond, VA).

Hexosamine Biosynthetic Pathway.

Protein isolation was performed as previously described[184]. Frozen heart and liver tissues were homogenized with modified ice-cold RIPA buffer, the supernatant was centrifuged twice at 13, 000 *g* for 10 min at 4°C, and then stored at -80°C until further use. We employed the Bradford assay for protein quantification, and total *O*-linked N-Acetylglucosamine (*O*-GlcNAc) expression evaluated by SDS-PAGE as described [184, 185] (CTD110.6, Santa Cruz Biotechnology Inc, Santa Cruz CA). Total *O*-GlcNAcylation expression (per lane) was quantified by densitometric analysis using β–actin (Cell Signaling, Beverly, MA) as a loading control.

Protein Kinase C Activity.

PKC activity was assessed by using a commercially available kit according to the manufacturer's instructions (Enzo Life Sciences, Farmingdale, NY). This is an ELISA-based method where a synthetic substrate is used for PKC activation that is measured by employing a polyclonal antibody that recognizes its phosphorylated form. Samples were homogenized in modified ice-cold RIPA buffer and the supernatant centrifuged twice at 13, 000 *g* for 10 min at 4°C. The active PKC control provided was serially diluted and added onto the 96 well-microtiter-plate (Corning Inc, Corning, NY) as controls. Homogenized tissue samples were subsequently added to appropriate wells, followed by the addition of ATP to initiate the reaction. The plate was incubated for 90 min at 30°C, after which the reaction was terminated by emptying contents of each well. The phosphospecific substrate antibody was added to wells followed by incubation at room temperature for 60 min. A peroxidase-conjugated secondary antibody was thereafter added and the assay was developed with tetramethylbenzidine substrate, where the intensity of color was proportional to PKC phosphotransferase activity. Color development was stopped with an acid solution and color intensity recorded in a microplate reader (EL 800 KC Junior Universal Microplate reader, Bio-Tek Instruments, Winooski Vermont, USA) at 450 nm. PKC activity was determined from the standard curve and expressed per volume of lysate per minute.

Polyol Pathway.

We assessed total D-sorbitol levels (cytosolic and mitochondrial components) as detailed in the instructions of a commercially obtained kit (Biovision K 631-100, Mountain View, CA). Briefly, liver and myocardial tissues were homogenized with modified ice-cold RIPA buffer, and the supernatant centrifuged twice at 13,000 *g* for 10 min at 4°C. Samples were subsequently incubated with 50 µl of reaction mix (assay buffer, enzyme mix, developer and probe) for 30 min at 37°C in a 96 well-microtiter-plate (Corning Inc, Corning, NY USA) in an orbital shaker incubator. Sorbitol levels were determined by evaluating the oxidation of sorbitol to fructose and the reaction's absorbance was recorded at 560 nm with a microplate reader (EL 800 KC Junior Universal Microplate reader, Bio-Tek Instruments, Winooski, VT). We calculated the sorbitol concentration (C) of samples by using the sample amount (nmol) from the standard curve (S_a), sample volume (µl) used (S_v) and the dilution factor (D); $C=S_a/S_v*D$.

Advanced Glycation End Products.

We determined methylglyoxal (MG) concentrations using the OxiSelect™ MG ELISA Kit (Cell Biolabs Inc, San Diego, CA 92126 USA). MG derivatives are formed from the non-enzymatic reaction of reducing carbohydrates such as glucose and carbonyl compounds (glyceraldehyde) in the Maillard reaction. Products of this reaction are referred to as AGEs. The kit measures the quantity of MG adduct in protein samples by comparing its absorbance with that of a known MG-BSA standard curve. Tissues were homogenized in modified ice cold RIPA buffer and the supernatant centrifuged twice at 13, 000 *g* for 10 min at 4°C. Protein quantification was performed using the Bradford assay and MG in the standard and protein samples were adsorbed (overnight at 4°C) onto a 96-well plate (Corning Inc, Corning, NY USA). This was followed by probing with an anti-MG specific monoclonal antibody for 60 min at room temperature. After a series of washing steps, an HRP-conjugated secondary antibody was added to all the wells and incubated for an hour at room temperature. A substrate solution was added to the wells and incubated for 5 to 20 min at room temperature on an orbital shaker for color development. The color development was stopped by adding a stop solution before reading absorbances at 450 nm with a microplate reader (EL 800 KC Junior Universal Microplate reader, Bio-Tek Instruments, Winooski, Vermont, USA). MG levels were calculated from the standard curve and are expressed as nmol per µg protein.

Enzyme Activity Assays

Whole tissue enzyme activities of 6-phosphogluconate (6PGD), citrate synthase (CS), medium-chain acyl-Coenzyme A dehydrogenase (MCAD), isocitrate dehydrogenase (ICDH), and G6PD were assayed from a single tissue homogenate and normalized to mg of wet tissue weight as described previously[154]. To obtain homogenized tissue, 10 – 20 mg of tissue was combined with 150 µL buffer containing 0.1 M Tris-HCl and 15 mM tricarballylic acid, pH 7.8. Tissue was homogenized in a Bullet Blender (Next Advance, Averill Park, NY) for 5 minutes on a setting of 8. All enzyme activities were assayed in duplicate for each sample.

To obtain G6PD activity, 10 μL of LV homogenate (10 μL of liver homogenate or 20 μL of hind-limb skeletal) muscle homogenate was added to cuvettes containing 490 μL of G6PD reaction mix (25 mM HEPES-Tris, 0.5 mM NADP+, 3.3 mM $MgCl_2$, 0.5 6-phosphogluconate [6PG], pH 7.8). The increase in light absorbance over 5 min was measured at 340 nm, after which 5 μL of 5 mM glucose 6-phosphate (G6P) was added, and the increase light absorbance at 340 nm was measured again. Activity was then determined by multiplying the slope to the molar concentration constant for NADPH (6.7 M^{-1}). To obtain G6PD activity, the slope of the absorbance without G6P was subtracted from the slope of the absorbance with G6P to obtain G6PD activity, because 6PGD, a downstream enzyme from G6PD in the pentose phosphate pathway, also produces NADPH, and the slope with G6P represents the activity of both enzymes.

For aconitase activity, 10 μL of LV homogenate (10 μL of liver homogenate or 20 μL of hind-limb skeletal muscle homogenate) was added to cuvettes containing 490 μL of aconitase reaction mix (0.083% chloroform, 1.67 mM sodium citrate, 26.7 mM triethanolamine, 0.5 mM NADP+, 0.5 mM $MgCl_2$, pH 7.4) , and the increase in absorbance at 340 nm was measured over 5 min. Activity was then determined by multiplying the slope to the molar concentration constant for NADPH (6.7 M^{-1}).

For ICDH activity, 10 μL of LV homogenate was added to cuvettes containing 490 μL of ICDH reaction mix (3.2 mM DL-isocitrate, 4.8 mM triethanolamine, 0.5 mM NADP+, 3.5 mM $MgCl_2$, pH 7.4), and the increase in absorbance at 340 nm was measured over 5 min. Activity was then determined by multiplying the slope to the molar concentration constant for NADPH (6.7 M^{-1}).

For CS activity, 0.5 μL of LV homogenate (1 μL of liver homogenate or 4 μL of hind-limb skeletal muscle homogenate) was added to cuvettes containing 500 μL of CS reaction mix (0.1 M Tris-HCl, 1.25 mM 5,5′-dithiobis[2-nitrobenzoic acid], pH 8). Then, 25 μL of 50 mM oxaloacetate and 5 mM acetyl-CoA were added to the reaction mixture, and the increase in absorbance at 412 nm was measured over 5 min. Activity was then determined by multiplying the slope to the molar concentration constant for 5,5′-dithiobis[2-nitrobenzoic acid] (13600 M^{-1}).

For MCAD activity, 5 μL of LV homogenate (5 μL of liver homogenate or 40 μL of skeletal muscle homogenate) was added to cuvettes containing 500 μ l of 100 mM KH_2PO_4, 1 mM EDTA, 0.5 mM sodium tetrathionate, and 200 μM ferrocenium hexafluorophosphate, pH 7.4. Then, 50 μL of 0.5 mM octanoyl-CoA was added to the reaction mixture, and the decrease in absorbance at 300 nm was measured over 5 min. Activity was then determined by multiplying the slope to the molar concentration constant for ferrocenium hexafluorophosphate (4300 M^{-1}).

We utilized a commercially available GAPDH activity assay according to the manufacturer’s instructions (Biomedical Research Service Centre, University at Buffalo, NY). The assay is based on the reduction of a water-soluble tetrazolium salt, 2-(4-Iodophenyl)-3-(4-nitrophenyl)-5-phenyl-2H-tetrazolium chloride (INT) to formazan (NADH-coupled reaction) exhibiting an absorption maximum at 492 nm. The intensity of the red color produced corresponds to the degree of GAPDH activity. Tissue samples were lysed with cell lysis buffer and protein concentrations diluted to fall within 0.2-2 mg/ml range. Ten µl of each sample was then pipetted onto the 96-well plate (Corning Inc, Corning NY), and the reaction was initiated by adding 50 µl of the GAPDH assay solution to each well. The plate was incubated at 37 °C for 60 min in an orbital shaking incubator. The reaction was stopped by addition of 50 µl of 3% acetic acid and the absorbance was measured at 492 nm using a microplate reader (EL 800 KC Junior Universal Microplate reader, Bio-Tek Instruments Inc, Winooski, VT). GAPDH activity is expressed as the relative optical density unit per g protein.

We evaluated gross overall apoptosis by employing a caspase activity assay (Biovision, Mountain View, CA). Tissues were homogenized with modified ice cold RIPA buffer, the supernatant was centrifuged twice at 13,000 *g* for 10 min at 4°C, and protein concentration was determined by a Bradford assay. The assay is based on spectrophotometric detection of the chromophore, p-nitroaniline (pNA) after cleavage of the labelled substrate amino acid sequence Asp-Glu-Val-Asp (DEVD)-pNA. The samples are added onto a 96 well-microtiter-plate (Corning Inc, Corning, NY) and incubated with the reaction mix and DEVD-pNA for 2 hours at 37 °C for 60 min in an orbital shaker incubator. The color intensity was quantified with a microplate reader (EL 800 KC Junior Universal Microplate reader, Bio-Tek Instruments, Winooski, VT) at 505 nm, and caspase 3 activity was expressed as arbitrary units per g protein.

Superoxide

Superoxide production was measured via lucigenin chemiluminescence.LV tissue was homogenized in MOPS (20 mmol/L) – sucrose (250 mmol/L) buffer (pH 7.4) containing 100 mmol/L phenylmethylsulfonyl fluoride, 10 µg/mL aprotinin, 10 µg/mL leupeptin, and 200 mmol/L pepstatin. This buffer system preserves intact cellular organelles in tissue homogenates[237]. Myocardial homogenate (20 µL) was added to lucigenin (5 μM) and Krebs solution buffered with 10mmol/L HEPES-NaOH (pH 7.4) to a final volume of 1 mL, and incubated at 37°C, and light emittance was measured as described[6]. The measurement was repeated after adding an NADPH regenerating system consisting of glucose 6-phosphate (200 μmol/L) and NADP+ (100 μmol/L) to each reaction.

NADPH

Myocardial NADPH levels were determined spectrophotometrically using a commercially available enzymatic method (BioVision, CA, USA). Homogenized tissue was centrifuged, and the supernatant (200 μl) was heated to 60°C for 30 min to decompose all NADP+, leaving NADPH intact. Samples were cooled on ice, and 50 μl of sample and 10 μl NADPH developer was added into each well on a 96 well plate, incubated for 1 hr and read at a 450 nm, as instructed by the manufacturer.

Lipid Peroxidation Products

Myocardial tissue concentrations of the lipid peroxidation products, malondialdehyde (MDA) and 4-hydroxyalkenals (4HA), were measured LV homogenates and normalized to tissue protein content (Oxford Biomedical Research, Oxford, MI). All samples were assayed in duplicate.

RT-qPCR

RNA was isolated using a commercially available kit according to the manufacturer's instructions (Qiagen, Valencia, CA), after which cDNA was generated as follows: 2 µg of RNA was combined with oligo(dT)$_{16}$ (4ul; Life Technologies, Grand Island, NY), random primers (3 µg), RNase inhibitor (10 U), dNTP (0.5 mM), DTT (10 mM), Superscript II reverse transcriptase (400 U; Life Technologies, Grand Island, NY), Superscript II 5x buffer (10 µL), and RNase-free water to a total volume of 50 µL. RNA, water, and primers were heated to 70° C for 10 minutes and then put on ice for 2 minutes, before adding the other reagents, to disrupt RNA secondary structures and allow primers to anneal. After all reagents were combined with each sample, samples were heated to 42° C for 1 hour, then heated to 70° C for 10 minutes, put immediately on ice, and then stored at -70° C until further use.

Messenger RNA was assessed by reverse transcription quantitative real time PCR with Taq man primers directed to G6PD, ANP, MHCβ, and MHCα, using cycle threshold (Ct) values from cyclophilin D or 16s ribosomal RNA for normalization (Applied Biosystems [ABI], Foster City, CA). In the myocardial infarction experiment, we validated the G6PD expression data using a second set of primers. The first set of primers spanned exons 12-13 (ABI #Mm00656735_g1), and the second set spanned exons 1-2 (ABI #Mm04260097_m1). Each reaction consisted of the following components: 1 µL cDNA template (containing 40 ng cDNA), 12.5 µL TaqMan PCR master mix (ABI, Foster City, CA), 10.25 µL nuclease-free water, and 1.25 µL TaqMan primer mix. The reaction was heated to 95° C for 10 minutes, and then cycled 40 times at 95° C for 15 seconds and 60° C for 1 minute. All qPCR reactions were performed in duplicate for each sample. Ct were obtained using a FAM fluorescence threshold of 215 dR.

References

(1) Beutler E. Glucose-6-phosphate dehydrogenase deficiency: a historical perspective. *Blood* 2008 January 1;111(1):16-24.

(2) Cappellini MD, Fiorelli G. Glucose-6-phosphate dehydrogenase deficiency. *Lancet* 2008 January 5;371(9606):64-74.

(3) Gupte SA, Levine RJ, Gupte RS et al. Glucose-6-phosphate dehydrogenase-derived NADPH fuels superoxide production in the failing heart. *J Mol Cell Cardiol* 2006 August;41(2):340-9.

(4) Gupte RS, Floyd BC, Kozicky M et al. Synergistic activation of glucose-6-phosphate dehydrogenase and NAD(P)H oxidase by Src kinase elevates superoxide in type 2 diabetic, Zucker fa/fa, rat liver. *Free Radic Biol Med* 2009 August 1;47(3):219-28.

(5) Gupte SA. Glucose-6-phosphate dehydrogenase: a novel therapeutic target in cardiovascular diseases. *Curr Opin Investig Drugs* 2008 September;9(9):993-1000.

(6) Gupte RS, Vijay V, Marks B et al. Upregulation of glucose-6-phosphate dehydrogenase and NAD(P)H oxidase activity increases oxidative stress in failing human heart. *J Card Fail* 2007 August;13(6):497-506.

(7) Rajasekaran NS, Connell P, Christians ES et al. Human alpha B-crystallin mutation causes oxido-reductive stress and protein aggregation cardiomyopathy in mice. *Cell* 2007 August 10;130(3):427-39.

(8) Serpillon S, Floyd BC, Gupte RS et al. Superoxide production by NAD(P)H oxidase and mitochondria is increased in genetically obese and hyperglycemic rat heart and aorta before the development of cardiac dysfunction. The role of glucose-6-phosphate dehydrogenase-derived NADPH. *Am J Physiol Heart Circ Physiol* 2009 July;297(1):H153-H162.

(9) Tian WN, Braunstein LD, Pang J et al. Importance of glucose-6-phosphate dehydrogenase activity for cell growth. *J Biol Chem* 1998 April 24;273(17):10609-17.

(10) Tian WN, Braunstein LD, Apse K et al. Importance of glucose-6-phosphate dehydrogenase activity in cell death. *Am J Physiol* 1999 May;276(5 Pt 1):C1121-C1131.

(11) Xu Y, Zhang Z, Hu J et al. Glucose-6-phosphate dehydrogenase-deficient mice have increased renal oxidative stress and increased albuminuria. *FASEB J* 2010 February;24(2):609-16.

(12) Zhang Z, Apse K, Pang J, Stanton RC. High glucose inhibits glucose-6-phosphate dehydrogenase via cAMP in aortic endothelial cells. *J Biol Chem* 2000 December 22;275(51):40042-7.

(13) Zhang Z, Liew CW, Handy DE et al. High glucose inhibits glucose-6-phosphate dehydrogenase, leading to increased oxidative stress and beta-cell apoptosis. *FASEB J* 2010 May;24(5):1497-505.

(14) Glucose-6-phosphate dehydrogenase deficiency. WHO Working Group. *Bull World Health Organ* 1989;67(6):601-11.

(15) Luzzatto L, Notaro R. Malaria. Protecting against bad air. *Science* 2001 July 20;293(5529):442-3.

(16) Beutler E. G6PD deficiency. *Blood* 1994 December 1;84(11):3613-36.

(17) GLASER L, BROWN DH. Purification and properties of d-glucose-6-phosphate dehydrogenase. *J Biol Chem* 1955 September;216(1):67-79.

(18) Persico MG, Viglietto G, Martini G et al. Isolation of human glucose-6-phosphate dehydrogenase (G6PD) cDNA clones: primary structure of the protein and unusual 5' non-coding region. *Nucleic Acids Res* 1986 March 25;14(6):2511-22.

(19) Takizawa T, Huang IY, Ikuta T, Yoshida A. Human glucose-6-phosphate dehydrogenase: primary structure and cDNA cloning. *Proc Natl Acad Sci U S A* 1986 June;83(12):4157-61.

(20) Naylor CE, Rowland P, Basak AK et al. Glucose 6-phosphate dehydrogenase mutations causing enzyme deficiency in a model of the tertiary structure of the human enzyme. *Blood* 1996 April 1;87(7):2974-82.

(21) Rowland P, Basak AK, Gover S, Levy HR, Adams MJ. The three-dimensional structure of glucose 6-phosphate dehydrogenase from Leuconostoc mesenteroides refined at 2.0 A resolution. *Structure* 1994 November 15;2(11):1073-87.

(22) Au SW, Naylor CE, Gover S et al. Solution of the structure of tetrameric human glucose 6-phosphate dehydrogenase by molecular replacement. *Acta Crystallogr D Biol Crystallogr* 1999 April;55(Pt 4):826-34.

(23) Au SW, Gover S, Lam VM, Adams MJ. Human glucose-6-phosphate dehydrogenase: the crystal structure reveals a structural NADP(+) molecule and provides insights into enzyme deficiency. *Structure* 2000 March 15;8(3):293-303.

(24) Cohen P, Rosemeyer MA. Subunit interactions of glucose-6-phosphate dehydrogenase from human erythrocytes. *Eur J Biochem* 1969 March;8(1):8-15.

(25) CHUNG AE, LANGDON RG. Human erythrocyte glucose 6-phosphate dehydrogenase. II. Enzyme-coenzyme interrelationship. *J Biol Chem* 1963 July;238:2317-24.

(26) CHUNG AE, LANGDON RG. Human erythrocyte glucose 6-phosphate dehydrogenase. I. Isolation and properties of the enzyme. *J Biol Chem* 1963 July;238:2309-16.

(27) Jain M, Brenner DA, Cui L et al. Glucose-6-phosphate dehydrogenase modulates cytosolic redox status and contractile phenotype in adult cardiomyocytes. *Circ Res* 2003 July 25;93(2):e9-16.

(28) Morelli A, Benatti U, Gaetani GF, De FA. Biochemical mechanisms of glucose-6-phosphate dehydrogenase deficiency. *Proc Natl Acad Sci U S A* 1978 April;75(4):1979-83.

(29) Frederiks WM, Kummerlin IP, Bosch KS, Vreeling-Sindelarova H, Jonker A, Van Noorden CJ. NADPH production by the pentose phosphate pathway in the zona fasciculata of rat adrenal gland. *J Histochem Cytochem* 2007 September;55(9):975-80.

(30) Meldrum NU, Tarr HL. The reduction of glutathione by the Warburg-Christian system. *Biochem J* 1935;29(1):108-15.

(31) Leopold JA, Loscalzo J. Oxidative enzymopathies and vascular disease. *Arterioscler Thromb Vasc Biol* 2005 July;25(7):1332-40.

(32) Longo L, Vanegas OC, Patel M et al. Maternally transmitted severe glucose 6-phosphate dehydrogenase deficiency is an embryonic lethal. *EMBO J* 2002 August 15;21(16):4229-39.

(33) Chevion M, Navok T, Glaser G, Mager J. The chemistry of favism-inducing compounds. The properties of isouramil and divicine and their reaction with glutathione. *Eur J Biochem* 1982 October;127(2):405-9.

(34) DERN RJ, WEINSTEIN IM, LEROY GV, TALMAGE DW, ALVING AS. The hemolytic effect of primaquine. I. The localization of the drug-induced hemolytic defect in primaquine-sensitive individuals. *J Lab Clin Med* 1954 February;43(2):303-9.

(35) ALVING AS, CARSON PE, FLANAGAN CL, ICKES CE. Enzymatic deficiency in primaquine-sensitive erythrocytes. *Science* 1956 September 14;124(3220):484-5.

(36) Beutler E, DERN RJ, FLANAGAN CL, ALVING AS. The hemolytic effect of primaquine. VII. Biochemical studies of drug-sensitive erythrocytes. *J Lab Clin Med* 1955 February;45(2):286-95.

(37) Beutler E, ROBSON M, BUTTENWIESER E. The mechanism of glutathione destruction and protection in drug-sensitive and non-sensitive erythrocytes; in vitro studies. *J Clin Invest* 1957 April;36(4):617-28.

(38) Beutler E. The glutathione instability of drug-sensitive red cells; a new method for the in vitro detection of drug sensitivity. *J Lab Clin Med* 1957 January;49(1):84-95.

(39) Kaplan M, Bromiker R, Hammerman C. Severe neonatal hyperbilirubinemia and kernicterus: are these still problems in the third millennium? *Neonatology* 2011;100(4):354-62.

(40) Schwartz HP, Haberman BE, Ruddy RM. Hyperbilirubinemia: current guidelines and emerging therapies. *Pediatr Emerg Care* 2011 September;27(9):884-9.

(41) Beutler E, Mitchell M. Special modifications of the fluorescent screening method for glucose-6-phosphate dehydrogenase deficiency. *Blood* 1968 November;32(5):816-8.

(42) Beutler E. A series of new screening procedures for pyruvate kinase deficiency, glucose-6-phosphate dehydrogenase deficiency, and glutathione reductase deficiency. *Blood* 1966 October;28(4):553-62.

(43) Monga A, Makkar RP, Arora A, Mukhopadhyay S, Gupta AK. Case report: Acute hepatitis E infection with coexistent glucose-6-phosphate dehydrogenase deficiency. *Can J Infect Dis* 2003 July;14(4):230-1.

(44) Pretsch W, Charles DJ, Merkle S. X-linked glucose-6-phosphate dehydrogenase deficiency in Mus musculus. *Biochem Genet* 1988 February;26(1-2):89-103.

(45) Sanders S, Smith DP, Thomas GA, Williams ED. A glucose-6-phosphate dehydrogenase (G6PD) splice site consensus sequence mutation associated with G6PD enzyme deficiency. *Mutat Res* 1997 March 4;374(1):79-87.

(46) Hunt SA, Abraham WT, Chin MH et al. 2009 focused update incorporated into the ACC/AHA 2005 Guidelines for the Diagnosis and Management of Heart Failure in Adults: a report of the American College of Cardiology Foundation/American Heart Association Task Force on Practice Guidelines: developed in collaboration with the International Society for Heart and Lung Transplantation. *Circulation* 2009 April 14;119(14):e391-e479.

(47) The Criteria Committee of the New York Heart Association. *Nomenclature and Criteria for Diagnosis of Diseases of the Heart and Great Vessels*. Boston: Little, Brown & Co; 1994.

(48) Lloyd-Jones D, Adams RJ, Brown TM et al. Heart disease and stroke statistics--2010 update: a report from the American Heart Association. *Circulation* 2010 February 23;121(7):e46-e215.

(49) Conrad CH, Brooks WW, Hayes JA, Sen S, Robinson KG, Bing OH. Myocardial fibrosis and stiffness with hypertrophy and heart failure in the spontaneously hypertensive rat. *Circulation* 1995 January 1;91(1):161-70.

(50) Shah MG, Cho S, Atwood JE, Heidenreich PA. Peripheral edema due to heart disease: diagnosis and outcome. *Clin Cardiol* 2006 January;29(1):31-5.

(51) Murray JF. Pulmonary edema: pathophysiology and diagnosis. *Int J Tuberc Lung Dis* 2011 February;15(2):155-60, i.

(52) Cho S, Atwood JE. Peripheral edema. *Am J Med* 2002 November;113(7):580-6.

(53) Frey N, Olson EN. Cardiac hypertrophy: the good, the bad, and the ugly. *Annu Rev Physiol* 2003;65:45-79.

(54) Bottini PB, Carr AA, Prisant LM, Flickinger FW, Allison JD, Gottdiener JS. Magnetic resonance imaging compared to echocardiography to assess left ventricular mass in the hypertensive patient. *Am J Hypertens* 1995 March;8(3):221-8.

(55) Cain PA, Ahl R, Hedstrom E et al. Age and gender specific normal values of left ventricular mass, volume and function for gradient echo magnetic resonance imaging: a cross sectional study. *BMC Med Imaging* 2009;9:2.

(56) Krumholz HM, Larson M, Levy D. Prognosis of left ventricular geometric patterns in the Framingham Heart Study. *J Am Coll Cardiol* 1995 March 15;25(4):879-84.

(57) Heineke J, Molkentin JD. Regulation of cardiac hypertrophy by intracellular signalling pathways. *Nat Rev Mol Cell Biol* 2006 August;7(8):589-600.

(58) Katz AM. Maladaptive growth in the failing heart: the cardiomyopathy of overload. *Cardiovasc Drugs Ther* 2002 May;16(3):245-9.

(59) Devereux RB, Roman MJ. Left ventricular hypertrophy in hypertension: stimuli, patterns, and consequences. *Hypertens Res* 1999 March;22(1):1-9.

(60) Haider AW, Larson MG, Benjamin EJ, Levy D. Increased left ventricular mass and hypertrophy are associated with increased risk for sudden death. *J Am Coll Cardiol* 1998 November;32(5):1454-9.

(61) Berenji K, Drazner MH, Rothermel BA, Hill JA. Does load-induced ventricular hypertrophy progress to systolic heart failure? *Am J Physiol Heart Circ Physiol* 2005 July;289(1):H8-H16.

(62) Kowey PR, Friechling TD, Sewter J et al. Electrophysiological effects of left ventricular hypertrophy. Effect of calcium and potassium channel blockade. *Circulation* 1991 June;83(6):2067-75.

(63) Cipriano C, Gosse P, Bemurat L et al. Prognostic value of left ventricular mass and its evolution during treatment in the Bordeaux cohort of hypertensive patients. *Am J Hypertens* 2001 June;14(6 Pt 1):524-9.

(64) Vakili BA, Okin PM, Devereux RB. Prognostic implications of left ventricular hypertrophy. *Am Heart J* 2001 March;141(3):334-41.

(65) Nagueh SF, Shah G, Wu Y et al. Altered titin expression, myocardial stiffness, and left ventricular function in patients with dilated cardiomyopathy. *Circulation* 2004 July 13;110(2):155-62.

(66) Rajabi M, Kassiotis C, Razeghi P, Taegtmeyer H. Return to the fetal gene program protects the stressed heart: a strong hypothesis. *Heart Fail Rev* 2007 December;12(3-4):331-43.

(67) Schwartz K, Carrier L, Lompre AM, Mercadier JJ, Boheler KR. Contractile proteins and sarcoplasmic reticulum calcium-ATPase gene expression in the hypertrophied and failing heart. *Basic Res Cardiol* 1992;87 Suppl 1:285-90.

(68) Neagoe C, Kulke M, del MF et al. Titin isoform switch in ischemic human heart disease. *Circulation* 2002 September 10;106(11):1333-41.

(69) Schwartz K, Carrier L, Chassagne C, Wisnewsky C, Boheler KR. Regulation of myosin heavy chain and actin isogenes during cardiac growth and hypertrophy. *Symp Soc Exp Biol* 1992;46:265-72.

(70) Suurmeijer AJ, Clement S, Francesconi A et al. Alpha-actin isoform distribution in normal and failing human heart: a morphological, morphometric, and biochemical study. *J Pathol* 2003 March;199(3):387-97.

(71) Nishikimi T, Yoshihara F, Morimoto A et al. Relationship between left ventricular geometry and natriuretic peptide levels in essential hypertension. *Hypertension* 1996 July;28(1):22-30.

(72) Rubattu S, Sciarretta S, Valenti V, Stanzione R, Volpe M. Natriuretic peptides: an update on bioactivity, potential therapeutic use, and implication in cardiovascular diseases. *Am J Hypertens* 2008 July;21(7):733-41.

(73) Troughton RW, Frampton CM, Yandle TG, Espiner EA, Nicholls MG, Richards AM. Treatment of heart failure guided by plasma aminoterminal brain natriuretic peptide (N-BNP) concentrations. *Lancet* 2000 April 1;355(9210):1126-30.

(74) Stanley WC, Recchia FA, Lopaschuk GD. Myocardial substrate metabolism in the normal and failing heart. *Physiol Rev* 2005 July;85(3):1093-129.

(75) Neubauer S. The failing heart--an engine out of fuel. *N Engl J Med* 2007 March 15;356(11):1140-51.

(76) Hoppel CL, Tandler B, Parland W, Turkaly JS, Albers LD. Hamster cardiomyopathy. A defect in oxidative phosphorylation in the cardiac interfibrillar mitochondria. *J Biol Chem* 1982 February 10;257(3):1540-8.

(77) Razeghi P, Young ME, Alcorn JL, Moravec CS, Frazier OH, Taegtmeyer H. Metabolic gene expression in fetal and failing human heart. *Circulation* 2001 December 11;104(24):2923-31.

(78) Barth AS, Kumordzie A, Frangakis C, Margulies KB, Cappola TP, Tomaselli GF. Reciprocal transcriptional regulation of metabolic and signaling pathways correlates with disease severity in heart failure. *Circ Cardiovasc Genet* 2011 October;4(5):475-83.

(79) Galvao TF, Brown BH, Hecker PA et al. High intake of saturated fat, but not polyunsaturated fat, improves survival in heart failure despite persistent mitochondrial defects. *Cardiovasc Res* 2011 November 8.

(80) O'Shea KM, Chess DJ, Khairallah RJ et al. omega-3 Polyunsaturated fatty acids prevent pressure overload-induced ventricular dilation and decrease in mitochondrial enzymes despite no change in adiponectin. *Lipids Health Dis* 2010;9:95.

(81) Kalsi KK, Smolenski RT, Pritchard RD, Khaghani A, Seymour AM, Yacoub MH. Energetics and function of the failing human heart with dilated or hypertrophic cardiomyopathy. *Eur J Clin Invest* 1999 June;29(6):469-77.

(82) Hecker PA, Galvao TF, O'Shea KM et al. High-sugar intake does not exacerbate metabolic abnormalities or cardiac dysfunction in genetic cardiomyopathy. *Nutrition* 2012 February 2.

(83) Vantrimpont P, Rouleau JL, Wun CC et al. Additive beneficial effects of beta-blockers to angiotensin-converting enzyme inhibitors in the Survival and Ventricular Enlargement (SAVE) Study. SAVE Investigators. *J Am Coll Cardiol* 1997 February;29(2):229-36.

(84) Sabbah HN. Biologic rationale for the use of beta-blockers in the treatment of heart failure. *Heart Fail Rev* 2004 April;9(2):91-7.

(85) Feldman D, Elton TS, Menachemi DM, Wexler RK. Heart rate control with adrenergic blockade: clinical outcomes in cardiovascular medicine. *Vasc Health Risk Manag* 2010;6:387-97.

(86) Zicha S, Tsuji Y, Shiroshita-Takeshita A, Nattel S. Beta-blockers as antiarrhythmic agents. *Handb Exp Pharmacol* 2006;(171):235-66.

(87) Communal C, Singh K, Pimentel DR, Colucci WS. Norepinephrine stimulates apoptosis in adult rat ventricular myocytes by activation of the beta-adrenergic pathway. *Circulation* 1998 September 29;98(13):1329-34.

(88) The Cardiac Insufficiency Bisoprolol Study II (CIBIS-II): a randomised trial. *Lancet* 1999 January 2;353(9146):9-13.

(89) Hjalmarson A, Goldstein S, Fagerberg B et al. Effects of controlled-release metoprolol on total mortality, hospitalizations, and well-being in patients with heart failure: the Metoprolol CR/XL Randomized Intervention Trial in congestive heart failure (MERIT-HF). MERIT-HF Study Group. *JAMA* 2000 March 8;283(10):1295-302.

(90) Packer M, Coats AJ, Fowler MB et al. Effect of carvedilol on survival in severe chronic heart failure. *N Engl J Med* 2001 May 31;344(22):1651-8.

(91) Lohse MJ, Engelhardt S, Eschenhagen T. What is the role of beta-adrenergic signaling in heart failure? *Circ Res* 2003 November 14;93(10):896-906.

(92) Hall JE. Control of blood pressure by the renin-angiotensin-aldosterone system. *Clin Cardiol* 1991 August;14(8 Suppl 4):IV6-21.

(93) Hall JE. The renin-angiotensin system: renal actions and blood pressure regulation. *Compr Ther* 1991 May;17(5):8-17.

(94) Mehta PK, Griendling KK. Angiotensin II cell signaling: physiological and pathological effects in the cardiovascular system. *Am J Physiol Cell Physiol* 2007 January;292(1):C82-C97.

(95) Struthers AD, MacDonald TM. Review of aldosterone- and angiotensin II-induced target organ damage and prevention. *Cardiovasc Res* 2004 March 1;61(4):663-70.

(96) Granger CB, McMurray JJ, Yusuf S et al. Effects of candesartan in patients with chronic heart failure and reduced left-ventricular systolic function intolerant to angiotensin-converting-enzyme inhibitors: the CHARM-Alternative trial. *Lancet* 2003 September 6;362(9386):772-6.

(97) Pitt B, Zannad F, Remme WJ et al. The effect of spironolactone on morbidity and mortality in patients with severe heart failure. Randomized Aldactone Evaluation Study Investigators. *N Engl J Med* 1999 September 2;341(10):709-17.

(98) Effects of enalapril on mortality in severe congestive heart failure. Results of the Cooperative North Scandinavian Enalapril Survival Study (CONSENSUS).

The CONSENSUS Trial Study Group. *N Engl J Med* 1987 June 4;316(23):1429-35.

(99) Effect of enalapril on survival in patients with reduced left ventricular ejection fractions and congestive heart failure. The SOLVD Investigators. *N Engl J Med* 1991 August 1;325(5):293-302.

(100) Brater DC. Diuretic therapy. *N Engl J Med* 1998 August 6;339(6):387-95.

(101) Patten RD, Hall-Porter MR. Small animal models of heart failure: development of novel therapies, past and present. *Circ Heart Fail* 2009 March;2(2):138-44.

(102) Grimard BH, Larson JM. Aortic stenosis: diagnosis and treatment. *Am Fam Physician* 2008 September 15;78(6):717-24.

(103) Verdecchia P, Carini G, Circo A et al. Left ventricular mass and cardiovascular morbidity in essential hypertension: the MAVI study. *J Am Coll Cardiol* 2001 December;38(7):1829-35.

(104) Pfeffer JM, Pfeffer MA, Braunwald E. Influence of chronic captopril therapy on the infarcted left ventricle of the rat. *Circ Res* 1985 July;57(1):84-95.

(105) Pfeffer MA, Pfeffer JM, Steinberg C, Finn P. Survival after an experimental myocardial infarction: beneficial effects of long-term therapy with captopril. *Circulation* 1985 August;72(2):406-12.

(106) Takimoto E, Champion HC, Li M et al. Chronic inhibition of cyclic GMP phosphodiesterase 5A prevents and reverses cardiac hypertrophy. *Nat Med* 2005 February;11(2):214-22.

(107) Heymes C, Bendall JK, Ratajczak P et al. Increased myocardial NADPH oxidase activity in human heart failure. *J Am Coll Cardiol* 2003 June 18;41(12):2164-71.

(108) Babior BM. NADPH oxidase: an update. *Blood* 1999 March 1;93(5):1464-76.

(109) Kuroda J, Ago T, Matsushima S, Zhai P, Schneider MD, Sadoshima J. NADPH oxidase 4 (Nox4) is a major source of oxidative stress in the failing heart. *Proc Natl Acad Sci U S A* 2010 August 31;107(35):15565-70.

(110) Infanger DW, Cao X, Butler SD et al. Silencing nox4 in the paraventricular nucleus improves myocardial infarction-induced cardiac dysfunction by attenuating sympathoexcitation and periinfarct apoptosis. *Circ Res* 2010 June 11;106(11):1763-74.

(111) Doerries C, Grote K, Hilfiker-Kleiner D et al. Critical role of the NAD(P)H oxidase subunit p47phox for left ventricular remodeling/dysfunction and survival after myocardial infarction. *Circ Res* 2007 March 30;100(6):894-903.

(112) Dixon LJ, Morgan DR, Hughes SM et al. Functional consequences of endothelial nitric oxide synthase uncoupling in congestive cardiac failure. *Circulation* 2003 April 8;107(13):1725-8.

(113) Xia Y, Dawson VL, Dawson TM, Snyder SH, Zweier JL. Nitric oxide synthase generates superoxide and nitric oxide in arginine-depleted cells leading to peroxynitrite-mediated cellular injury. *Proc Natl Acad Sci U S A* 1996 June 25;93(13):6770-4.

(114) Moens AL, Takimoto E, Tocchetti CG et al. Reversal of cardiac hypertrophy and fibrosis from pressure overload by tetrahydrobiopterin: efficacy of recoupling nitric oxide synthase as a therapeutic strategy. *Circulation* 2008 May 20;117(20):2626-36.

(115) Porras AG, Olson JS, Palmer G. The reaction of reduced xanthine oxidase with oxygen. Kinetics of peroxide and superoxide formation. *J Biol Chem* 1981 September 10;256(17):9006-103.

(116) Cappola TP, Kass DA, Nelson GS et al. Allopurinol improves myocardial efficiency in patients with idiopathic dilated cardiomyopathy. *Circulation* 2001 November 13;104(20):2407-11.

(117) Hayashi K, Kimata H, Obata K et al. Xanthine oxidase inhibition improves left ventricular dysfunction in dilated cardiomyopathic hamsters. *J Card Fail* 2008 April;14(3):238-44.

(118) Dai DF, Johnson SC, Villarin JJ et al. Mitochondrial oxidative stress mediates angiotensin II-induced cardiac hypertrophy and Galphaq overexpression-induced heart failure. *Circ Res* 2011 April 1;108(7):837-46.

(119) Dai DF, Hsieh EJ, Liu Y et al. Mitochondrial proteome remodelling in pressure overload-induced heart failure: the role of mitochondrial oxidative stress. *Cardiovasc Res* 2012 January 1;93(1):79-88.

(120) Chess DJ, Stanley WC. Role of diet and fuel overabundance in the development and progression of heart failure. *Cardiovasc Res* 2008 July 15;79(2):269-78.

(121) Ogden CL, Carroll MD, Curtin LR, McDowell MA, Tabak CJ, Flegal KM. Prevalence of overweight and obesity in the United States, 1999-2004. *JAMA* 2006 April 5;295(13):1549-55.

(122) Alberti KG, Eckel RH, Grundy SM et al. Harmonizing the metabolic syndrome: a joint interim statement of the International Diabetes Federation Task Force on Epidemiology and Prevention; National Heart, Lung, and Blood Institute; American Heart Association; World Heart Federation; International Atherosclerosis Society; and International Association for the Study of Obesity. *Circulation* 2009 October 20;120(16):1640-5.

(123) Kenchaiah S, Evans JC, Levy D et al. Obesity and the risk of heart failure. *N Engl J Med* 2002 August 1;347(5):305-13.

(124) Jensen G, Nyboe J, Appleyard M, Schnohr P. Risk factors for acute myocardial infarction in Copenhagen, II: Smoking, alcohol intake, physical activity, obesity, oral contraception, diabetes, lipids, and blood pressure. *Eur Heart J* 1991 March;12(3):298-308.

(125) Yusuf S, Hawken S, Ounpuu S et al. Obesity and the risk of myocardial infarction in 27,000 participants from 52 countries: a case-control study. *Lancet* 2005 November 5;366(9497):1640-9.

(126) Lewis CE, McTigue KM, Burke LE et al. Mortality, health outcomes, and body mass index in the overweight range: a science advisory from the American Heart Association. *Circulation* 2009 June 30;119(25):3263-71.

(127) Voulgari C, Tentolouris N, Dilaveris P, Tousoulis D, Katsilambros N, Stefanadis C. Increased heart failure risk in normal-weight people with metabolic syndrome compared with metabolically healthy obese individuals. *J Am Coll Cardiol* 2011 September 20;58(13):1343-50.

(128) Kanasaki K, Koya D. Biology of obesity: lessons from animal models of obesity. *J Biomed Biotechnol* 2011;2011:197636.

(129) Mathe D. Dyslipidemia and diabetes: animal models. *Diabete Metab* 1995 April;21(2):106-11.

(130) Ren J, Ma H. Impaired cardiac function in leptin-deficient mice. *Curr Hypertens Rep* 2008 December;10(6):448-53.

(131) Ren J, Dong F, Cai GJ et al. Interaction between age and obesity on cardiomyocyte contractile function: role of leptin and stress signaling. *PLoS One* 2010;5(4):e10085.

(132) Kim JY, van de WE, Laplante M et al. Obesity-associated improvements in metabolic profile through expansion of adipose tissue. *J Clin Invest* 2007 September;117(9):2621-37.

(133) Wauman J, Tavernier J. Leptin receptor signaling: pathways to leptin resistance. *Front Biosci* 2011;17:2771-93.

(134) Ashwin PJ, Dilipbhai PJ. Leptin and the cardiovascular system: a review. *Recent Pat Cardiovasc Drug Discov* 2007 June;2(2):100-9.

(135) Dardeno TA, Chou SH, Moon HS, Chamberland JP, Fiorenza CG, Mantzoros CS. Leptin in human physiology and therapeutics. *Front Neuroendocrinol* 2010 July;31(3):377-93.

(136) Thakker GD, Frangogiannis NG, Bujak M et al. Effects of diet-induced obesity on inflammation and remodeling after myocardial infarction. *Am J Physiol Heart Circ Physiol* 2006 November;291(5):H2504-H2514.

(137) Park SY, Cho YR, Kim HJ et al. Unraveling the temporal pattern of diet-induced insulin resistance in individual organs and cardiac dysfunction in C57BL/6 mice. *Diabetes* 2005 December;54(12):3530-40.

(138) Matsushima S, Kinugawa S, Yokota T et al. Increased myocardial NAD(P)H oxidase-derived superoxide causes the exacerbation of postinfarct heart failure in type 2 diabetes. *Am J Physiol Heart Circ Physiol* 2009 July;297(1):H409-H416.

(139) Thakker GD, Frangogiannis NG, Zymek PT et al. Increased myocardial susceptibility to repetitive ischemia with high-fat diet-induced obesity. *Obesity (Silver Spring)* 2008 December;16(12):2593-600.

(140) Chess DJ, Lei B, Hoit BD, Azimzadeh AM, Stanley WC. Effects of a high saturated fat diet on cardiac hypertrophy and dysfunction in response to pressure overload. *J Card Fail* 2008 February;14(1):82-8.

(141) Welsh JA, Sharma A, Abramson JL, Vaccarino V, Gillespie C, Vos MB. Caloric sweetener consumption and dyslipidemia among US adults. *JAMA* 2010 April 21;303(15):1490-7.

(142) Johnson RK, Appel LJ, Brands M et al. Dietary sugars intake and cardiovascular health: a scientific statement from the American Heart Association. *Circulation* 2009 September 15;120(11):1011-20.

(143) Nishida C, Uauy R, Kumanyika S, Shetty P. The joint WHO/FAO expert consultation on diet, nutrition and the prevention of chronic diseases: process, product and policy implications. *Public Health Nutr* 2004 February;7(1A):245-50.

(144) Stanhope KL, Havel PJ. Fructose consumption: considerations for future research on its effects on adipose distribution, lipid metabolism, and insulin sensitivity in humans. *J Nutr* 2009 June;139(6):1236S-41S.

(145) Stanhope KL, Schwarz JM, Keim NL et al. Consuming fructose-sweetened, not glucose-sweetened, beverages increases visceral adiposity and lipids and decreases insulin sensitivity in overweight/obese humans. *J Clin Invest* 2009 May;119(5):1322-34.

(146) Mellor KM, Ritchie RH, Davidoff AJ, Delbridge LM. Elevated dietary sugar and the heart: experimental models and myocardial remodeling. *Can J Physiol Pharmacol* 2010 May;88(5):525-40.

(147) Third Report of the National Cholesterol Education Program (NCEP) Expert Panel on Detection, Evaluation, and Treatment of High Blood Cholesterol in Adults (Adult Treatment Panel III) final report. *Circulation* 2002 December 17;106(25):3143-421.

(148) Halton TL, Willett WC, Liu S et al. Low-carbohydrate-diet score and the risk of coronary heart disease in women. *N Engl J Med* 2006 November 9;355(19):1991-2002.

(149) Beulens JW, de Bruijne LM, Stolk RP et al. High dietary glycemic load and glycemic index increase risk of cardiovascular disease among middle-aged women: a population-based follow-up study. *J Am Coll Cardiol* 2007 July 3;50(1):14-21.

(150) Liu S, Willett WC, Stampfer MJ et al. A prospective study of dietary glycemic load, carbohydrate intake, and risk of coronary heart disease in US women. *Am J Clin Nutr* 2000 June;71(6):1455-61.

(151) Sharma N, Okere IC, Duda MK et al. High fructose diet increases mortality in hypertensive rats compared to a complex carbohydrate or high fat diet. *Am J Hypertens* 2007 April;20(4):403-9.

(152) Sharma N, Okere IC, Barrows BR et al. High-sugar diets increase cardiac dysfunction and mortality in hypertension compared to low-carbohydrate or high-starch diets. *J Hypertens* 2008 July;26(7):1402-10.

(153) Chess DJ, Lei B, Hoit BD, Azimzadeh AM, Stanley WC. Deleterious effects of sugar and protective effects of starch on cardiac remodeling, contractile dysfunction, and mortality in response to pressure overload. *Am J Physiol Heart Circ Physiol* 2007 September;293(3):H1853-H1860.

(154) Chess DJ, Xu W, Khairallah R et al. The antioxidant tempol attenuates pressure overload-Induced cardiac hypertrophy and contractile dysfunction in mice fed a high-fructose diet. *Am J Physiol Heart Circ Physiol* 2008 October 17;295(6):H2223-H2230.

(155) Bouchard-Thomassin AA, Lachance D, Drolet MC, Couet J, Arsenault M. A high-fructose diet worsens eccentric left ventricular hypertrophy in experimental volume overload. *Am J Physiol Heart Circ Physiol* 2011 January;300(1):H125-H134.

(156) Levitan EB, Mittleman MA, Wolk A. Dietary glycemic index, dietary glycemic load, and incidence of heart failure events: a prospective study of middle-aged and elderly women. *J Am Coll Nutr* 2010 February;29(1):65-71.

(157) Mellor K, Ritchie RH, Meredith G, Woodman OL, Morris MJ, Delbridge LM. High-fructose diet elevates myocardial superoxide generation in mice in the absence of cardiac hypertrophy. *Nutrition* 2010 July;26(7-8):842-8.

(158) Singh R, Singh AP, Singh M, Krishan P. Impact of obesity on hypertension-induced cardiac remodeling: role of oxidative stress and its modulation by gemfibrozil treatment in rats. *Free Radic Biol Med* 2011 January 15;50(2):363-70.

(159) Dong F, Zhang X, Yang X et al. Impaired cardiac contractile function in ventricular myocytes from leptin-deficient ob/ob obese mice. *J Endocrinol* 2006 January;188(1):25-36.

(160) Saraiva RM, Minhas KM, Zheng M et al. Reduced neuronal nitric oxide synthase expression contributes to cardiac oxidative stress and nitroso-redox imbalance in ob/ob mice. *Nitric Oxide* 2007 May;16(3):331-8.

(161) Kurtz B, Thibault HB, Raher MJ et al. Nitric oxide synthase 3 deficiency limits adverse ventricular remodeling after pressure overload in insulin resistance. *Am J Physiol Heart Circ Physiol* 2011 November;301(5):H2093-H2101.

(162) Brownlee M. Biochemistry and molecular cell biology of diabetic complications. *Nature* 2001 December 13;414(6865):813-20.

(163) Tsutsui H, Kinugawa S, Matsushima S. Mitochondrial oxidative stress and dysfunction in myocardial remodelling. *Cardiovasc Res* 2009 February 15;81(3):449-56.

(164) Cocco P, Todde P, Fornera S, Manca MB, Manca P, Sias AR. Mortality in a cohort of men expressing the glucose-6-phosphate dehydrogenase deficiency. *Blood* 1998 January 15;91(2):706-9.

(165) Meloni L, Manca MR, Loddo I et al. Glucose-6-phosphate dehydrogenase deficiency protects against coronary heart disease. *J Inherit Metab Dis* 2008 June;31(3):412-7.

(166) Park J, Choe SS, Choi AH et al. Increase in glucose-6-phosphate dehydrogenase in adipocytes stimulates oxidative stress and inflammatory signals. *Diabetes* 2006 November;55(11):2939-49.

(167) Lee JW, Choi AH, Ham M et al. G6PD up-regulation promotes pancreatic beta-cell dysfunction. *Endocrinology* 2011 March;152(3):793-803.

(168) Park J, Rho HK, Kim KH, Choe SS, Lee YS, Kim JB. Overexpression of glucose-6-phosphate dehydrogenase is associated with lipid dysregulation and insulin resistance in obesity. *Mol Cell Biol* 2005 June;25(12):5146-57.

(169) Matsui R, Xu S, Maitland KA et al. Glucose-6 phosphate dehydrogenase deficiency decreases the vascular response to angiotensin II. *Circulation* 2005 July 12;112(2):257-63.

(170) Matsui R, Xu S, Maitland KA et al. Glucose-6-phosphate dehydrogenase deficiency decreases vascular superoxide and atherosclerotic lesions in apolipoprotein E(-/-) mice. *Arterioscler Thromb Vasc Biol* 2006 April;26(4):910-6.

(171) Carette C, Dubois-Laforgue D, Gautier JF, Timsit J. Diabetes mellitus and glucose-6-phosphate dehydrogenase deficiency: from one crisis to another. *Diabetes Metab* 2011 February;37(1):79-82.

(172) Meloni T, Pacifico A, Forteleoni G, Meloni GF. G6PD deficiency and diabetes mellitus in northern Sardinian subjects. *Haematologica* 1992 January;77(1):94-5.

(173) Saeed TK, Hamamy HA, Alwan AA. Association of glucose-6-phosphate dehydrogenase deficiency with diabetes mellitus. *Diabet Med* 1985 March;2(2):110-2.

(174) Saha N. Association of glucose-6-phosphate dehydrogenase deficiency with diabetes mellitus in ethnic groups of Singapore. *J Med Genet* 1979 December;16(6):431-4.

(175) Sobngwi E, Gautier JF, Kevorkian JP et al. High prevalence of glucose-6-phosphate dehydrogenase deficiency without gene mutation suggests a novel genetic mechanism predisposing to ketosis-prone diabetes. *J Clin Endocrinol Metab* 2005 August;90(8):4446-51.

(176) Wan GH, Tsai SC, Chiu DT. Decreased blood activity of glucose-6-phosphate dehydrogenase associates with increased risk for diabetes mellitus. *Endocrine* 2002 November;19(2):191-5.

(177) Amin KA, Kamel HH, bd Eltawab MA. Protective effect of Garcinia against renal oxidative stress and biomarkers induced by high fat and sucrose diet. *Lipids Health Dis* 2011;10:6.

(178) Park JH, Choi JC, Sung MH, Kang JH, Chang MJ. High molecular weight poly-gamma-glutamic acid regulates lipid metabolism in rats fed a high-fat diet and humans. *J Microbiol Biotechnol* 2011 July;21(7):766-75.

(179) Xu Y, Osborne BW, Stanton RC. Diabetes causes inhibition of glucose-6-phosphate dehydrogenase via activation of PKA, which contributes to oxidative stress in rat kidney cortex. *Am J Physiol Renal Physiol* 2005 November;289(5):F1040-F1047.

(180) Jain M, Cui L, Brenner DA et al. Increased myocardial dysfunction after ischemia-reperfusion in mice lacking glucose-6-phosphate dehydrogenase. *Circulation* 2004 February 24;109(7):898-903.

(181) Han CY, Umemoto T, Omer M et al. NADPH oxidase-derived reactive oxygen species increases expression of monocyte chemotactic factor genes in cultured adipocytes. *J Biol Chem* 2012 January 27.

(182) Han CY, Umemoto T, Omer M et al. NADPH oxidase-derived reactive oxygen species increases expression of monocyte chemotactic factor genes in cultured adipocytes. *J Biol Chem* 2012 January 27.

(183) Fang CX, Dong F, Thomas DP, Ma H, He L, Ren J. Hypertrophic cardiomyopathy in high-fat diet-induced obesity: role of suppression of forkhead transcription factor and atrophy gene transcription. *Am J Physiol Heart Circ Physiol* 2008 September;295(3):H1206-H1215.

(184) Rajamani U, Essop MF. Hyperglycemia-mediated activation of the hexosamine biosynthetic pathway results in myocardial apoptosis. *Am J Physiol Cell Physiol* 2010 July;299(1):C139-C147.

(185) Rajamani U, Joseph D, Roux S, Essop MF. The hexosamine biosynthetic pathway can mediate myocardial apoptosis in a rat model of diet-induced insulin resistance. *Acta Physiol (Oxf)* 2011 June;202(2):151-7.

(186) Nishikawa T, Edelstein D, Du XL et al. Normalizing mitochondrial superoxide production blocks three pathways of hyperglycaemic damage. *Nature* 2000 April 13;404(6779):787-90.

(187) Reclos GJ, Hatzidakis CJ, Schulpis KH. Glucose-6-phosphate dehydrogenase deficiency neonatal screening: preliminary evidence that a high percentage of partially deficient female neonates are missed during routine screening. *J Med Screen* 2000;7(1):46-51.

(188) Bendall JK, Cave AC, Heymes C, Gall N, Shah AM. Pivotal role of a gp91(phox)-containing NADPH oxidase in angiotensin II-induced cardiac hypertrophy in mice. *Circulation* 2002 January 22;105(3):293-6.

(189) Moens AL, Kass DA. Tetrahydrobiopterin and cardiovascular disease. *Arterioscler Thromb Vasc Biol* 2006 November;26(11):2439-44.

(190) Spencer NY, Yan Z, Boudreau RL et al. Control of hepatic nuclear superoxide production by glucose 6-phosphate dehydrogenase and NADPH oxidase-4. *J Biol Chem* 2011 March 18;286(11):8977-87.

(191) Yokota T, Kinugawa S, Hirabayashi K et al. Oxidative stress in skeletal muscle impairs mitochondrial respiration and limits exercise capacity in type 2 diabetic mice. *Am J Physiol Heart Circ Physiol* 2009 September;297(3):H1069-H1077.

(192) Matsushima S, Kinugawa S, Ide T et al. Overexpression of glutathione peroxidase attenuates myocardial remodeling and preserves diastolic function in

diabetic heart. *Am J Physiol Heart Circ Physiol* 2006 November;291(5):H2237-H2245.

(193) Han CY, Umemoto T, Omer M et al. NADPH oxidase-derived reactive oxygen species increases expression of monocyte chemotactic factor genes in cultured adipocytes. *J Biol Chem* 2012 January 27.

(194) Pandolfi PP, Sonati F, Rivi R, Mason P, Grosveld F, Luzzatto L. Targeted disruption of the housekeeping gene encoding glucose 6-phosphate dehydrogenase (G6PD): G6PD is dispensable for pentose synthesis but essential for defense against oxidative stress. *EMBO J* 1995 November 1;14(21):5209-15.

(195) Brooks SP, Lampi BJ. Time course of enzyme changes after a switch from a high-fat to a low-fat diet. *Comp Biochem Physiol B Biochem Mol Biol* 1997 October;118(2):359-65.

(196) mir-Ahmady B, Salati LM. Regulation of the processing of glucose-6-phosphate dehydrogenase mRNA by nutritional status. *J Biol Chem* 2001 March 30;276(13):10514-23.

(197) Risse S, Schulke B, Dargel D, Fischer K. [Behavior of some parameters of lipid and energy metabolism. 2. Activity of citrate synthase, ATP citrate lyase, fatty acid synthase, and glucose-6-phosphate dehydrogenase in liver of growing rats on diets differing in fat content]. *Nahrung* 1976;20(6):613-8.

(198) ROSSI F. [Decrease of glucose-6-phosphate dehydrogenase activity prevented by choline in the liver of rats on high fat diet]. *Boll Soc Ital Biol Sper* 1959 November 15;35:1400-2.

(199) Salati LM, mir-Ahmady B. Dietary regulation of expression of glucose-6-phosphate dehydrogenase. *Annu Rev Nutr* 2001;21:121-40.

(200) Spolarics Z. A carbohydrate-rich diet stimulates glucose-6-phosphate dehydrogenase expression in rat hepatic sinusoidal endothelial cells. *J Nutr* 1999 January;129(1):105-8.

(201) Hecker PA, O'Shea KM, Galvao TF, Brown BH, Stanley WC. Role of Adiponectin in the Development of High Fat Diet-induced Metabolic Abnormalities in Mice. *Horm Metab Res* 2010 December 16.

(202) Ferrannini E, Gastaldelli A, Iozzo P. Pathophysiology of prediabetes. *Med Clin North Am* 2011 March;95(2):327-viii.

(203) Wiesenfeld SL, Petrakis NL, Sams BJ, Collen MF, Cutler JL. Elevated blood pressure, pulse rate and serum creatinine in Negro males deficient in glucose-6-phosphate dehydrogenase. *N Engl J Med* 1970 April 30;282(18):1001-2.

(204) Roden M. Mechanisms of Disease: hepatic steatosis in type 2 diabetes--pathogenesis and clinical relevance. *Nat Clin Pract Endocrinol Metab* 2006 June;2(6):335-48.

(205) Cantu D, Schaack J, Patel M. Oxidative inactivation of mitochondrial aconitase results in iron and H2O2-mediated neurotoxicity in rat primary mesencephalic cultures. *PLoS One* 2009;4(9):e7095.

(206) Cleary MP, Zisk JF. Anti-obesity effect of two different levels of dehydroepiandrosterone in lean and obese middle-aged female Zucker rats. *Int J Obes* 1986;10(3):193-204.

(207) Katz J, Landau BR, Bartsch GE. The pentose cycle, triose phosphate isomerization, and lipogenesis in rat adipose tissue. *J Biol Chem* 1966 February 10;241(3):727-40.

(208) Taubes G. Insulin resistance. Prosperity's plague. *Science* 2009 July 17;325(5938):256-60.

(209) Ananthakrishnan R, Li Q, Gomes T, Schmidt AM, Ramasamy R. Aldose reductase pathway contributes to vulnerability of aging myocardium to ischemic injury. *Exp Gerontol* 2011 September;46(9):762-7.

(210) Facundo HT, Brainard RE, Watson LJ et al. O-GlcNAc Signaling is Essential for NFAT-Mediated Transcriptional Reprogramming During Cardiomyocyte Hypertrophy. *Am J Physiol Heart Circ Physiol* 2012 March 9.

(211) Bing RJ, Gudbjarnason S, Tschopp H, Braasch W. Molecular changes in myocardial infarction in heart muscle. *Ann N Y Acad Sci* 1969 January 31;156(1):583-93.

(212) Han CY, Umemoto T, Omer M et al. NADPH oxidase-derived reactive oxygen species increases expression of monocyte chemotactic factor genes in cultured adipocytes. *J Biol Chem* 2012 January 27.

(213) Chess DJ, Lei B, Hoit BD, Azimzadeh AM, Stanley WC. Deleterious effects of sugar and protective effects of starch on cardiac remodeling, contractile dysfunction, and mortality in response to pressure overload. *Am J Physiol Heart Circ Physiol* 2007 September;293(3):H1853-H1860.

(214) von HS, Lainscak M, Springer J, Anker SD. Cardiac cachexia: a systematic overview. *Pharmacol Ther* 2009 March;121(3):227-52.

(215) Han CY, Umemoto T, Omer M et al. NADPH oxidase-derived reactive oxygen species increases expression of monocyte chemotactic factor genes in cultured adipocytes. *J Biol Chem* 2012 January 27.

(216) Chess DJ, Lei B, Hoit BD, Azimzadeh AM, Stanley WC. Deleterious effects of sugar and protective effects of starch on cardiac remodeling, contractile dysfunction, and mortality in response to pressure overload. *Am J Physiol Heart Circ Physiol* 2007 September;293(3):H1853-H1860.

(217) Nishizawa T, Iwase M, Kanazawa H et al. Serial alterations of beta-adrenergic signaling in dilated cardiomyopathic hamsters: possible role of myocardial oxidative stress. *Circ J* 2004 November;68(11):1051-60.

(218) Groh S, Zong H, Goddeeris MM et al. Sarcoglycan complex: implications for metabolic defects in muscular dystrophies. *J Biol Chem* 2009 July 17;284(29):19178-82.

(219) Chess DJ, Lei B, Hoit BD, Azimzadeh AM, Stanley WC. Deleterious effects of sugar and protective effects of starch on cardiac remodeling, contractile dysfunction, and mortality in response to pressure overload. *Am J Physiol Heart Circ Physiol* 2007 September;293(3):H1853-H1860.

(220) Duda MK, O'Shea KM, Lei B et al. Low-carbohydrate/high-fat diet attenuates pressure overload-induced ventricular remodeling and dysfunction. *J Card Fail* 2008 May;14(4):327-35.

(221) Joyeux-Faure M, Rossini E, Ribuot C, Faure P. Fructose-fed rat hearts are protected against ischemia-reperfusion injury. *Exp Biol Med (Maywood)* 2006 April;231(4):456-62.

(222) Jordan JE, Simandle SA, Tulbert CD, Busija DW, Miller AW. Fructose-fed rats are protected against ischemia/reperfusion injury. *J Pharmacol Exp Ther* 2003 December;307(3):1007-11.

(223) Jakob SM, Stanga Z. Perioperative metabolic changes in patients undergoing cardiac surgery. *Nutrition* 2010 April;26(4):349-53.

(224) Missihoun C, Zisa D, Shabbir A, Lin H, Lee T. Myocardial oxidative stress, osteogenic phenotype, and energy metabolism are differentially involved in the initiation and early progression of delta-sarcoglycan-null cardiomyopathy. *Mol Cell Biochem* 2009 January;321(1-2):45-52.

(225) Reue K, Phan J. Metabolic consequences of lipodystrophy in mouse models. *Curr Opin Clin Nutr Metab Care* 2006 July;9(4):436-41.

(226) Chess DJ, Lei B, Hoit BD, Azimzadeh AM, Stanley WC. Deleterious effects of sugar and protective effects of starch on cardiac remodeling, contractile dysfunction, and mortality in response to pressure overload. *Am J Physiol Heart Circ Physiol* 2007 September;293(3):H1853-H1860.

(227) Shusterman V, Usiene I, Harrigal C et al. Strain-specific patterns of autonomic nervous system activity and heart failure susceptibility in mice. *Am J Physiol Heart Circ Physiol* 2002 June;282(6):H2076-H2083.

(228) Toye AA, Lippiat JD, Proks P et al. A genetic and physiological study of impaired glucose homeostasis control in C57BL/6J mice. *Diabetologia* 2005 April;48(4):675-86.

(229) Rebuffe-Scrive M, Surwit R, Feinglos M, Kuhn C, Rodin J. Regional fat distribution and metabolism in a new mouse model (C57BL/6J) of non-insulin-dependent diabetes mellitus. *Metabolism* 1993 November;42(11):1405-9.

(230) Barrick CJ, Rojas M, Schoonhoven R, Smyth SS, Threadgill DW. Cardiac response to pressure overload in 129S1/SvImJ and C57BL/6J mice: temporal- and background-dependent development of concentric left ventricular hypertrophy. *Am J Physiol Heart Circ Physiol* 2007 May;292(5):H2119-H2130.

(231) Sicinski P, Geng Y, Ryder-Cook AS, Barnard EA, Darlison MG, Barnard PJ. The molecular basis of muscular dystrophy in the mdx mouse: a point mutation. *Science* 1989 June 30;244(4912):1578-80.

(232) Arber S, Hunter JJ, Ross J, Jr. et al. MLP-deficient mice exhibit a disruption of cardiac cytoarchitectural organization, dilated cardiomyopathy, and heart failure. *Cell* 1997 February 7;88(3):393-403.

(233) Inoguchi T, Li P, Umeda F et al. High glucose level and free fatty acid stimulate reactive oxygen species production through protein kinase C--dependent activation of NAD(P)H oxidase in cultured vascular cells. *Diabetes* 2000 November;49(11):1939-45.

(234) Adams JW, Sakata Y, Davis MG et al. Enhanced Galphaq signaling: a common pathway mediates cardiac hypertrophy and apoptotic heart failure. *Proc Natl Acad Sci U S A* 1998 August 18;95(17):10140-5.

(235) D'Angelo DD, Sakata Y, Lorenz JN et al. Transgenic Galphaq overexpression induces cardiac contractile failure in mice. *Proc Natl Acad Sci U S A* 1997 July 22;94(15):8121-6.

(236) Gupte SA. Targeting the Pentose Phosphate Pathway in Syndrome X-related Cardiovascular Complications. *Drug Dev Res* 2010 May 1;71(3):161-7.

(237) Mohazzab KM, Wolin MS. Sites of superoxide anion production detected by lucigenin in calf pulmonary artery smooth muscle. *Am J Physiol* 1994 December;267(6 Pt 1):L815-L822.